University of Kentucky Master's Theses   Graduate School

2004

AN INVESTIGATION OF IMAGE PROCESSING TECHNIQUES FOR PAINT DEFECT DETECTION USING A MACHINE VISION SYSTEM

Ashish V. Kamat

University of Kentucky, kamat@engr.uky.edu

Right click to open a feedback form in a new tab to let us know how this document benefits you.

ABSTRACT OF THESIS

AN INVESTIGATION OF IMAGE PROCESSING TECHNIQUES FOR PAINT DEFECT DETECTION USING A MACHINE VISION SYSTEM

Detection and inspection of metal surface corrosion in the ballast tanks of U.S. Navy ships has been a long time problem. The adverse climatic conditions to which the ballast tanks are exposed and the uneven geometry of ballast tanks makes the visual inspection process of surface coatings a difficult job. Thousands of tanks are inspected yearly, with the average cost of an individual tank inspection at approximately $8-15 thousand/each. To aid the visual inspection process, this research is conducted to develop a new technique to automate the visual task of metal surface inspection by image acquisition and post processing. The best results of image processing are achieved by the enhanced contrast between the paint defect and the background using a newly developed optically active additive (OAA) used in paints. Thorough investigation of image processing algorithms has been carried out and a background of imaging theory and experiments is illustrated in this work.

Keywords: Optically active additive, image acquisition, image processing.

Ashish V. Kamat

November 29, 2004

AN INVESTIGATION OF IMAGE PROCESSING TECHNIQUES FOR PAINT DEFECT DETECTION USING A MACHINE VISION SYSTEM

By

Ashish Vijay Kamat

Dr. Kozo Saito

(Director of Thesis)

Dr. George Huang

(Director of Graduate Studies)

Date: 11/29/2004

RULES FOR THE USE OF THESIS

Unpublished thesis submitted for the Master's degree and deposited in the University of Kentucky Library are as a rule open for inspection, but are to be used only with due regard to the rights of the authors. Bibliographical references may be noted, but quotations or summaries of parts may be published only with the permission of the author, and with the usual scholarly acknowledgements.

Extensive copying or publication of the thesis in whole or in part also requires the consent of the Dean of the Graduate School of the University of Kentucky.

A library that borrows this thesis for use by its patrons is expected to secure the signature of each user.

<u>Name</u>   <u>Date</u>

_____

_____

_____

_____

_____

_____

_____

THESIS

Ashish Vijay Kamat

The Graduate School

University of Kentucky

2004

AN INVESTIGATION OF IMAGE PROCESSING TECHNIQUES FOR PAINT DEFECT DETECTION USING A MACHINE VISION SYSTEM

THESIS

A thesis submitted in partial fulfillment of the requirements for the degree of Master of Science in Mechanical Engineering at the University of Kentucky

By

Ashish Vijay Kamat

Lexington, Kentucky

Director: Dr. Kozo Saito, Professor of Mechanical Engineering

Lexington, Kentucky

2004

TO MY MOTHER

Acknowledgments

I would like to express my gratitude and appreciation to all the individuals whose support and guidance have helped me achieve my thesis objective. I am deeply indebted to Dr. Kozo Saito who has been an exceptional mentor and inspiration for me. Your presence was always encouraging and your counsel always insightful. I would like to thank Dr. Abraham Salazar, who has been my true advisor in every aspect of the thesis and helped me improve the work through his insights. Thank you, I have greatly enjoyed working for you.

Further, I wish to thank the members of my thesis evaluation committee, Dr. Keith Rouch and Dr. Abraham Salazar for their evaluation.

I would also like to thank my research buddies, Belal Gharaibeh and Mangesh Kolharkar, who worked meticulously to achieve the research goals and supported me in the experimental work. I would also like to thank Mr. Paul Gossen and Mr. Jay Angal from the National Surface Treatment Center for their valuable comments and suggestions.

The most valuable encouragement and support was provided by my family and friends which helped me succeed in this task. Finally, I would like to thank all the members of Industrial Applications and Engineering Science (IAES) group for their support and advice throughout. You guys are great !

Table of Contents

List of Tables

List of Figures

Chapter 1

Introduction

The painting of the ships during and after construction is a highly complex technology. In principle, different surfaces of the ship require different painting treatments depending on the function of the surface and its exposure to potentially corrosive environment. Since corrosion is defined as the deterioration of a metallic substrate [1] that reacts with its environment, in corrosion prone areas, the typical procedure has been to apply a multi-coat painting with the aim of building enough film thickness to minimize corrosion onset, for example, through pinholing. Table 1 summarizes the paint systems for topside and superstructure paints, boottopping, and bottoms.

It is obvious that the lifetime of a ship is greatly influenced by its ability to withstand corrosion, particularly in the ballast tanks. The annual cost of corrosion and corrosion protection in the United States is estimated by the National Association of Corrosion Engineers (NACE) to be in excess of 10 billion dollars [2]. To fulfill the demand for a long service life, the vessel should ideally be protected with a high-quality system already at the new building stage. Shipboard tanks and voids make up significant percentage of below deck space and are necessary components for normal operation pertaining to seawater buoyancy control, damage control, seawater compensated fuel storage, and a number of other essential tasks, such as combined holding (CHT), potable water storage and sludge. Ballast tanks represent more than 50% of the entire coated area per vessel [2], and as large parts of the ballast tank areas are inaccessible during service, the quality of surface preparation and application is of crucial importance.

The size and quantity of these tanks vary considerably for each class of ship, with the typical numbers of tanks per ship in excess of 300 for carriers, 75-100 for cruisers or destroyers and up to 75 large tanks in amphibious assault ships [2, 3]. Operationally, each tank may see different degrees of service depending on mission requirements, thus creating widely variable maintenance concerns, in addition to those problems routinely anticipated for each tank type. As a result, up to 50% of tank maintenance is due to hidden damage or unplanned work.

Table 1 Summary of 'conventional' marine paint types [1]

Surface	Paint System	Binder type	Coats	Dry Film Thickness	Total Average Film Thickness
Bottom	Primer	Oil-modified phenolic; bitumen	3-4	40-60	~265
	Barrier coat No.1 anti-corrosive	Bitumen/limed rosin	1	50-60	
	Anti-fouling	'Soluble matrix' based on boiled oil/limed rosin; Cu or TBTO toxicant	1	50-75	
Boottopping	Primer 655	Tung/linseed-modified phenolic	2-3	40-60	~200
	Finish	Tung-modified phenolic	2	40-60	
Topside and superstructure		Medium oil length linseed alkyd (55-60% O.L.)	2	50	~220
	Undercoat	Medium oil length linseed alkyd (50-55% O.L.)	1	50	
	Enamel	Long oil length soya alkyd (65% O.L.)	1-2	35-50	

Since the primary function of paints is to prevent corrosion [1, 3] that causes the loss of structural integrity of metal surfaces, ballast tank preservation scenario utilizes paints as the primary corrosion barrier. They may be required to provide the solution to aesthetic or protective problems, or both. Aesthetic concerns vary considerably, depending on the specific industry. The selection of coating depends on, the intended use of the surface, the surface activity, desired time between coatings (service life), aesthetic desires of the ship owner and final the cost of the coating itself. Paints or surface coatings offers a high degree of protection to the metal substrate from corrosion and helps in shielding the exchange of ions between the bare metal and the surroundings that triggers oxidation. In addition to problems of corrosion, the fouling of ships' bottoms with marine organisms leads to increased drag on vessel and hence to increased fuel consumption. Fouling causes the fuel to be consumed at the rate of about 170 tons per day. Paints are used as an anti-corrosive and anti-fouling substance.

Figure 1.1 Condition of ballast tank after 10 years

The maintenance of a ballast tank consists of more than just re-painting the metal surfaces, because tank inspection and assessment alone requires the need for manual opening,

3

gas freeing, staging and entry of trained personnel. Thousands of tanks are inspected yearly, with the average cost of an individual tank inspection at approximately $8K-15K [2]. For this, each tank must be inspected at least once every dry dock cycle, or nominally at least every 5 to 7 years depending on service or ship class. Once tanks are identified for refurbishment, costs soar to over $250 million/year to perform the maintenance. This covers only a fraction of the thousands of Navy tanks in service. Of these costs, which provide for staging, surface preparation and coating application, dollars are spent on those tanks that are in a worst condition. For this methodology to work effectively, all tanks should be monitored, assesses and correctly identified for maintenance only when the condition of the preservation warrants repair.

The geometry is often unique for each tank and maintenance work is often complicated by many complex structure members, such as baffles, edges, corners, etc. Ballast tanks are serviced only when the ship is in the dock of a shipyard (not functioning). However, this does not necessarily mean that the painting and inspection process is a simple task. Working conditions, where maintenance is typically needed, are often difficult and provides less than ideal coatings quality assurance scenarios. As a result, certain structural members, such as edges, corners, etc, often remain inadequately coated and inspected, as a result of which provide best possible environmental conditions as sources of metal corrosion.

Figure 1.2 Condition of ballast tank after 5 years

Over the recent years, major changes have taken place in painting practices and paint formulation to meet the needs. Because of the tonnage limitations, fewer crews are available to do maintenance painting on a much larger ship. This has required the development of paints that

require the ship to undergo less frequent and shorter periods in dry dock. To achieve this, paints giving higher build with fewer coats yet providing improved performance have had to be produced.

However, mere application of paints does not solve the problem of corrosion protection. This is where paint failure and improper inspection comes into picture. Approximately 85 percent of all premature coating failures are a result of poor surface preparation, inadequate mixing, thinning, and/or poor coating application [13]. Onsite quality control inspection during surface preparation and coating application procedures can help prevent failures of these types. Proper inspection techniques must be combined with knowledgeable instrument use, good common sense, and through documentation of work activities and inspection checkpoints to help ensure specification compliance. Coatings on metal surfaces, whether for marine, industrial or domestic uses, rely heavily on the quality of the initial application for their performance. Factors affecting this application such as surface preparation, coating thickness and continuity, number of coats as well as subsequent coating damage caused by heat, abrasion, climate and impacts must be taken into account when considering performance.

The reasons for paint failure are legion. Nevertheless some reasons for failure are readily identifiable, and attempts can be made to combat them. Marine paints based upon autoxidizable binders have the seeds of degradation within them [17]. The oxidation process does not stop when the film has dried. Oxidation proceeds, giving an increasingly cross-linked film. Oxidation products are lost from the film, the net effect being embrittlement ultimately to the stage that changes in the substrate cannot be accommodated. The final effect is cracking and flaking of the film.

The Steel Structures Painting Council (SSPC) Paint Application Guide No. 5, "Guide to Maintenance Painting Programs," provides procedures for planning and carrying out a maintenance painting program.

To prevent corrosion in ballast tanks, the maintenance program is carried out in following steps:

Step 1) Visual survey: Either a minimal walk-through survey, a mid-level, or a detailed survey, depending on the duration of the program, is carried out. It involves a subjective visual assessment of the overall condition of the coatings within a given

area of tanks. The deterioration of the coating is assessed quantitatively in terms of visible corrosion, peeling, blistering, flaking, etc.

Step 2) Physical tests of coating integrity: The existing adhesion within the paint system is inspected and depending on its condition, an overcoating is recommended.

Step 3) Coating thickness Inspection: The film thickness of the entire system, as well as individual layers, is important. This information and the corresponding adhesion may determine the type, level, and degree of surface preparation required if overcoating is recommended.

Step 4) Substrate condition: The underlying substrate is examined for the presence of underfilm corrosion, rust scale, mill scale, or deterioration typical of the substrate itself.

Of all the above mentioned inspection procedures, the visual survey of the tank is the most crucial and time consuming process. Moreover, the interpretation of the survey data requires the ability to change field tests results into meaningful information, which is done by skilled and experienced personnel. Because of the complicated nature of some of the structures it is also almost impossible to carry out an adequate survey of vital parts of the structure with any degree of certainty as to the completeness of the survey.

Visual tests are widely used for in-process and product inspections. Organoleptic visual tests (i.e., those relying on the human eye) have drawbacks [6]. If momentarily distracted, an inspector may overlook discontinuities. Also, the passage of years is increasing industry's need for automation, productions lines are getting faster, and users are demanding better surface quality. Today's demand for higher performance and faster throughput exceed the abilities of visual tests by humans. Consequently, visual tests made by the human eye are being replaced by automated visual testing using optical equipment and unstaffed inspection stations. Surface inspection entails not only optical considerations but also insight into the user industry and peripheral technologies, such as computer, system and human engineering, operational technology, quality control, and user demand trends.

1.1 Research Objective:

The objective of this research is to develop image processing algorithms that would be incorporated in a machine vision system which would replace the visual inspection process of paints for ballast tanks.

In achieving this goal, the research aims a thorough investigation of different post processing algorithms that are been used in the field of machine vision and apply them accordingly to the data collected through imaging experiments. The research also investigates possible solutions for surface inspection that are in use in today's world and propose a possible method that can fit well to the problem of coating's inspection. Figure 1.3 gives an overview of the fields that surround the surface inspection system. In the arena of Non-destructive inspection technique, the purpose of this program is to provide a technique/methodology to enable the detection and characterization of surface paint defects, either pinholes or holidays, for ship ballast tanks and to predict the requirements of a vision system. This would include the development of a theory to support the idea of an Optically Active Additive (OAA) as an aid to visual imaging technique. The research is also directed towards selection of optimum parameters that govern the vision system in a ballast tank and would justify the use of OAA in the paint. The outcome of this study will also help in creating a set of specifications and testing the technical feasibility of the system.

For confidentiality purposes the different vendors providing paint for our analysis would be referred to as Vendor A, Vendor B and Vendor C in order to maintain the data integrity. The two types of additives would also be referred to as Additive X and Additive Y. The characterization of the paint system and the ambient lights will form the base line to design imaging experiments. The optimum parameters that govern the image quality will be derived through a number of combinations of imaging experiments. The geometry of imaging experimental setup and parameters will be replicated in the prototype for the field trial.

PHYSICS
  METTALOGRAPHY
  SURFACE PROPERTIES
  DISLOCATION

CONTROL ENGINEERING
  SIGNAL PROCESSING TECHNOLOGY
  AUTOMATION TECHNOLOGY
  ROBOTICS

MAINTENANCE
TECHNOLOGY

OPTICS
  LASER TECHNOLOGY
  OPTICAL SENSOR
  ILLUMINATION TECHNOLOGY
  COLORING ENGINEERING

ERGONOMICS
ORGANOLEPTICS
HUMAN RESOURCES

OPERATION
  UNDERSTANDING THE
  MANUFACTURING PROCESS

COMPUTER
TECHNOLOGY
SYSTEM ENGINEERING

QUALITY ASSURANCE
QUALITY CONTROL
ROCESS CONTROL

BIOLOGY

INFORMATION PROCESSING
IN BRAIN AND VISION

DEMAND FOR QUALITY
UNDERSTANDING THE
NEEDS AND
MANUFACTURING
PROCESS OF CONSUMER

**SURFACE
INSPECTION**

ARTIFICIAL INTELLIGENCE
  EXPERT SYSTEM
  EXPERTISE
  LEARNING NEURAL NETWORK

MANAGEMENT
  INVESTEMENT EFFECTS

ELECTRONICS

SEMICONDUCTOR TECHNOLOGY
DIGITAL PROCESSING
TRANSISTOR TECHNOLOGY

IMAGE PROCESSING
TECHNOLOGY

EXPERTISE TO DEVELOP AND
  CONSTRUCT AN ORGANIZATION
EXPERTISE TO DEVELOP
  HUMAN RELATIONS

ELECTRICAL ENGINEERING
  POWER
  GROUND
  NOISE

MATHEMATICS
  FOURIER SERIES
  STATISTICAL ANALYSIS
  DISCRMINANT FUNCTION
  PRINCIPAL COMPONENT
  ANALYSIS
  MULTIVARIATE ANALYSIS

MECHANICS
  DESIGN
  MANUFACTURING

Figure 1.3 Various fields surrounding the surface inspection

1.2   Thesis structure:

This research effort has addressed the problem of tank coating inspection from two directions. The first has been the detection of optimum percent loading of OAA required in the primer that will aid in deciding the factors governing the vision system. This is achieved by performing a set of spectroscopic experiments on the paint samples provided by different vendors.

The second aspect is the development of a prototype and the imaging experiments associated with it. This includes, testing of the paint samples in different ambient light conditions, different image capturing techniques and the use of optical filters that would help in the process of image processing.

The research is basically reviewed from three different aspects. The first aspect is addressed in Chapter 2 that illustrates the literature survey and the existing techniques that are in use for surface inspection in industry. This also includes understanding the basic parameters of machine vision systems and defining the customer needs which are covered in Chapter 3. The second aspect of the study covers the experimental part that investigates the effects of ambient light conditions on the excitation intensity of fluorescence emission. The data gathered from these experiments helped in building the prototype, the details of which are also covered in Chapter 4. Finally the last aspect of this research discusses the development of image processing algorithms and its applications depending upon the type of the paint defects that are analyzed. The chapter also shows how the lighting conditions and the uncontrolled parameters can produce complexities in the processed images in the form of false positives.

Chapter 2

Literature Review and Our Approach

2.1   Coatings Inspection Background:

a) Approximately 85 percent of all premature coating failures are a result of poor surface preparation, inadequate mixing, thinning, and/or poor coating application [3]. Onsite quality control inspection during surface preparation and coating application procedures can help prevent failures of these types. Proper inspection techniques must be combined with knowledgeable instrument use, good common sense, and through documentation of work activities and inspection checkpoints to help ensure specification compliance.

b) Paint covers a multitude of mistakes. Without a form of onsite quality control, determining the cause of a problem can be difficult. Coatings inspection can increase the life of a coating system by reducing the number of shortcuts taken by the painter.

c) The amount of inspection and the specific inspection checkpoints will vary with the type and size of the coating project. Some of the quality control inspection procedures are:

- Pre-surface preparation inspection
- Ambient conditions
- Compressed air cleanliness
- Surface profile
- Surface cleanliness
- Paint storage, mixing, and thinning procedures
- Application techniques
- Wet and dry coating thickness
- Pinhole detection
- Adhesion
- Cure

2.2   Techniques for surface inspection using ultraviolet light:

Ultraviolet (UV) sources have the shortest optical wavelengths and hence have much higher energies than longer wave visible light. The UV region of the spectrum is generally considered to be from 40 to 400 nm. It may be further subdivided on the basis of functional

characteristics into three regions: the near UV (300 to 400 nm), the far UV (200 to 300 nm), and vacuum UV (40 to 200 nm). Ultraviolet or UV lighting should be considered when the part to be inspected fluoresces or when fluorescent tracers can be added to the part to be added without problem. Some examples of materials that fluoresce naturally are grease, fluorescent penetrant dyes (used for crack detection), and some food products [7, 9]. An example of the use of tracer technique is the inclusion of a fluorescent additive to solder flux to allow easier inspection for flux residue after soldering. With UV lighting, all visible lighting except that emitted by the fluorescence material can be omitted, yielding very high image contrasts.
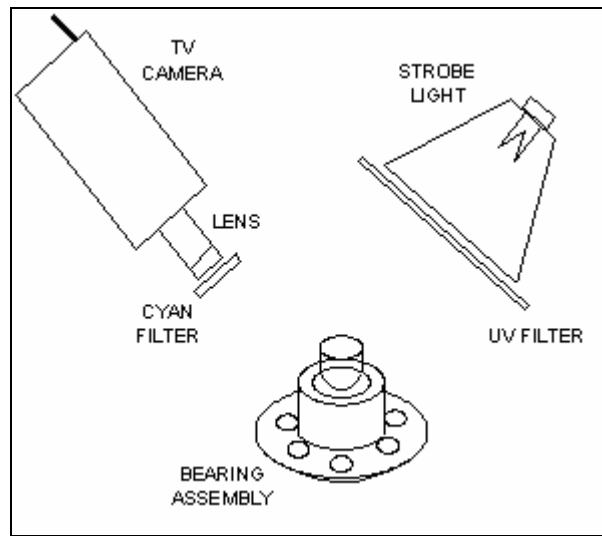
Figure 2.1 Strobe UV lighting arrangement (after Novini, 1985)

One practical application of UV illumination is in the detection of greases. In one assembly application reported by Novini (1985), under visible light there is little or no contrast between dark-colored grease and similar colored background [6]. The use of UV illumination dramatically improves image contrast by reducing background radiance to a low value. Most greases, when exposed to UV radiation, emit light at a longer wavelength (fluoresce). Since that background does not fluoresce, a good contrast is produced and the grease is easily detected. This application used a xenon flash-lamp as both the primary source of UV illumination and as a strobe source for minimizing motion blur of the moving workpiece. The spectral response of a xenon flash-lamp goes deep into the ultraviolet (UV) range and therefore allows its use as a UV source for these applications. To generate only UV light, it is necessary to place a filter in front of the flash lamp to reject most of the visible light while allowing the UV light to pass through.

Direct imaging of metal-surface defects is possible using fluorescent dye-penetrant methods. Bodziak (1986) reports that an innovative technique for using longwave UV excited fluorescent metal dyes to enhance image contrast for inspection of industrial parts assemblies [6]. The application involves the assembly of spacers, locking washers, and gears into a differential gearbox for a rear-wheel drive car. Rear axles are inserted into the gearbox and held there with two C-washers fitted into grooves milled into the axles. Because of the close proximity of the various components in the gearcase, it is very difficult to visually inspect for the presence and correct installation of the C-washers [15, 16]. Such an inspection application would also appear to be difficult to automate. To aid the human inspector, the C-washers are electroplated with copper to make them easier to see within the clutter of the gearcase. The solution for the automated MV inspection task uses a similar philosophy: the contrast of the part is increased with respect to the background clutter. To the MV system, however, copper plating is virtually indistinguishable from the spectral content of the reflections from the steel parts. Hence, a number of phosphorescent and fluorescent paints, dyes, and inks were tested. The rationale for the use of phosphorescent paint was that under the strobe illumination, the phosphorescent-painted washers would continue to glow after the strobe was off, and the shutter to the camera could then be opened.

UV light is widely used with a secondary illumination process, from fluorescence. Fluorescent tracers have been used extensively in industry in non-destructive testing of materials [15]. Fluorescent penetrant dyes are used to detect the presence of surface flaws in a wide variety of materials. One important thing to consider when using fluorescent tracers under UV illumination is that very low visible light levels are involved (the fluoresced light returning to the camera). The cameras that are used must have relatively high response at the fluorescent wavelength to obtain satisfactory SNR.

Another area of intense use of UV illumination is wafer processing and inspection. UV light sources are used in the inspection of IC wafers to determine film thickness and compositional homogeneity.

2.3 Existing paint inspection instrument and techniques:

Table 2 Technologies investigated for assessment of seawater ballast tank and compensating fuel tanks aboard US Navy ships [17]

Technique	Pro	Con
Microwave, Near and Far Field	Near field technology promises hand held device for micro inspection	Microwaves effected by water, tank structures and moisture on walls
Optical Coherent Topography	Ability to detect coatings disbondment	Micro area analysis
Optical Visible Light	Ability to document damage and retain good color rendering	Requires supplemental lighting
Color Visible Imaging/CCD	Real-time Spectrographic analysis, visual record/documentation, reliable and durable	Analysis program required
Infrared Spectrometer	Ability to provide area damage documentation and some localized features	Affected by temp variation/moisture/silt/salinity barrier on tank walls, Limited effectiveness
Ultra Sound	Hold promise in near future	Affected by tank structure
Fiber Optic Corrosion Monitors	Ability to monitor and detect corrosion initiation sites	Monitors micro areas
Electrochemical Impedance Spectroscopy	Determine coatings porosity and relative coatings properties	Localized information, complex installation and limited interpretation
Electrochemical Reference Cell	Currently utilized in seawater ballast and compensating fuel tanks	Requires electrolyte for operation
Coatings Fluorescent Dyes	Ability to detect holidays in surface coatings	Not proven inspection method and not applicable to old tanks

2.3.1 Tank Monitoring Systems:

Ballast tank spaces include seawater tanks for ballast and damage control, compensated fuel tanks, fuel/oil service, potable water storage, and combined holding tanks (CHT) [17]. These spaces have coatings as the primary corrosion control element and a cathodic protection system as the secondary element to minimize coating degradation and effects of galvanic corrosion. Navy Research Laboratory (NRL) has developed a Tank Monitoring System (TMS), an unmanned tank entry method for inspection and qualification of tank integrity. The TMS system includes an in-situ corrosion sensor (fig) which is installed in the tank to monitor the coating integrity, the corrosion status, and cathodic protection functionality.
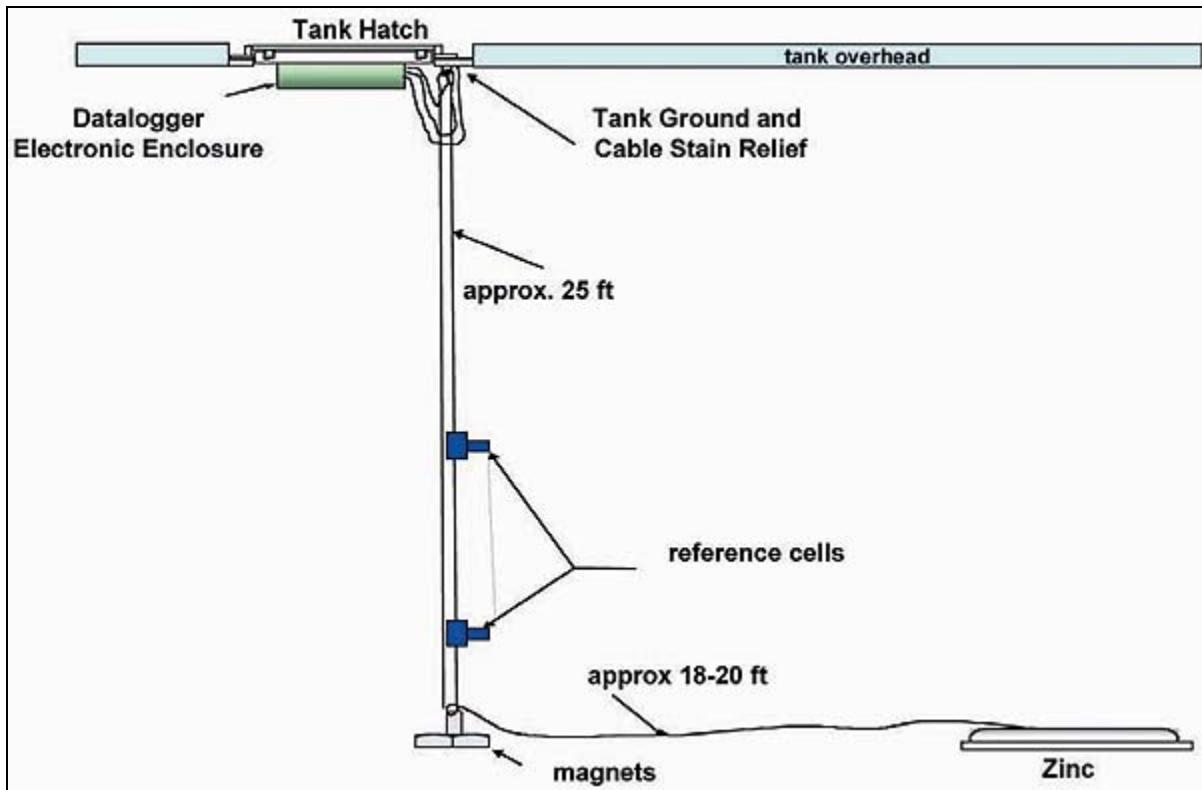
Figure 2.2 Schematic of Tank Monitoring System

For each sensor, a minimum of two reference cells are suspended in the tank, with one always residing near the bottom, while the others are arranged to correspond to intermediate and filled states. Upon filling, the lower water reference cell registers the change in potential almost immediately, as the tank fills. The upper reference cells begin to read once the water reaches

them. The upper areas of the tank will be better indicated on these cells and will report the relative time it takes to fully polarize and protect these areas.

Figure 2.3 Tank Monitoring System

These sensors can be installed with minimal impact to the tank and provide continual in-situ performance data whenever the tank is filled or when seawater displaces the fuel in a compensated fuel tank. Sensors can be installed in a variety of forms and data handling configurations, from completely internal watertight systems to fully integrated computerized ship systems.

2.3.2   Insertable Stalk Inspection System (ISIS) and Remotely Operated Paint Inspector (ROPI):

The ISIS system is inserted into a ballast tank entry point. Motorized pan and tilt stages allow for changes in the camera direction of view [17, 18]. The ROPI system is deployed using a small remote undersea vehicle.

Figure 2.4 Insertable Stalk Inspection System (ISIS)

ISIS currently incorporates a 72:1 zoom-capable charge-coupled device (CCD) camera that allows for continuous optical changes from 6m x 6m to 0.3m x 0.3m when the camera is located 7.5 m from the surface. The video camera and the motorized pan and still stages are integrated to the end of a long stalk. A mechanical sub-system is used to hold the stalk and provides a means to secure the system to the bolts on the hatch at the ballast tank entry point.
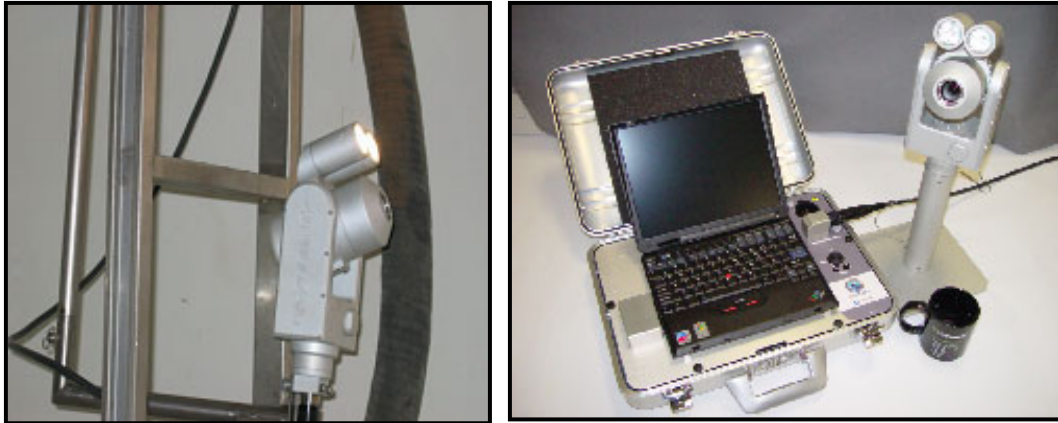
(a)   (b)

Figure 2.5 (a) Video camera for ISIS   (b) Image Acquisition for ISIS

The mechanical sub-system allows the stalk to be lowered to a desired depth within the ballast tank. ISIS is inserted up to 3 m into the tank through a personnel entry hatch and is mounted to the hatch. The operator then records high-resolution images (stills) and video of all tank surfaces for later analysis.

The ROPI system is essentially a mini-ROV, whose dimensions allow entry through the ~ 13 X 21-in. tank hatches. The ROPI is ideal for use in tanks that are ballasted and those having numerous obstructions that would prevent useful implementation of the ISIS system. The ROPI system is equipped with two cameras, one forward looking (the main imaging camera) and a rear looking camera (to aid in navigation). A total 340 W of lighting with intensity control are included onboard for adequate lighting in a variety of conditions. The ROPI is outfitted with an autohover system that will allow for smooth vertical evaluation of tank surfaces. To perform an inspection ROPI is swum to a particular location and camera parameters are appropriately adjusted while the video is recorded using the digital video recorder.

2.3.3 Low voltage wet sponge pinhole detectors:

The low voltage wet sponge pinhole detectors are used for finding discontinuities in nonconductive coatings applied to conductive metal surfaces [2]. Pinhole testing also can be used to locate conductivity on rivets, bolt threads, etc. The low voltage detector is suitable for use on coatings up to 0.51 mm (20 mils) in thickness. The basic unit consists of the detector, a ground cable, and a sponge electrode. The ground cable is firmly attached to the bare substrate, and the sponge electrode is saturated with tap water. When the electrode is moved across the entire surface, the water permits a small current to flow through the pinholes down to the substrate. When the current reaches the substrate, the circuit is completed to the detector unit and an audible signal indicates that a pinhole or discontinuity is present. Pinhole testing has certain limitations. For example, in some situations, pinholes can be visually detected, though the detector does not sound, because the pinholes do not penetrate to the substrate. Conversely, the detector may sound to indicate the presence of a void when none exists because the coating itself may be conductive as a result of metallic pigmentation or entrained solvent.

2.3.4 High-voltage holiday detectors:

High-voltage holiday detectors basically function on the same operating principle as the low-voltage units, except the sponge is not used [2]. The instrument consists of testing unit capable of producing various voltage outputs, a ground cable, and an electrode made of neoprene, rubber, brass, or steel. High-voltage units are available up to 20,000 V and more. High-voltage holiday inspection frequently is required on pipelines and other critical applications. A spark will jump from the electrode through the coating down to the substrate at pinholes, holidays, or missed areas and simultaneously trigger an audible and/or visual signaling device in the unit. The rule of thumb for high voltage testing is 100 to 125 V per mil. Too high a test voltage sometimes damages the film. Even when the testing voltage is properly set, a spark may penetrate a thin, intact area of the coating and create a void that must be repaired.

2.4   The fluorescence phenomenon:

A theoretical molecule has two electronic energy states, E_0 (ground state) and E_1 (excited state). Each electronic state has several vibrational states [5]. Incident polychromatic light (photons) excite the molecules that are in state E_0 and makes them temporarily populate the excited vibrational states of E_1.
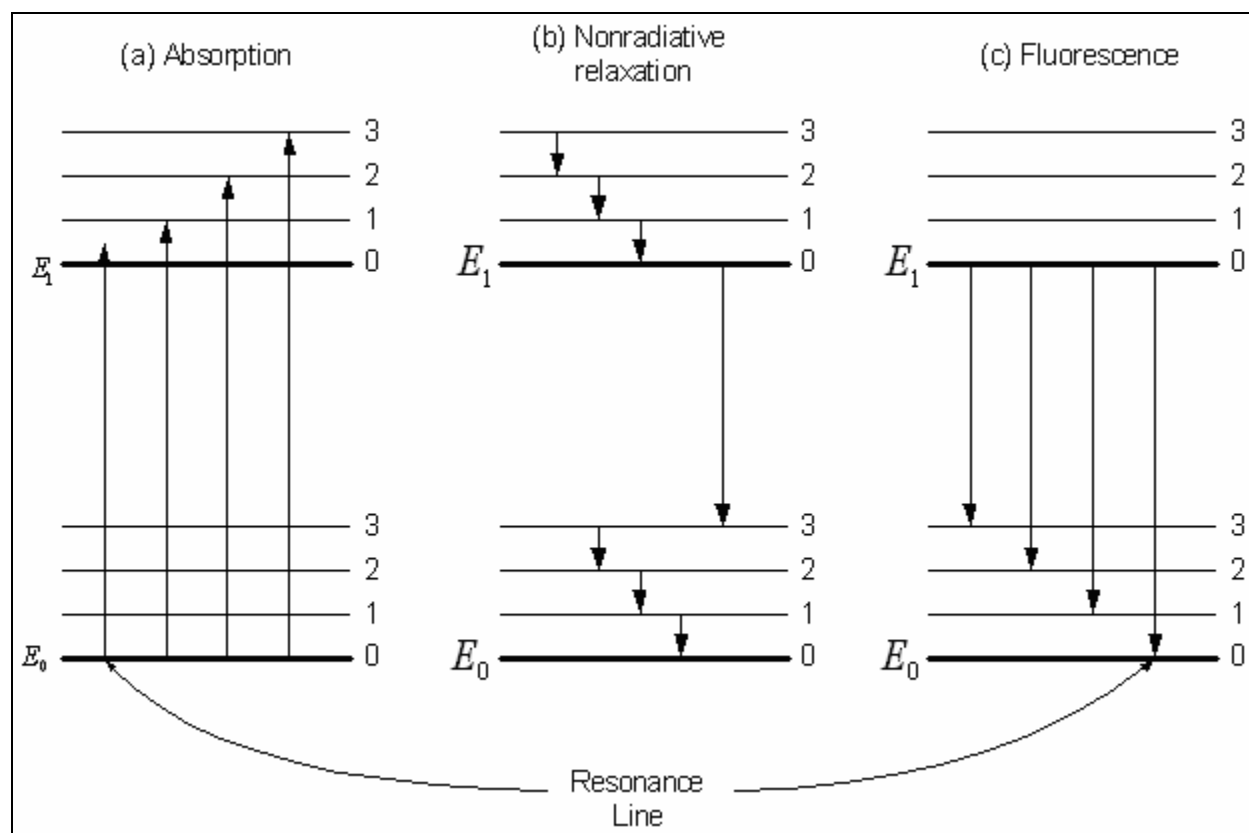
Figure 2.6 The energy level diagram of (a) absorption (b) non-radiative relaxation (c) fluorescent emission. [5]

The vibrational excited state has an average lifetime of only 10^{-15} s. The molecule rapidly loses its vibrational energy and goes down to the electronic energy state E_1. This relaxation process is non-radiative, and it is caused by the collisions with other molecules to which the vibrational energy is transferred. This induces a slight increase of the temperature of the medium. The excited state E_1 has a lifetime varying between 10^{-6} and 10^{-9} s. There are two ways for the molecule to give up its excess energy. One of them is called internal conversion, a nonradiative relaxation for which the mechanism is not fully understood. The transition occurs between

19

E_1 and the upper vibrational state of E_0 (Figure b), and the lost energy raises the temperature of the medium. The other possible relaxation process is fluorescence. It takes place by emitting a photon of energy corresponding to the transition between E_1 and a vibrational state of E_0 (Figure c). The remaining excess energy with respect to E_0 is lost by vibrational relaxation. To quantify the number of photons emitted by fluorescence, the quantum yield is introduced as the rate of absorbed photons that are released by radiative relaxation.

The wavelength band of absorbed radiation that is responsible for the excitation of the molecules is called the excitation spectrum. This spectrum consists of lines whose wavelengths correspond to the energy differences between excited vibrational states of E_1 and the ground electronic state E_0 (according to the energy difference ΔE produced by the absorption of a photon of wavelength lambda: $\Delta E = \dfrac{hc}{\lambda}$, where h is Plank's constant and c is the speed of light).

The fluorescence emission spectrum (or fluorescence spectrum), on its part, consists of lines that correspond to the energy differences between the electronic level E_1, and the vibrational state of E_0. The multitude of lines in both spectra is difficult to resolve and makes them look like continuous spectra. The fluorescence spectrum is made up of lines of lower energy than the absorption spectrum. This wavelength shift between the absorption band and the fluorescence band is called Stokes shift.

The shape of the fluorescence emission spectrum does not depend on the spectrum of the absorbed light, but on the probability of the transition between the excited state E_1 and the vibrational states of E_0. Often, the fluorescence spectrum looks like a mirror image of the excitation spectrum (Add spectrum Figure) due to the fact that the differences between vibrational states are about the same in ground and excited states.

The fluorescence spectrum is measured with a fluorescence spectrometer [5, 8]. A sample of unknown fluorescence substance is excited with a monochromatic light beam whose wavelength is within the excitation band of the molecule. The emitted light is analyzed, and the resulting spectrum is the fluorescence spectrum. Its amplitude is maximal when the wavelength of the incident light corresponds to the maximum absorption of the fluorescent molecule.

At high concentrations, the behavior of the fluorescent substance is no longer linear. The absorption is too large, and no light can pass through to cause excitation. Temperature, dissolved

oxygen, and impurities reduce the quantum yield, which in turn reduces fluorescence. This phenomenon is called quenching.

The fluorescent light emission process follows a Poisson distribution [7], adding a signal-dependent (multiplicative) noise component. Multiplicative signal processes can yield non-linear effects that are difficult both to model and compensate for. The signal in fluorescence imaging can be divided into two parts: the signal from the fluorescence relaxation process itself, and the noise of the detection process. Since the fluorescence signal is usually very low in flux density, it has a Poisson type energy distribution P (k); that is, the joint probability of the occurrence of a photon flux of k is

$$P(k) = \frac{\lambda^k}{k!} e^{-\lambda}$$

where λ is both the mean and the variance of the Poisson distribution P, and k = 0, 1,.….

The noise power N (RMS) of a Poisson distributed signal is $N = \sqrt{S}$, where S is the RMS signal power: $\left(S = \sum k.P \right)$. With the lower SNRs involved in fluorescence imaging, it is important that detector noise (which has an additive Gaussian distribution) be taken into account.

When the photon count expectation value (λ) is low, the SNR will degrade according to the above noise process. To improve the signal, the mean value λ must be increased. This can be done either by increasing the intensity of the UV light source or by longer integration times in the sensor:

$$S(x, y) = \int_0^t S(x, y, t) dt$$

The use of high UV lighting levels can be problematical, e.g. the surrounding target area may be damaged, the system optics can degrade more rapidly, a significant health hazard may result, etc. Moreover, at some point the fluorescence relaxation process becomes saturated (producing some maximum level of flux), the signal to longer increases, and there is no further improvement in the SNR. Finally, the increased excitation power can damage the sample being imaged. Workpiece damage, called bleaching, as well as system damage, also results if the exposure time is increased. As an alternative to increasing the signal and/or exposure time, image processing techniques can be applied to attenuate the effects of the noise.

2.4.1   Theory of additives:

An additive is defined as one of the substances included in a paint formulation at a low level, which nevertheless has a marked effect on the properties of the paint [1]. Optically active additives (OAA) are similar to fluorescent whitening agents or optical brighteners. These materials absorb ultraviolet wavelengths and re-emit the energy in the visible waveband. The OAA used in the paints are chosen to emit in the blue and green region and a comparative study is made on the basis of their visual contrast with the background. In recent years, OAA have found significant applications in surface inspection techniques and ongoing research is conducted to improve their short emission life and reduction in cost.

2.5   Light scattering and absorption by paint films:

Light refracted into the paint film is partly absorbed by the medium (resin or varnish), but mainly encounters particles where it is scattered, absorbed, or transmitted in various proportions. Light scattering by pigment particle depends on its size, relative to the wavelength of the light, and its refractive index ratio to that of the medium. Absorption by a pigment particle depends on the path length of light through the particle and on the excitation coefficient (absorbance) of the pigmentary material for the particular wavelength.

2.5.1   Reflection at interfaces:

Light transmitted through a paint film is partly absorbed by the substrate and partly reflected; a proportion of the reflected light eventually re-emerges, so that the film appears lighter over a more reflective substrate [1].
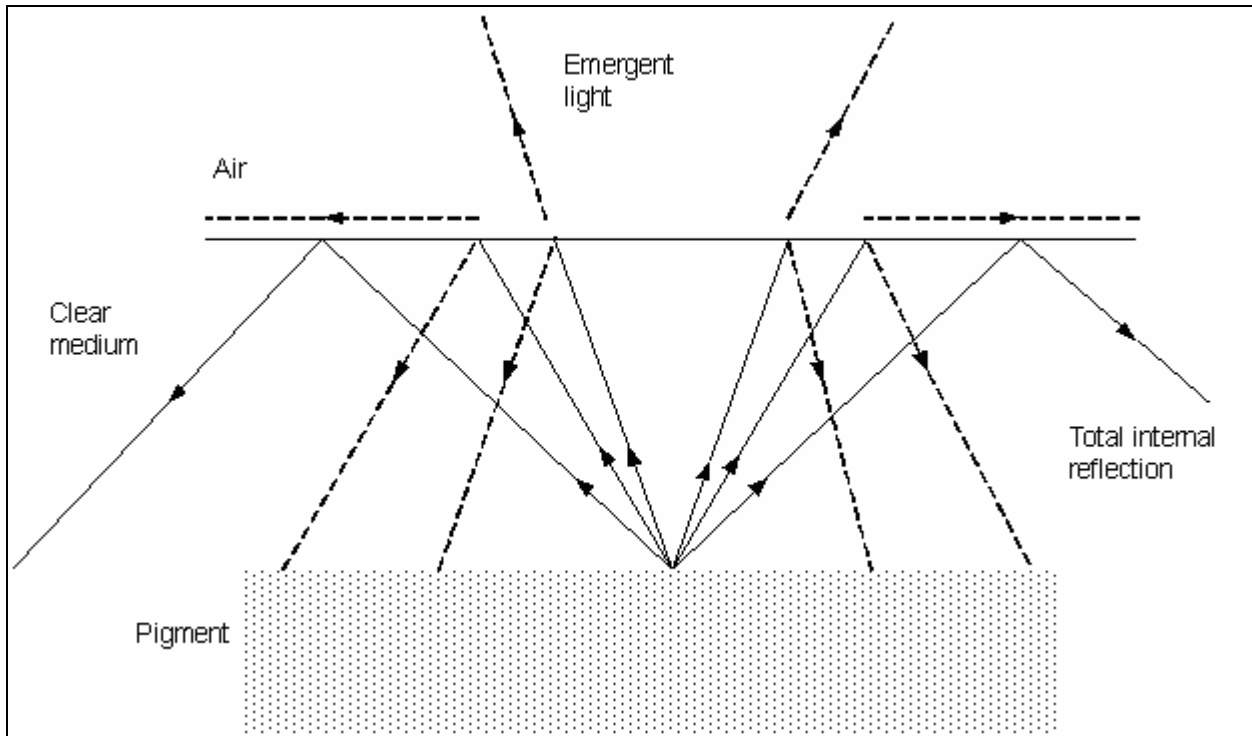
Figure 2.7 Internal reflection at paint/air interface

When incident beam of light is absorbed by a paint film, a considerable portion (usually over one half) of the light scattered back, diffusely, from a pigment layer is internally reflected at the paint/air interface (Figure 2.7), and thus is attenuated again by absorption by pigment or substrate before reaching the interface for a second time. A similar situation occurs at the paint/substrate interface where light is inter-reflected between the substrate and the pigmented layer. (Figure 2.8) indicates some of the infinite series of inter-reflections that occur until all the light has been absorbed or has emerged finally from the film.

The effect of the air/paint interface is calculated by summing the geometric progressions of inter-reflections. The result obtained is

$$R_T = R_E + \frac{(1-R_E)(1-R_I)R_P}{(1-R_I R_P)}$$

where R_T is the reflectivity of the glossy paint film,

R_E the external reflection coefficient of the interface,

R_I the internal reflection coefficient of the interface,

R_P the reflectivity of the pigmented layer over its substrate.
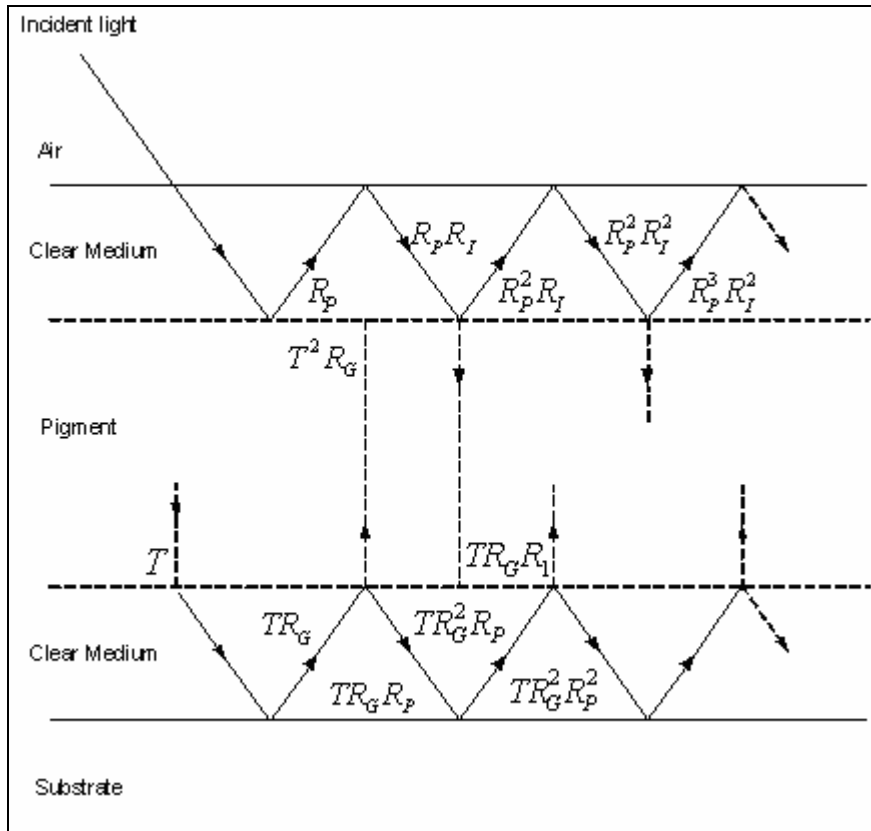
Figure 2.8 Inter-reflections at surface and substrate

2.5.2 Scattering by white pigments:

White pigments are made from transparent, almost colorless materials used in paint as fine particles. The relationship between particle size and light scattering was investigated by Mie in 1908 [1] who showed that maximum scattering per unit amount of material occurred for a particle diameter rather less than the wavelength of light. The curve refers to single scattering, i.e. light scattered only once by each particle, but in practice the optimum size is not greatly modified in paint films, except at very high levels of pigmentation where scattering by more closely spaced particles is considerably reduced.

2.5.3 Absorption by pigments:

All pigments absorb radiation of some wavelengths, but for white pigments the absorption becomes strong only in the ultra-violet region [1]. Most colored pigments absorb strongly for parts of visible light spectrum but are transparent for others. In a film where colored pigment is mixed with white scattering particles the total absorption and hence the depth of color depends on the particle size of the colored pigment. Provided that the particles are fully dispersed, absorption increases steadily as particle size is reduced. This is because the cross-section of each particle is proportional to d^2, where d is the particle diameter, and the number of particles per unit volume is proportional to $1/d^3$. Hence the total cross-section offered to the light is proportional to $1/d$.

2.6 Physics of Image Formation:

In any machine vision system application, it is important to understand the analytical function, a mathematical model of the behavior of light source. Equally important is to predict the model of the system optics, sensors, and surfaces to yield a prediction of what an image output by an MV system design will look like. In this section, an analytical relation between image irradiance and the scene radiance that govern the principles of image formation is been developed. The amount of light falling onto a patch of unit surface area is termed as illuminance. Illuminance £ is amount of luminous flux through a unit of surface area [8]. The SI unit for illuminance £ is meter-candle (m.cd), the amount of illumination falling on to the inner surface of the sphere of a 1-m radius with an isotropic central 1-cd source. This unit is more commonly termed as **lux** and is given in terms of lm/m^2.

The following table serves as a reference for understanding the relative differences between various **lux** levels:

Table 3 Representative levels of source intensities [8]

Lux	Description
100,000	Clear sky, mid-day, sunlight
32,000	Cloudy sky, mid-day, sunlight
2,000	Cloudy sky, 1 hr after sunrise
600	Department store counters
450	Average office fluorescent lighting
175	Streetlights at night
10	Candlelight at 20 cm; pocket flashlight
0.3	Bright clear moonlight night

The radiance R of a passive surface consists of reflected light from one or more sources (or other surfaces). This surface radiance depends on the direction of observation, the direction from which the surface is illuminated, the illumination level, and the reflection properties of the surface. The irradiance falling onto a surface oriented perpendicular to the light source direction can be readily calculated, provided the radiant intensity N_S of the light source (in the direction of the receiving surface) is known, as well as the distance d_O between the source and the surface. Irradiance is defined as the flux per unit area.
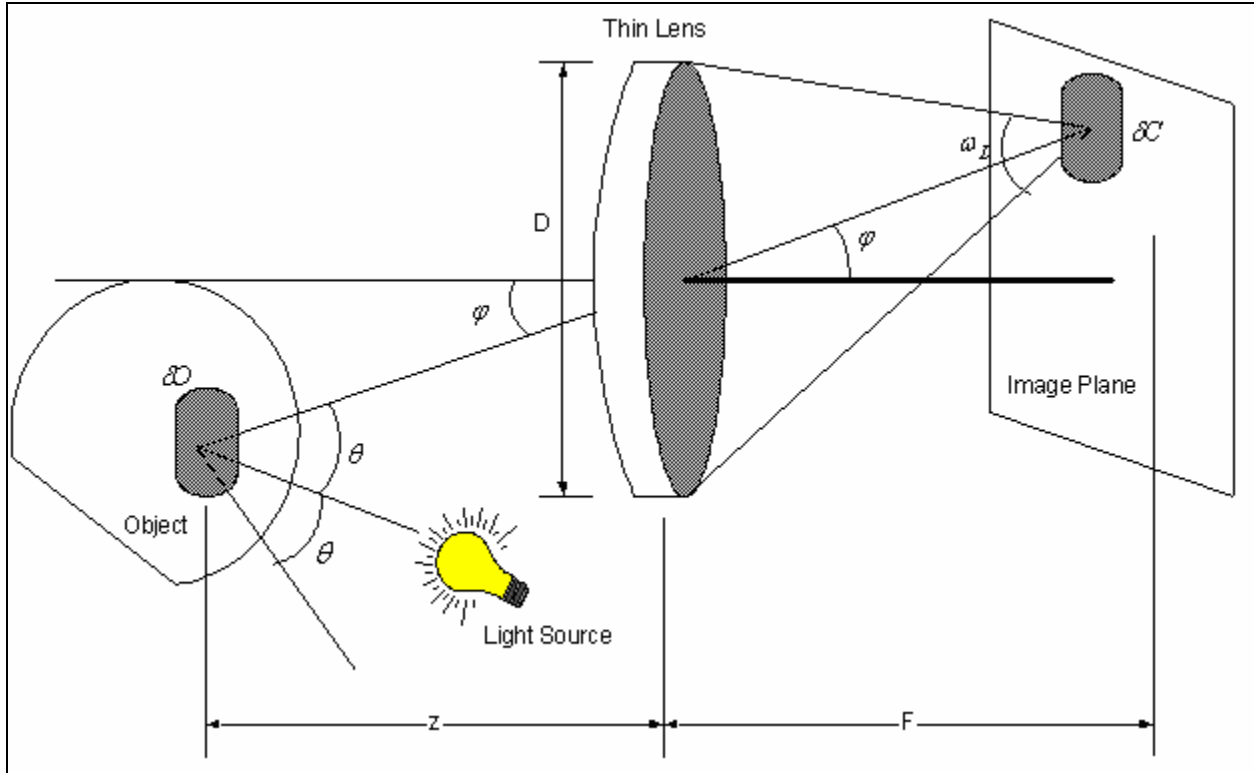
Figure 2.8 Schematic illustrating the principle of image formation

The radiant power W_O falling onto a patch O of area A_O of a receiving surface is called the degree of irradiance I_O of the object surface and is given as:

$$I_O = \frac{W_O}{A_O} = \frac{N_S\left(A_O / d_O^2\right)}{A_O} = \frac{N_S}{d_O^2}$$

Thus, the irradiance falling onto a perpendicular surface patch O is proportional to the inverse square of the distance to the light source.

If the receiving surface is located in a direction at an angle θ with respect to the axis of illumination, the receiving surface normally 'sees' a source of reduced intensity $(A_O \cos\theta)$.

Hence the irradiance on the surface will be proportional to the cosine of the angle of $\hat{i}$:

$$I_O = \frac{N_S}{d_O^2} \cos\theta$$

If the receiving surface normal $\hat{o}$ is tilted at an angle φ with respect to $\hat{i}$, then this becomes

$$I_O = \frac{N_S}{d_O^2} \cos\theta \cos\varphi$$

The underlying assumption for the application of inverse-square law and the cosine law is that the light source can be considered to be a 'point-source'.

The object, which are now the fluorescent particles dispersed in the paint, now becomes a source surface and the sensor plane assumes the role of the receiving surface.

The following theory now focuses on determining how much of the light from an object patch gets through the lens and falls onto the camera image (surface of the sensor).

For an object patch which is at an angle to the optical axis, the solid angle solid angle subtended at the center of the lens is given by

$$\omega_L = \frac{\left(\pi D_L^2 / 4\right)\cos\varphi}{\left(z/\cos\varphi\right)^2} = \frac{\pi}{4}\left(\frac{D_L}{z}\right)^2 \cos^3\varphi$$

The radiance of the object patch remains constant through the optical system and is given as

$$R = \frac{W}{\omega A}$$

The image flux falling onto the camera surface is given by

$$W_C = R_O \omega_O A_O = R_O \omega_C A_C$$

where ω_O the solid angle is subtended by the object patch and A_O is the area of the object patch.

Hence the proportion of flux falling onto a patch of area δO is given by

$$\delta W_C = R_O \omega_O \left(\delta O \cos\theta\right)$$

Substituting for ω_O gives

$$\delta W_C = R_O \left[\frac{1}{4}\pi\left(\frac{D_L}{z}\right)^2 \cos^3\varphi\right]\delta O \cos\theta$$

This amount of light flux δW_C is spread over the sensor image spot area of δC, so its irradiance is

$$I_C = \frac{\delta W_C}{\delta C}$$

$$I_C = R_O \left[\frac{1}{4} \pi \left(\frac{D_L}{z} \right)^2 \cos^3 \varphi \right] \frac{\delta O}{\delta C} \cos \theta$$

The solid angle of the cone of rays leading to the spot on the object is equal to the solid angle of the cone of rays leading to the corresponding spot on the image sensor. This gives:

$$\frac{\delta C \cos \varphi}{(F / \cos \varphi)^2} = \frac{\delta O \cos \theta}{(z / \cos \varphi)^2}$$

$$\frac{\delta O}{\delta C} = \frac{\cos \varphi}{\cos \theta} \left(\frac{z}{F} \right)^2$$

Generalizing the above equation to the entire sensor surface, the total irradiance falling onto the camera surface is

$$I_C = R_O \left[\frac{1}{4} \pi \left(\frac{D_L}{z} \right)^2 \cos^3 \varphi \right] \left[\frac{\cos \varphi}{\cos \theta} \left(\frac{z^2}{F^2} \right) \right] \cos \theta$$

$$I_C = \left[\frac{\pi}{4} \frac{D_L^2}{F^2} \cos^4 \varphi \right] R_O$$

The image irradiance I_C is proportional to scene radiance R_O, with the proportionality factor being the term within the brackets.

2.7 Sample Preparation and Procurement:

In order to study the characteristics of the optically active additive (OAA) and the relation between the paint film thickness and fluorescence emission, there was a need to produce painted samples with varying film thickness. Accordingly, paint samples were created with different percentage loading of OAA and different film thicknesses. Laboratory tests were subsequently performed on these paint samples with deferent test conditions. The experiments and their subsequent results will be discussed in chapter 4 and chapter 5.

Pre-surface Preparation Inspection:

a) Prior to starting surface preparation and coating work, it is necessary to determine that the structure is ready for surface preparation and painting. The blast-cleaning process

redistributes heavy deposits of grease, oil, dust, dirt, and other contaminants, if they are not removed.

b) The specifications may require that weld spatter be removed and sharp edges be rounded. Unusual spitting in the steel substrate may require grinding, filling, etc. before blast cleaning. Large-scale repairs of this type, however, can be quite costly and time consuming.

2.7.1 Test sample preparation for pin-hole defect detection and study of lighting conditions:

In any method of paint application, either an excess of paint is applied and the surplus is removed, or the desired thickness of paint is put directly during application. Dipping is in the first category, and electrodeposition, spraying, brushing, and roller application are in the second. The application methods that were employed for our experiments are spraying and drawdown (Knife-coating). For sprayed samples, panels of 4"x 8" area were blasted to a 1.5 – 2.5 mil profile at SSPC – SP5 finish. This essentially means that it was ensured that the panel is free from surface imperfections, such as rolling marks, scores, and corrosion. They were degreased thoroughly with trichloroethylene and dried. The drawdown panels were 6" x 12" cold roll steel. The spray application of panels was done by 30:1 airless spray pump using number 19-spray tip. Two thicknesses of 8 and 12 mils were sprayed. The Knife-coating or drawdown method is employed when a very thin coating is required on a flat and usually continuous sheet material. Excess coating is applied by any suitable technique, and the coating thickness is then reduced by passing the web under a doctor knife (an angled metal blade) or an air knife (a curtain of high-velocity air directed onto the web). Viscosity can be relatively high, since the pressure of the knife determines film thickness, and the appearance requirement is not exacting. The drawdown samples of 4, 6 and 10 mils were created using a fixed 4 edge steel blade.

The process of paint making requires extensive use of various types of mixers for the blending and mixing of resins, solvents, additives, and intermediates in order to complete the make-up of paint formulations and obtain a homogenous product after the dispersion stage. The OAA from two different vendors was mixed with the epoxy paints in the ratio described by the MSDS, by a heavy duty portable mixer that was capable of dispensing the pigment in the paint.

2.7.2 Preparation of 3D test panels to simulate holidays and missed areas:

Apart for the study of spectroscopic experiments and pin-hole defect detection, there was a need to procure paint samples that will represent the actual missed areas and holidays in ballast tanks. This resulted in producing five, 3-D test panels made of 1/16" gauge steel sheets having geometries similar to that found in ballast tanks of Navy ships. The defects that were taken into consideration while making these panels were missed areas at corners and at edges. These are the areas which are difficult to inspect and can be sources of corrosion if not painted appropriately. For the purpose of this thesis we have designated these panels as B1, B2 and B3 where "B" stands for Box shape and T1 and T2 where "T" stands for a T-shape plate welded to a flat plate. The models were MEK wiped before painting, but not blasted or scarified. The panels were sprayed with a 30:1 airless spray gun under 80 psi pressure.

2.8 Experimental Set-up:

Although there are some general guidelines for lighting and imaging setups, every machine vision application has its own unique peculiarities that have to be dealt with. A crucial issue in any imaging problem is the selection of an appropriate light source(s) that highlights features of interest. The lighting geometry, i.e. relative positions of light source, camera, and the object, is also equally important. Also, the combination of optical filters, that decide the wavelength of light incident on the sample and the camera sensor, are important aspects of the vision system. The experimental-set up was directed towards achieving the best possible image of the paint defect and deciding the parameters of the system. It forms a integral part of this research and is discussed in brief.

2.8.1 Equipments and specifications:
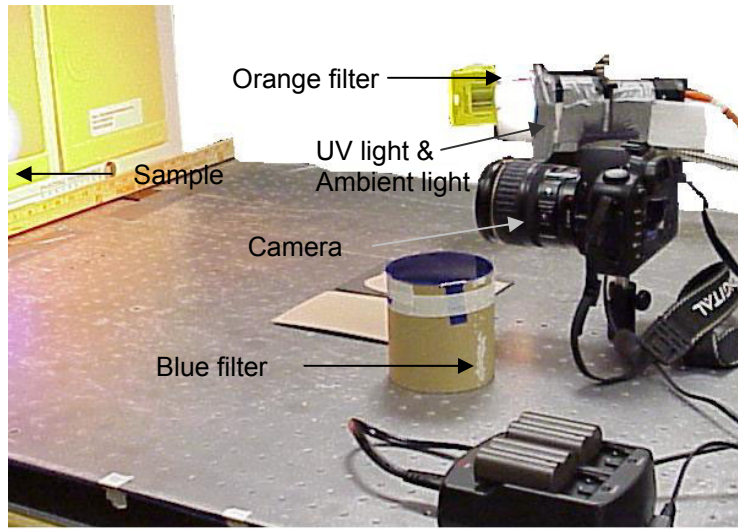
Figure 2.9 Experimental Set-up

TOP VIEW
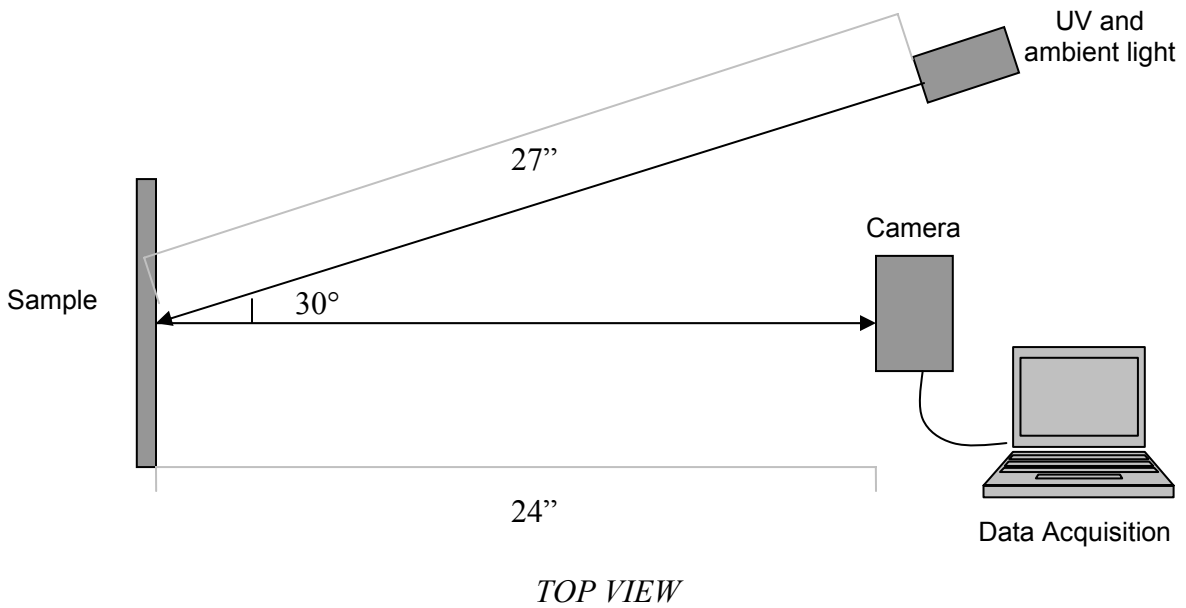
Figure 2.10 Schematic of Experimental Set-up

Following are the parameters and the conditions that were applied during the study of imaging experiments:

Table 4 Array of parameters used in imaging experiments

PARAMETER CATEGORY	VARIATIONS/ CONDITIONS
Image resolution	Small, Small interpolated, Medium, Medium interpolated, Large, Large interpolated
Samples	Vendor A-Additive X-0.5%-4 mils, Vendor B-Additive X-0.1%-4 mils, Vendor B-Additive X- Commercial- 4 mils
Lighting condition	Ultraviolet only, Ambient only, Ultraviolet with ambient
Ambient lights	Spot light, Halogen lamp, Diffused spot light, Diffused halogen lamp
Light intensity (lux)	50, 100, 200, 400, 800
Detector filters	No filter, UV filter, Blue filter, polarized filter
Ambient light filters	No filter, Orange filter

2.9   Development of Product Matrix:

To implement a vision system, it was needed to know precisely the objectives of the inspection process and the user requirements of the system. That makes it essential to understand the characteristics of the surface defects which the vision system will examine, as well as the specifications of the ballast tank. A typical vision system is made up of many components. Each component constitutes a link in the chain of successful machine vision application. A simple machine vision system might comprise the following:

- An optical sensor
- A digital camera
- Proper illumination
- A frame grabber
- Specific software for image processing

- Digital signal hardware or a network connection to report results

A compromise has to be reached between the system requirements and the objectives of the task to be accomplished. It was extremely important to analyze the proposed application and identify the process variables.

Preliminary studies and tests using a machine vision system indicated that such a system could be designed to satisfy the constraints of small size, limited required servo region, incorporation of an operator-assisted mode, and to provide a logical means of discriminating a target from its surroundings. Based on these preliminary findings, the following set of requirements was used as a guide for the machine vision system development:

1. The detection technology must

   - Resolve a 0.5 mm diameter void/discontinuity in the coating.

   - Distinguish between true coating discontinuity and surface irregularities caused by tank geometry, weld spatter, and irregular coating surfaces.

   - Be portable. It can be carried and operated by one person, and operated one-handed.

   - Be capable of assessing an area hidden from the line-of-sight of the assessor (e.g. behind a T-stiffener) or a 4"-8" wide swath.

   - Be used effectively by a certified coating inspector with less than 30 min additional training.

   - Provide an appropriate field-of-view to the operator who can barely see through his full face respiratory mask.

   - Require minimal maintenance and provide trouble-free operation.

2. The camera and supporting equipment

   - Be untethered and battery powered. If at all it is tethered, it should operate with 120 V AC supply.

   - Not employ hazardous materials or hazardous energy sources to ensure operational safety; particularly the UV light source and the operating procedures must be designed not to cause any eye or skin damage to the operator and paint applicators.

   - Be capable of rapidly acquiring and processing an image to avoid impeding the assembly process. Current rework time is less than 5%, but inspection time is 20%.

Chapter 3

Experiments

3.1 Introduction:

Machine vision applications all have one characteristic in common and that is to obtain feature information from the scene. The term used to describe this condition is contrast [18]. Contrast is created by variations in shades of grey or changes in color. The technique used to discern these changes is a function of the item to be analyzed, the optical sensor and the illumination. This chapter deals with the design of the laboratory experiments to deal with the factors to be considered when selecting the optimum illumination technique.

Most applications using machine vision requires some form of controlled lighting to obtain consistent data from an optical image. Where unstable illumination condition exists, the signal processing grows in complexity. This chapter will address various illumination techniques to enhance features, and in many cases, reduce the complexity of image processing.

3.2 Interaction of Objects with Light:

A visual sensor does not see an object but rather sees light as emitted or reflected by the object. Incident light can be reflected, front scattered, absorbed, transmitted, and/or backscattered [7, 18]. This distribution varies with the composition, surface qualities, and geometry of the object as well as with the wavelength of the incident light.

Control of lighting conditions implies the elimination of problems such as random fluctuations, unwanted gradation across the field-of-view, inadequate intensity, unhelpful coloration etc. which occur with ambient light. At a higher level it refers to the control of the position and intensity of the lighting source or sources so that the desired information within the scene can be highlighted and unwanted information, which unnecessarily complicates subsequent analysis, is suppressed.

3.3 Structured Lighting:

Although the goal of different lighting paradigms is the enhancement of contrast of particular object features, the goal of structured lighting is to yield direct 3D information about the object. The basic approach with structured lighting is to project a known (structured) pattern of light onto an object and then use the measured distortions in this pattern to calculate the 3D characteristics degree of the object's surface. The goal is to generate a degree of object radiance R_O for features of interest sufficient to produce an acceptable level of image irradiance I_C for a good image [6]. At the same time, for good contrast, the radiance of the background areas should be low. The irradiance I_O onto the object, interacts with the object's reflectivity characteristics (R) to generate an effective object radiance R_O seen by the sensor I_C. The range of R_O values required for an acceptable image is determined for the most part by the location of the sensor, its sensitivity, and the imaging optics. To yield the required irradiance I_O onto the object, a specific lighting design is developed that will produce the desired distribution of R_S over the $\hat{i}$ with respect to the feature's location and orientation.

3.3.1 Front illumination:

Frontlighting techniques are utilized when surface features [18], rather than object outlines, are imaged. Frontlighting is also used when backlighting is impractical. The purpose is to flood the area of interest with light such that the surface characteristics will act as the defining features in the image.

3.3.2 Specular Illumination (Darkfield):

Darkfield lighting is used in applications where surface defects such as pits and scratches are to be detected. The light striking a specular or mirror type surface reflects off at an angle that is equal to or opposite to the incident ray. The only illumination that is returned to the sensor, when it is positioned at an angle other than the reflection angle, is scattered energy from the perturbation in the surface. For flaw free surfaces, very little light is diffused and scattered upward to the camera, so the surface appears dark. Any abrupt change in the surface height (e.g.

the presence of a flaw) causes a localized point of reflection and increases the amount of light scattered to the camera, thus facilitating detection of a defect.
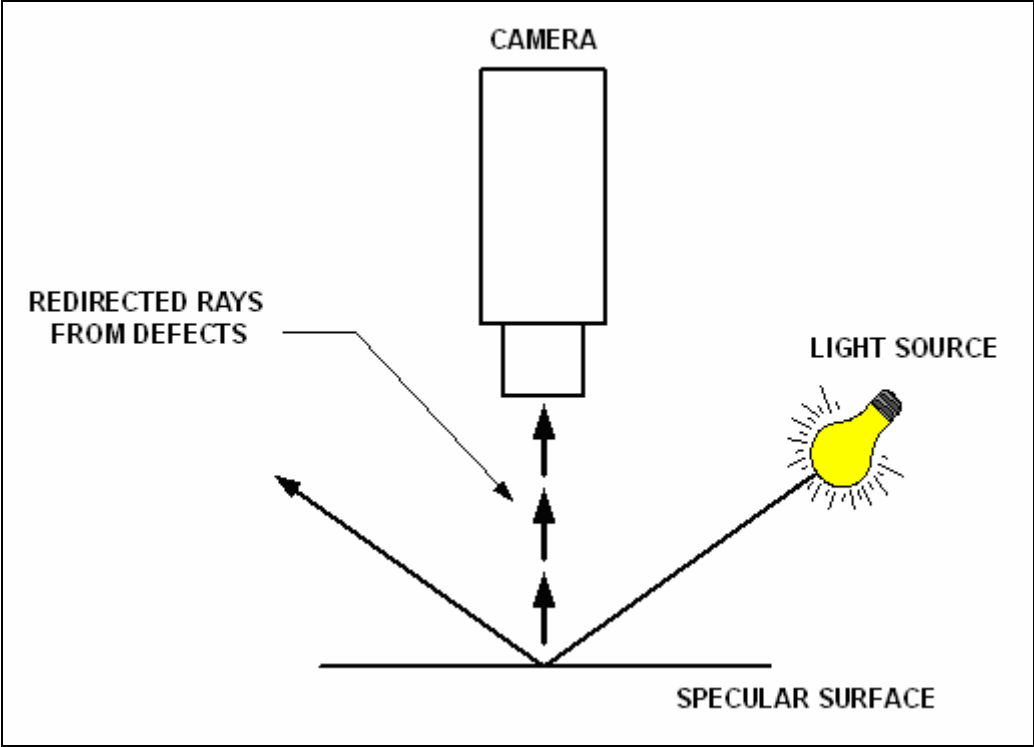

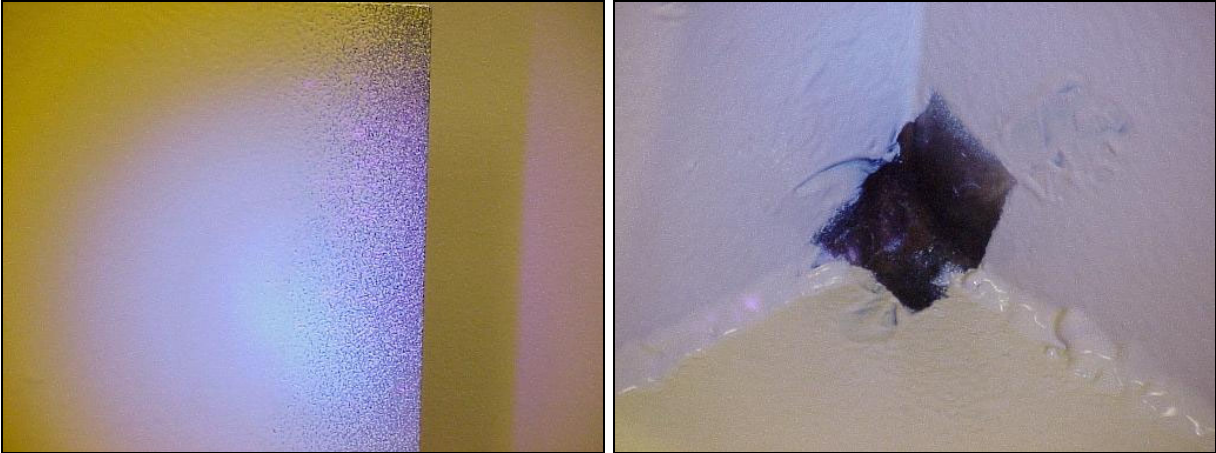**Figure 3.1 Schematic showing Darkfield illumination technique**

Figure 3.2 Sample images of surface defects observed under darkfield illumination

3.3.3   Specular Illumination (Brightfield):

This uses the same principle as Darkfield; however, the sensor is positioned in line with the reflected ray [18]. The angle of lighting is determined primarily by the height of the surface features to be detected.   The higher the feature, the larger the angle can be; the smaller the feature height, the shallower the angle must be. The camera is located at the opposite reflection angle. The only time no reflected light returns to the camera is when there is a deformity in the specular surface that scatters the light away from the reflected light. The uniformity of illumination is very important when using this technique, since the defect contrast may be small with respect to the entire output signal amplitude.
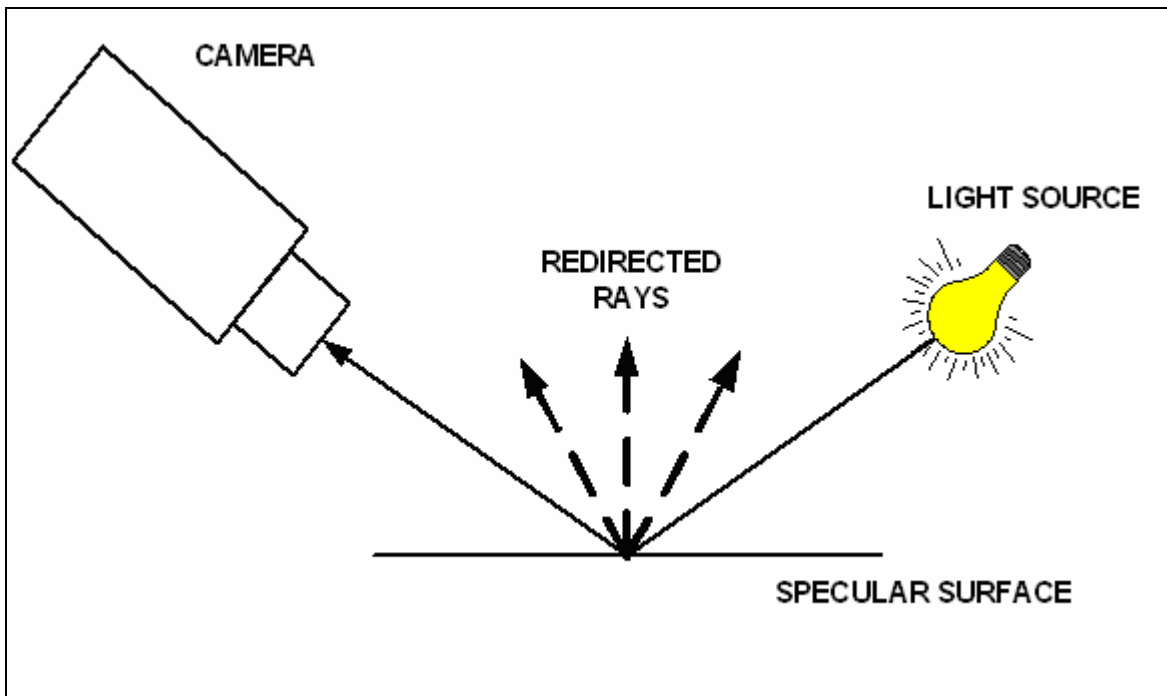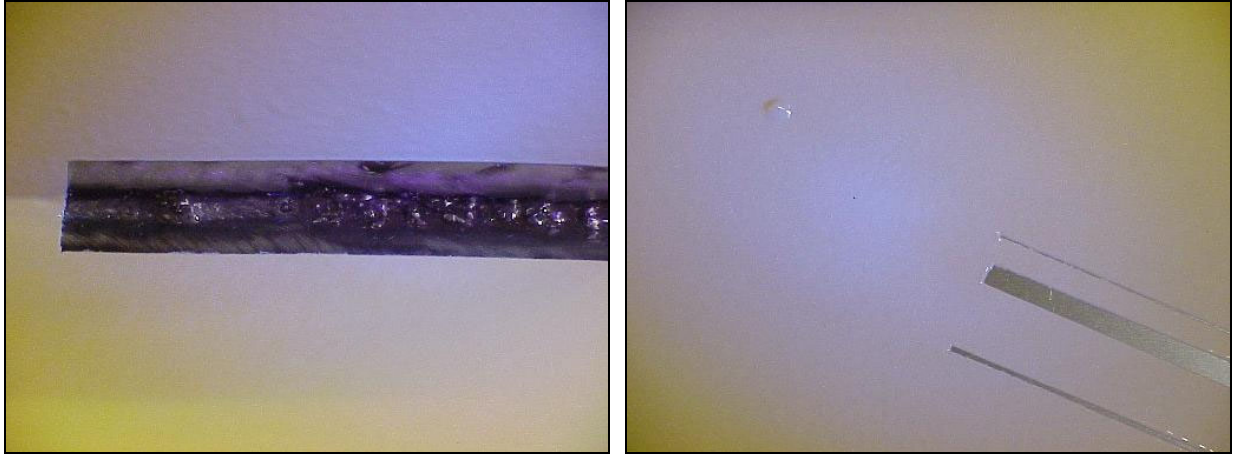

Figure 3.3 Schematic showing Brightfield illumination technique

Figure 3.4 Sample images of surface defects observed under brightfield illumination

3.4   Design of Experiments:

The design of experiments is a set of experimental study based on human visual color interpretation, operating in the spectral bandwidth of 450nm to 650 nm. Visual imaging data is collected using a high-resolution digital color camera that makes possible to observe different surface irregularities (defects and holidays). This data can be further analyzed and can be collaborated as a technique for automated paint inspection and evaluation.

The experiments demonstrate the use of optical filters used with the imaging system, the illumination system, or both. Their primary task is to enable the vision system to detect colors, to improve the contrast of the image, or simple to protect the camera lens.

Following is a set of laboratory experiments that were conducted to study the combined effect of ambient light, ultraviolet light, optical filters, and diffusers on the appearance of the image and the image processing capabilities to detect the smallest surface defect:

1. Study the effect of ambient light and optical filters on drawdown and sprayed samples.
2. Study the effect of room light, camera flash light and optical filters on drawdown samples.
3. Study the effect of variable illumination of ambient light and presence of spot light.
4. Compare the effect of room daylight, industrial light and spot light on paint surface appearance of drawdown, sprayed and 3D paint samples.

3.4.1 Study the effect of ambient light and optical filters on drawdown and sprayed samples:

Ambient or surrounding light plays a significant role in machine vision applications and has to be considered in the experimental set-up to simulate conditions similar to that in ship ballast tanks. The ballast tanks are equipped with significant amount of white/halogen light that helps inspector during the inspection process. To study, what affect the white light can have on the appearance of the image, we conducted some experiments. The following observations summarize the optimum lighting conditions and the combination of optical filters that would produce the best image for processing.

The white light used in these experiments is a silver back-coated bulb of 30 W. Also, a blue optical filter that fits over the digital camera and a orange gelatin filter that fits over the bulb are used. With these parameters in consideration, the following images are recorded.

3.4.1.1 Drawdown Samples

(a)   (b)
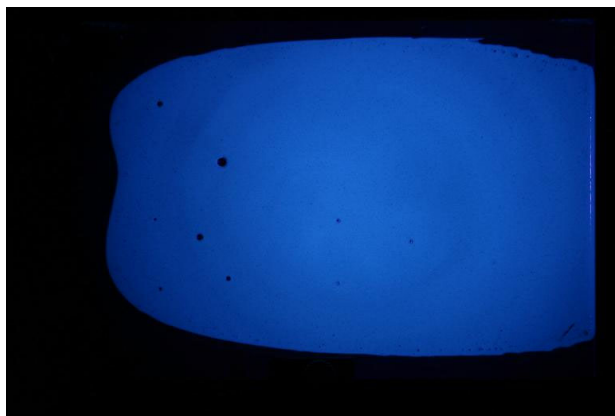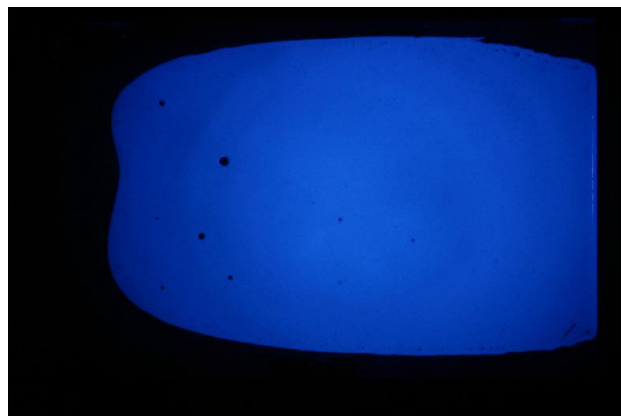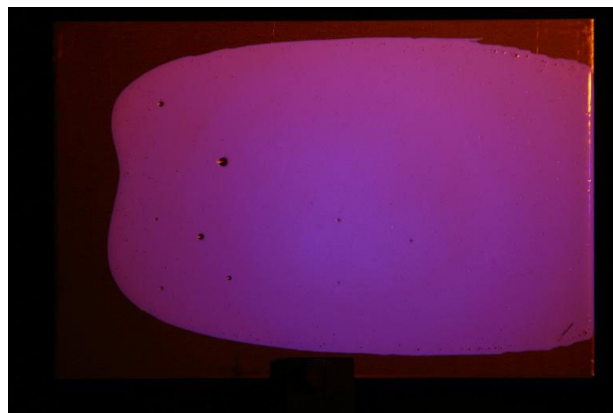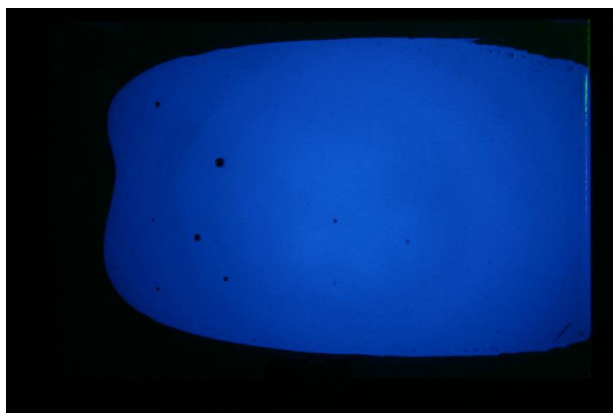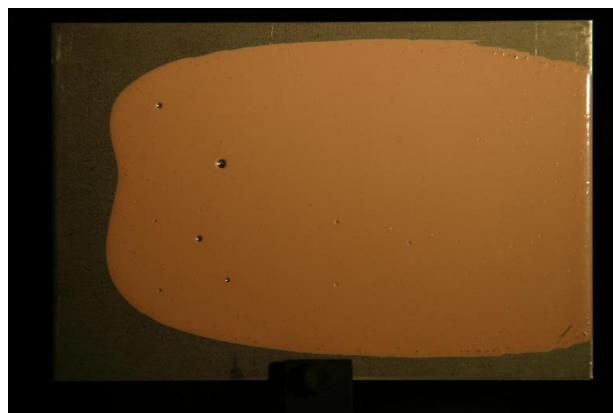
Figure 3.5 Drawdown sample from Vendor A with 0.5% loading of Additive X observed under (a) UV light only (b) UV light only with blue filter over the camera (c) UV and white light (d) UV and white light with orange filter (e) UV and white light with orange filter, blue filter over the camera (f) white light only (g) white light with blue filter over the camera (h) white light with orange filter over the camera
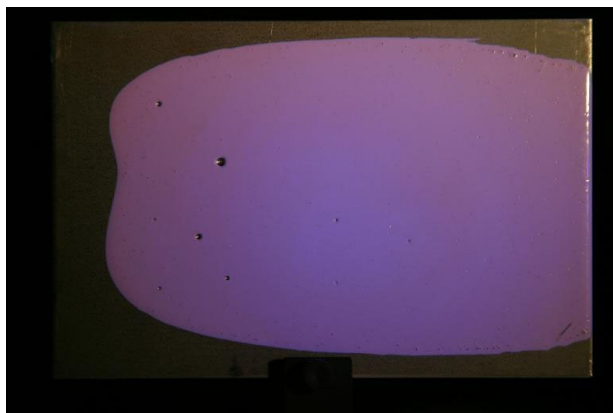
3.4.1.2 Sprayed Samples

(a)

(b)

(c)

(d)

(e)

(f)

| (g) | (h) |

Figure 3.6 Sprayed sample from Vendor A with 0.5% loading of Additive X observed under (a) UV light only (b) UV light only with blue filter over the camera (c) UV and white light (d) UV and white light with orange filter (e) UV and white light with orange filter, blue filter over the camera (f) white light only (g) white light with blue filter over the camera (h) white light with orange filter over the camera

3.4.1.3 Observations:

- The visual appearance and the behavior (excitation wavelength) of drawdown and sprayed samples is almost the same irrespective of the ambient light and the filters used.

- The best contrast between the defects and the background, that would also simplify the image processing, is obtained with a combination when white light with orange filter is used wi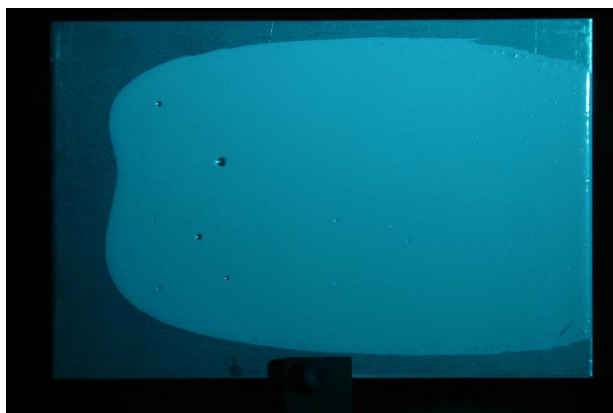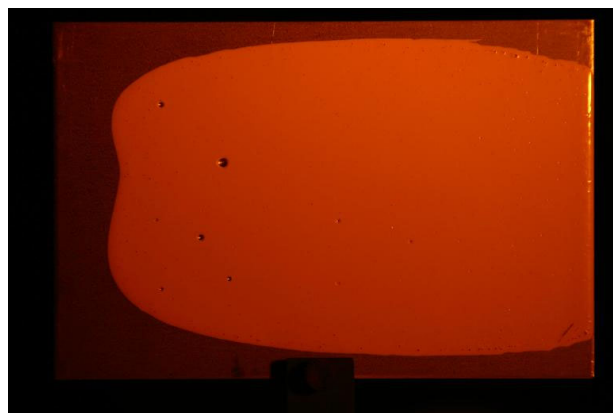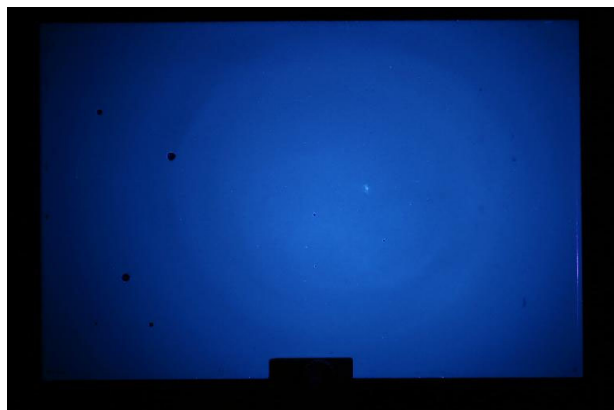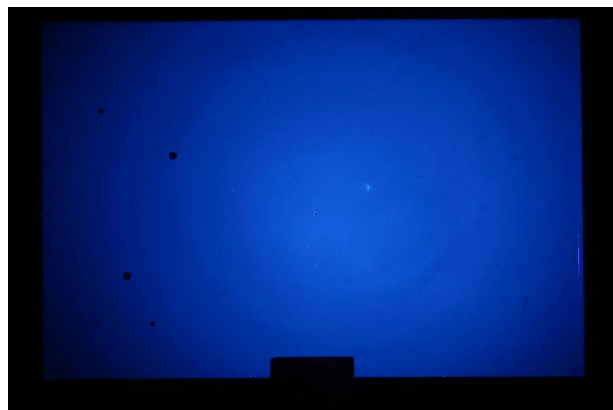th UV light and a blue filter over the camera (Figure 4.5(e) and 4.6(e)). This observation is also supported by corresponding spectroscopic results.

- With no ambient light present, the presence of blue filter over the camera can hardly be justified (see Figure 4.5 (b) and 4.6 (b)), the reason being the absence of any other wavelength other than the excited wavelength of light.

- With no blue filter over the camera, and with UV and white light present, the wavelength of light falling on the camera sensor is shifted more in the purple region of visible spectrum of light (see Figure 4.5 (d) and 4.6 (d)).

- Finally, with no UV light present, there is no excitation of fluorescent additive and contrast between the defects and the background is not sufficient enough to detect the defects (see Figure 4.5 (f), (g), (h) and 4.6 (f), (g), (h)).

- Image comparison is done on the basis of smallest visible defect, absence of false positives and shadows, and the best contrast achieved.

3.4.2 Study the effect of room light, camera flashlight and optical filters on drawdown samples:

Camera flashlights have an UV component present in their spectrum. The following experiments were conducted to study if the camera flash light is sufficient enough to excite the optically active additive in the paint samples and produce a better contrast between the defect and the background. This might eliminate the need of a separate UV source and make the design much simpler. In addition to this, two additional filters, an orange filter on the camera and a blue filter over the white ambient light were also tested with to study their combined effects on the paint appearance. Paint samples from two different vendors were used and the results are documented.

| (a) | (b) | (c) |
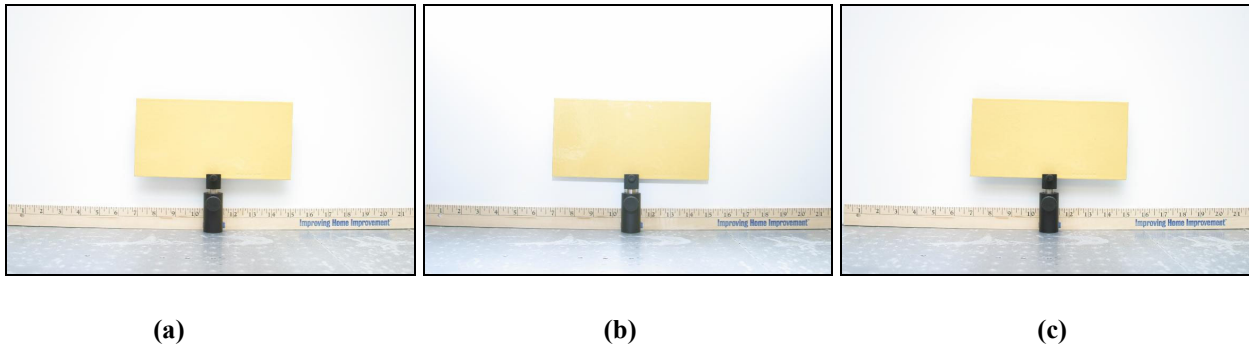
Figure 3.7 Sprayed sample for Vendor A with 0.1 % loading of Additive X observed under (a) direct camera at 45 deg. to the normal (b) direct flash at 90 deg. to the normal (c) Indirect flash not facing paint surface.
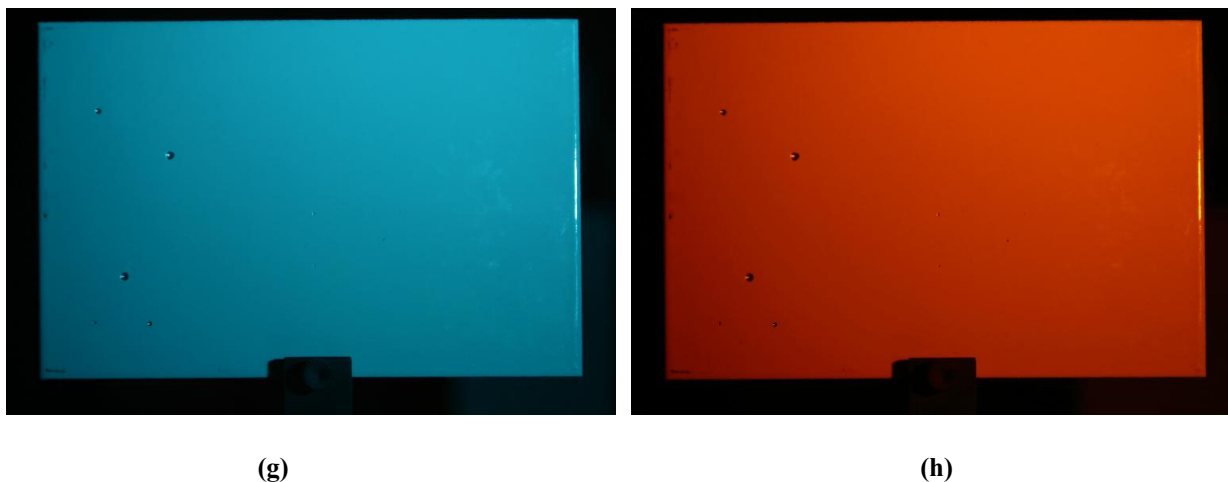
(a)   (b)   (c)

Figure 3.8 Sprayed sample for Vendor A with 0.1 % loading of Additive X observed under (a) Room light only (b) Room light and white light with orange filter (c)UV and white light with orange filter, blue filter over the camera. No other light (room light) other that white light was present.

(a)   (b)   (c)

Figure 3.9 Sprayed sample for Vendor A with 0.1 % loading of Additive X observed under (a) UV and white light with orange filter (b) UV light with blue filter, white light with orange filter (c) white light with orange filter over the camera. No other light (room light) other that white light was present.
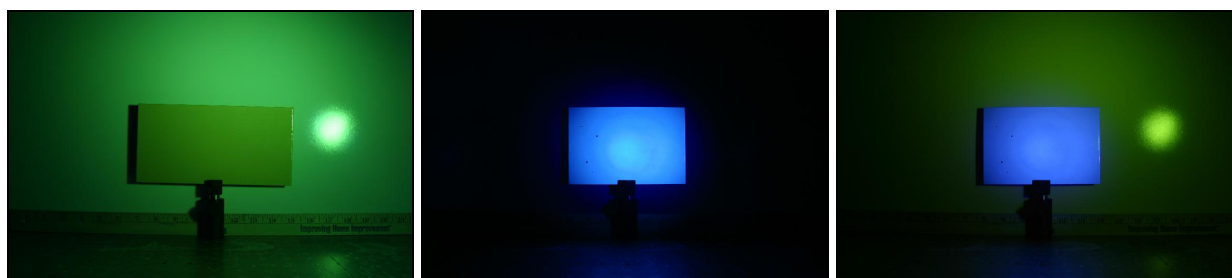
(a)   (b)   (c)

Figure 3.10 (a) Sprayed sample for Vendor A with 0.1 % loading of Additive X observed under white light with orange filter, blue filter over the camera; Sprayed sample for Vendor B with 0.5 % loading of Additive X observed under (b) UV light only (c) UV and white light with orange filter, blue filter over the camera.

45

(a)	**(b)**	**(c)**

Figure 3.11 Sprayed sample for Vendor B with 0.5 % loading of Additive X observed under (a) UV light with UV filter over the camera (b) UV light with blue filter over the camera (c) UV light with UV filter and white light with orange filter. No other light (room light) other that white light was present.
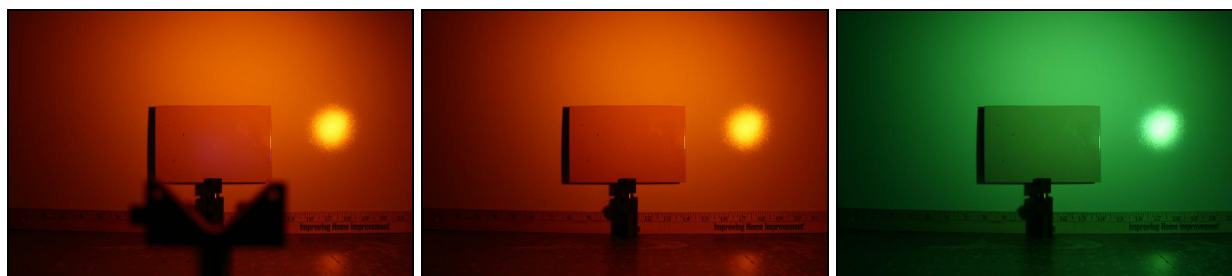
(a)	**(b)**	**(c)**

Figure 3.12 Sprayed sample for Vendor B with 0.5 % loading of Additive X observed under (a) white light only and with orange filter over the camera (b) white light only with orange filter (c) white light with orange filter and blue filter over the camera. No other light (room light) other that white light was present.

3.4.2.1   *Observations:*

The images reveal a lot of data and help answer some intricate problems related to visual imaging.

- Firstly, the assumption that the UV component in the camera flash light might be sufficient enough to excite the fluorescent pigment, could not be proved since the flash was too bright to saturate the pigment and made hardly possible to detect the defects.
- A comparison of light emission properties from two different vendors was made.

- Another objective of these experiments was to verify the maximum area that can be covered without compromising the smallest defect detection. It was observed that an area of 22" x 12" can be covered.

- However, in achieving this, it was hard to eliminate the spot light reflection effect that would make the processing more complicated.

- Another drawback of the system is that the UV light source limited the maximum area to be inspected because of a collimated beam.

- Again, the contrast between the defects and the background is more significant with a combination of UV and white light with an orange filter over the white light and a blue filter over the camera.

3.4.3 Study the effect of variable illumination of ambient light and presence of spot light:

As noted in the previous set of experiments that the ambient light plays an important role in deciding the image processing algorithms, we performed more experiments to investigate the approximate ambient light intensity, a parameter that will be controlled in the actual ballast tank for the vision system to work efficiently. While doing so, care was taken to keep the percent loading of the fluorescent additive constant and also the paint film thickness. The spot light used to simulate the ambient light effect was a 40 W, silver coated bulb. Also, the samples from only one vendor were tested to counter any variation in paint properties. Sample images were captured for 50 lux, 100 lux, 200 lux, 400 lux and 800 lux ambient light.
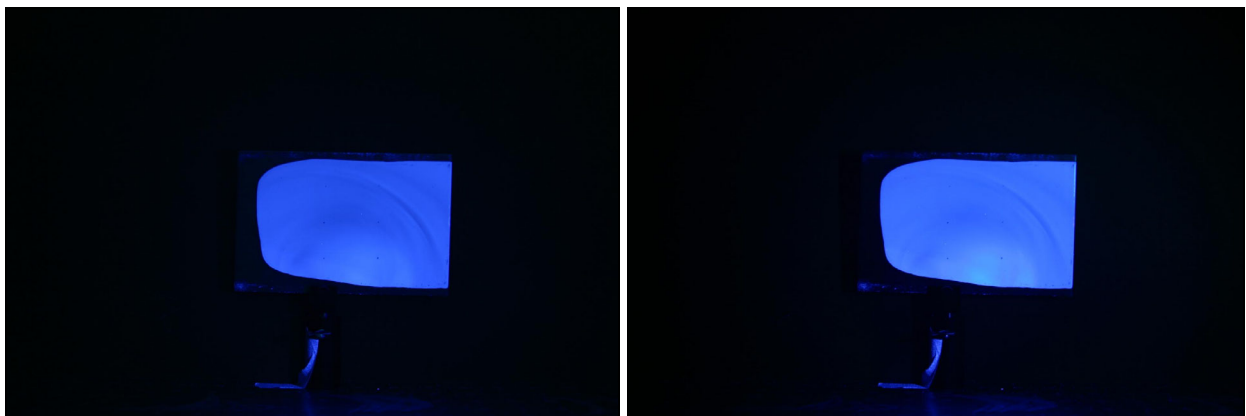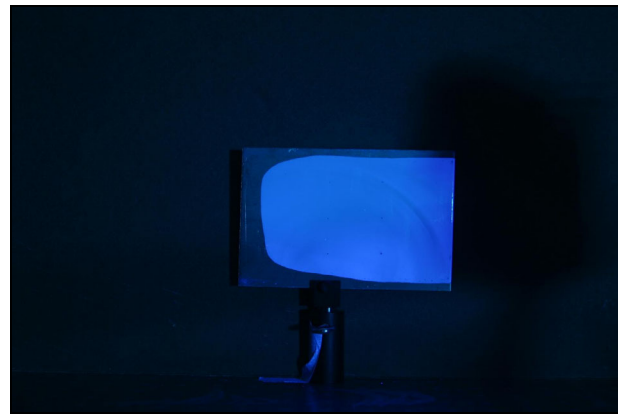
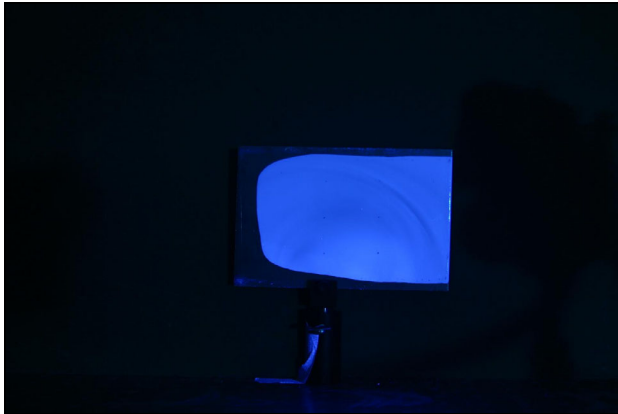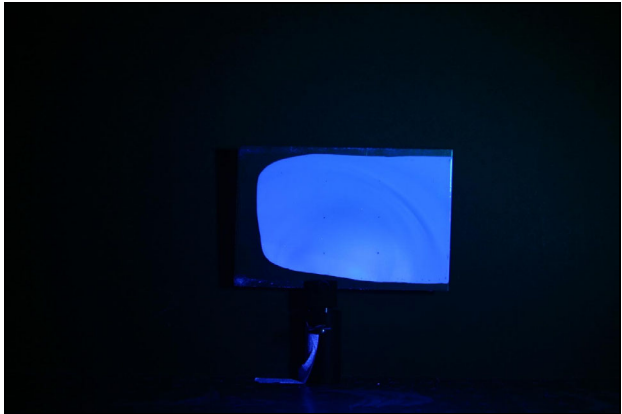<div align="center">(i)   (j)</div>

Figure 3.13 Drawdown sample from Vendor B with 0.5% loading of Additive X observed under UV light (a) 50 lux of ambient light and no spot light (b) 50 lux of ambient light and spot light (c) 100 lux of ambient light and no spot light (d) 100 lux of ambient light and spot light (e) 200 lux of ambient light and no spot light (f) 200 lux of ambient light and spot light (g) 400 lux of ambient light and no spot light (h) 400 lux of ambient light and spot light (i) 800 lux of ambient light and no spot light (j) 800 lux of ambient light and spot light

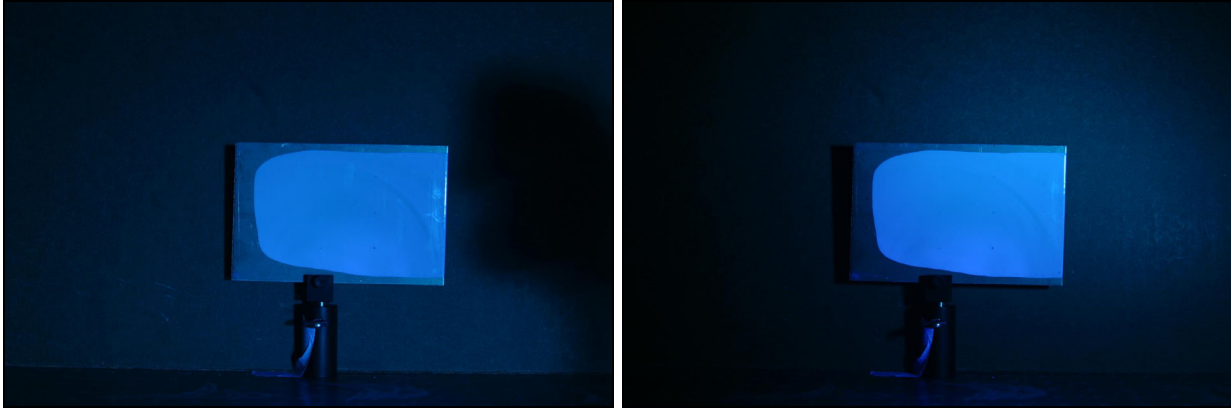### *3.4.3.1 Observations:*

- The UV source was a collimated light beam of varying intensity. It was more concentrated at the center and its intensity decreased in the outward direction.

- This would not excite the fluorescent additive uniformly over the paint area under consideration, producing concentric ring pattern, thus making it hard to detect pinhole defects. This effect was more dominant in the absence of ambient light (Figure 4.13 (a), (c), (e), (g), (i)).

- Ambient light helps in uniformly illuminating the paint sample thus eliminating the need to design complex image processing algorithms.

- The effect of ambient light can be seen prominently as the intensity increases from 200 lux to 800 lux. The best results are produced with 400 lux of ambient light.

- Again, the difference between the area illuminated by UV and white light limits the area under inspection.

- The experiments also emphasize the need for structured lighting geometry to eliminate the effect of shadows produced in the field of view as can be seen in Figure 4.13 (g) and (i).

3.4.4 Compare the effect of room daylight, industrial light and spot light on paint surface appearance of drawdown, sprayed and 3D paint samples

Prior to testing the prototype in the field, there was a need to decide on the artificial ambient light conditions that would be incorporated in the prototype. It was also essential to know beforehand the exact behavior (intensity) of daylight that might interfere in the image acquisition process. Following experiments show a comparative study of industrial light and spot light. Another objective of these experiments is to understand the change in fluorescence emission in relation to paint film thickness. An attempt has been made to keep the combined light intensity constant that is incident over the sample.
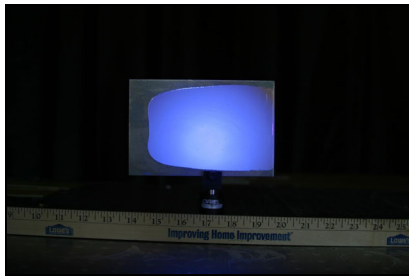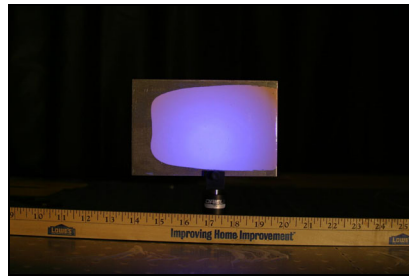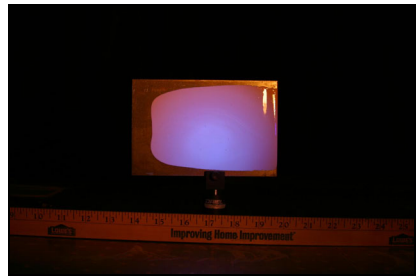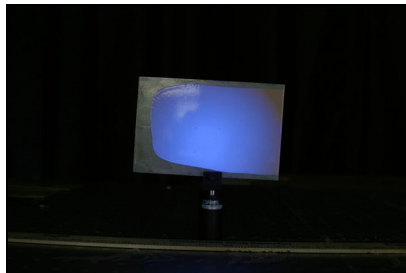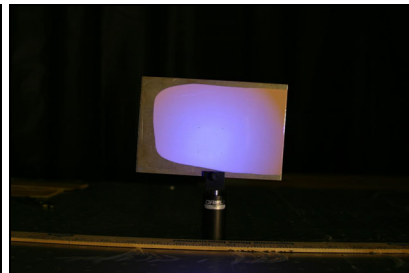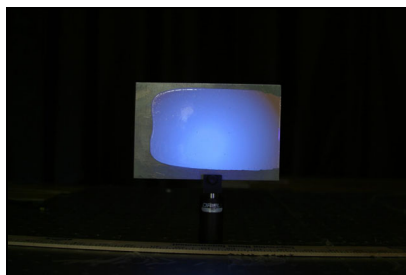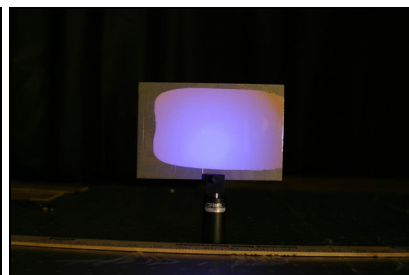
(a)	(b)	(c)
(e)	(f)	(g)
(g)	(h)	(i)

Figure 3.14 Drawdown sample from Vendor B with 0.5% loading of Additive X observed under UV light and (a) 200 lux daylight; 4 mil DFT sample (b) 400 lux industrial light; 4 mil DFT sample (c) 400 lux spot light; 4 mil DFT sample (d) 250 lux daylight; 6 mil DFT sample (e) 400 lux industrial light; 6 mil DFT sample (f) 400 lux spot light; 6 mil DFT sample (g) 200 lux daylight; 8 mil DFT sample (h) 400 lux industrial light; 8 mil DFT sample (i) 400 lux spot light; 8 mil DFT sample
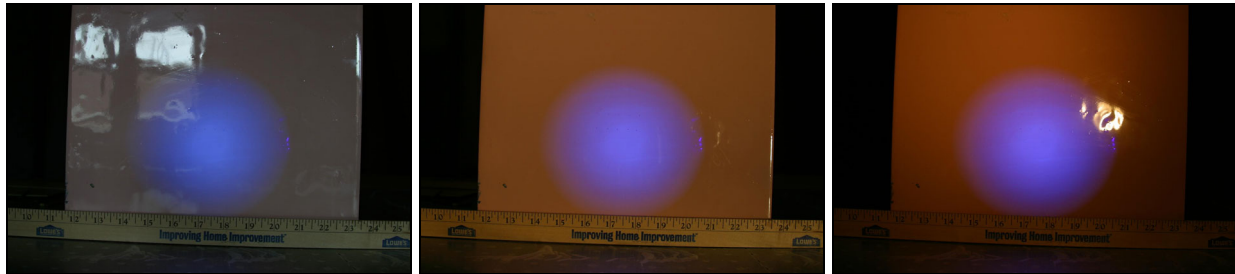
| (a) | (b) | (c) |

Figure 3.15 Drawdown sample from Vendor B (commercial) with Additive X observed under UV light and (a) 300 lux daylight; 25 mil DFT sample (b) 400 lux industrial light (c) 400 lux spot light
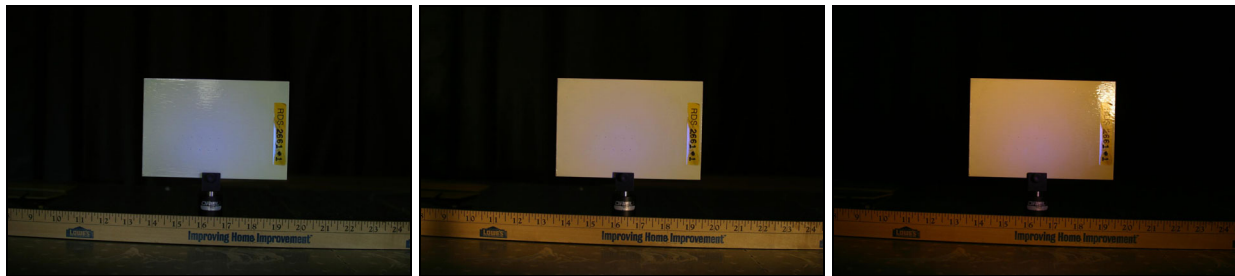
| (a) | (b) | (c) |

Figure 3.16 Sprayed sample from Vendor C with Additive X observed under UV light and (a) 200 lux daylight (b) 400 lux industrial light (c) 400 lux spot light
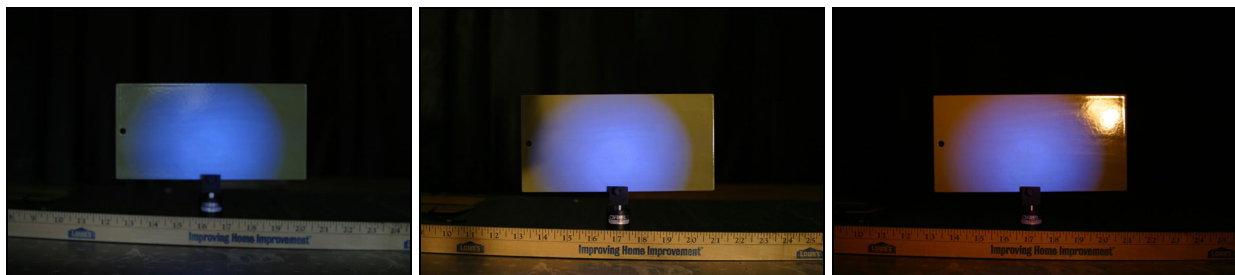
| (a) | (b) | (c) |

Figure 3.17 Sprayed sample from Vendor D with Additive X observed under UV light and (a) 200 lux daylight; 15 mil DFT sample (b) 400 lux industrial light (c) 400 lux spot light

51
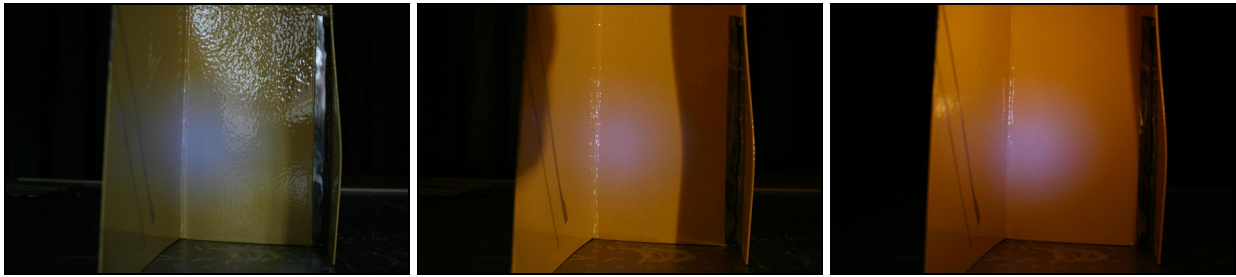
Figure 3.18 T-section from Vendor A with Additive X observed under UV light and (a) 200 lux daylight (b) 400 lux industrial light (c) 400 lux spot light. The T-section sample is painted with the commercial percent of additive that cannot be published due to propriety reasons.

3.4.4.1   Observations:

- Fluorescence emission increases in direct proportion to the paint DFT. This observation is also supported from the spectroscopic results.

- 200 lux of daylight does not have much effect on the fluorescence emission property of the paint. However, the 4 mils sample shows a better contrast under daylight conditions as compared with 6 and 8 mils (Figure 4.14 (a), (e), and (g)).

- Use of spot light produces a source reflection in the image field-of-view that interferes with the fluorescence emission. So the effective area under inspection is reduced (Figure 4.14 (c), (g), and (i)). The reflection is eliminated using a diffuser instead of direct light.

3.5 Prototype Development:

After a series of laboratory experiments, there was a need to design and fabricate a prototype that could be capable of gathering preliminary field results. The efforts were directed in consolidating the basic machine vision components viz. the high end digital camera, a collimated UV light source, a white light source and a light diffuser, all fabricated with the help of poly-vinyl chloride (PVC) pipes and steel plates. The light controlling experiments described earlier in this chapter, helped to decide the specifications of an optimum image in terms of quality, area covered, smallest defect size, and image size. Moreover, the results obtained from the spectroscopy experiments supported in the development of the prototype. Because of the time constraint, most of the components are off-shelf items and a few were fabricated in-house. Following data was gathered from the light controlling and spectroscopy experiments, which helped in the development of the prototype:

- Distance of detector/ camera from sample: **24"**
- Distance of UV light and ambient light from sample: **27"**
- Angle between light assembly and detector/camera: **30°**
- Image size: **24" x 18"**
- Prototype optimized for: **Additive X**
- Prototype optimized for : **0.5% loading or less**
- Ambient light used**: 40 W Spot light (Light C in spectroscopy experiments)**
- Preferred filter for ambient light: **Orange**
- Preferred filter for detector/ camera: **Blue**

The main components used in the prototype fabrication are listed in the table below:

Table 5 Raw material used in prototype

Description	Quantity
Hot rolled mild steel plate 3.25" x 4.75"	1
Hot rolled mild steel plate 5" x 6.5"	1
90° elbow joint for 1" diameter PVC pipe	8
45° elbow joint for 1" diameter PVC pipe	1
T-joint for 1" diameter PVC pipe	3
2" steel pipe holders	3
1" PVC pipes 4.5" long	4
1" PVC pipes 2" long	2
1" PVC pipes 5.5" long	2
1" PVC pipes 5" long	1
End cap for 1" PVC pipe	1
Locking nut for reflector	1

- *Camera mounting plate*
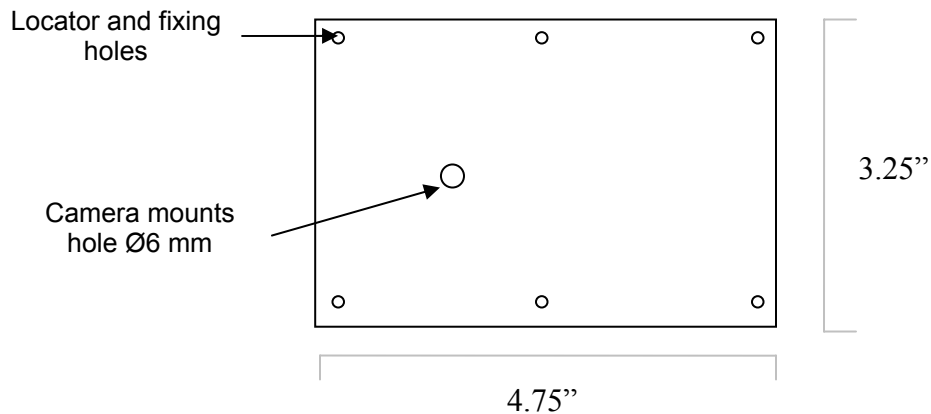
Figure 3.19 Camera mounting plate for prototype

- *Lamp mounting plate*
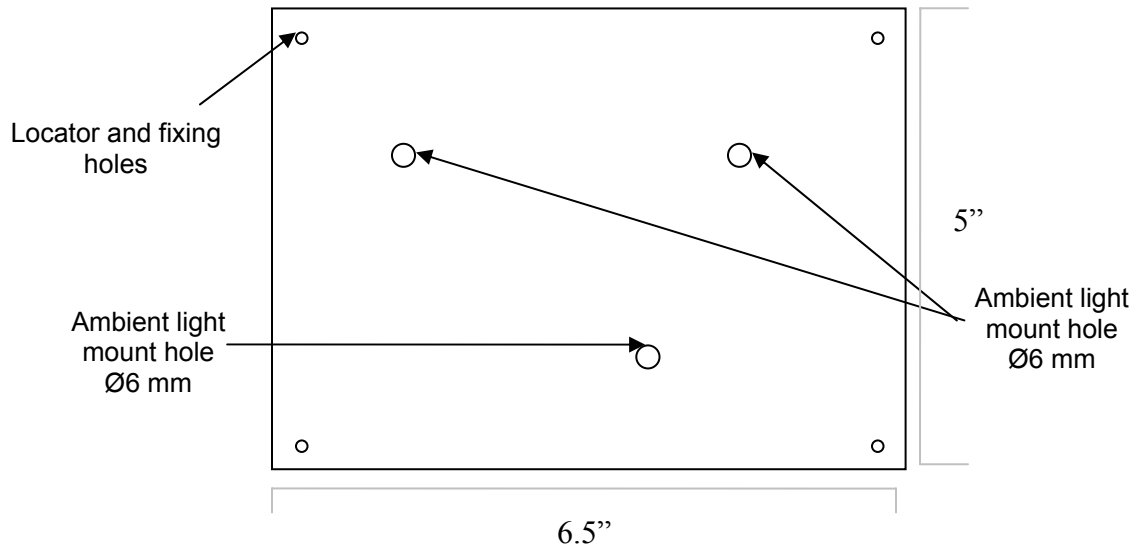
Figure 3.20 Lights mounting plate for prototype

- *Holding rod:* Made from PVC pipe and padded with foam to make it more ergonomic to hold. The length of rod is 5"
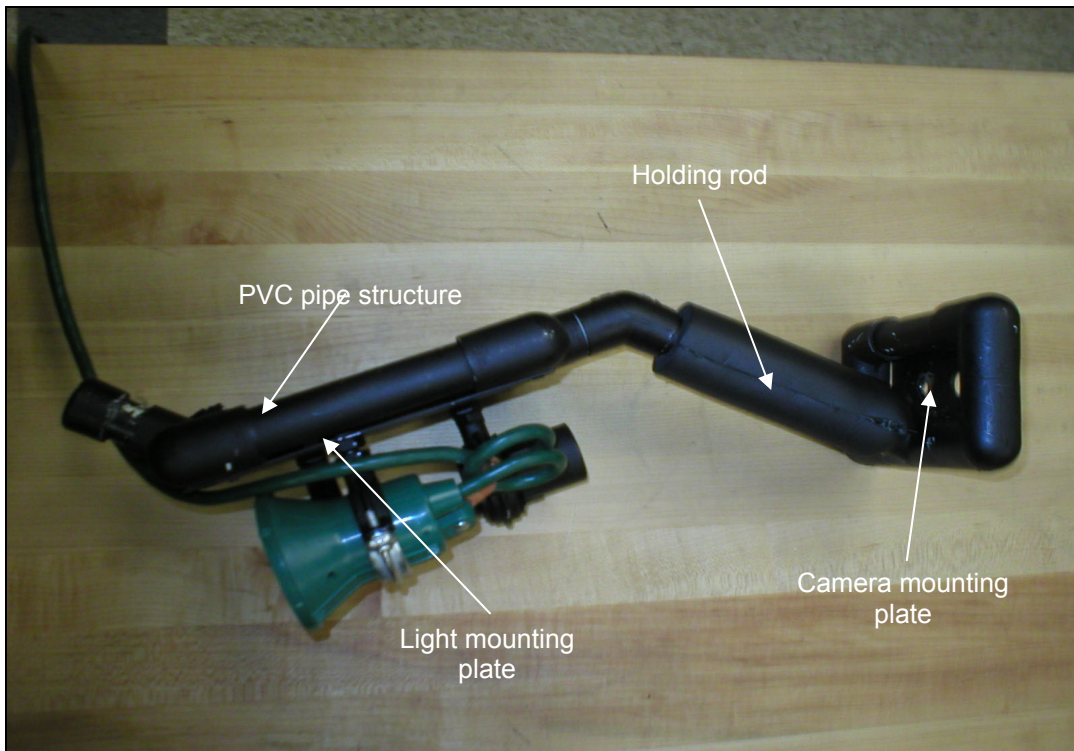
Figure 3.21 PVC structure made for the prototype

- *PVC structure*: PVC structure was fabricated using PVC pipes of 1" in diameter, T-joints, elbow joints and locking nut. The pipes were cut to the desired size and glued together with the joints.
- *Pipe holders:* The pipe holders were used on the light mounting plate to hold the ambient light and the UV lamp

All the fabrication of plates which included cutting, drilling and assembly was completed in-house

3.5.1 Prototype geometry

The basic aim in the prototype design was to keep the angle between the camera and the reflected UV light 30°. The final design which maintains this angle is represented in the schematic below.
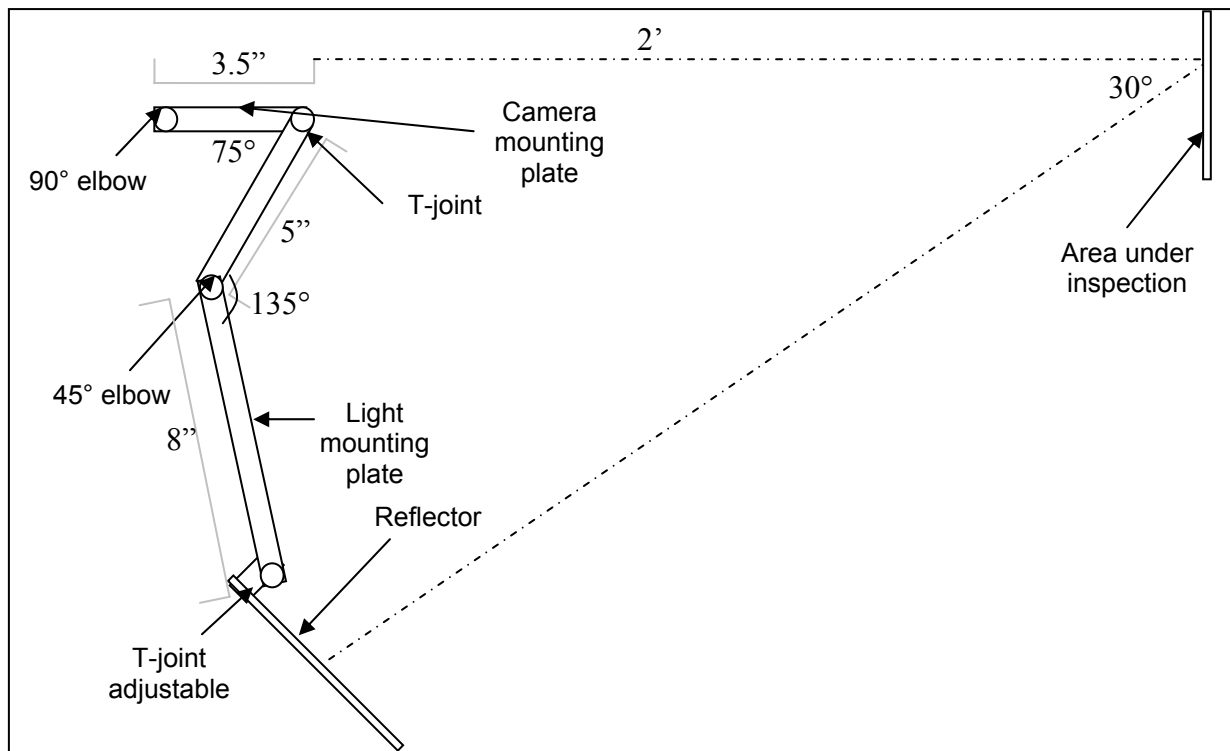
Figure 3.22 Schematic of prototype design

The other dimensions of the PVC pipes and the plates were decided according to the dimensions of the light sources and the digital camera. An effort was made to keep the weight of the prototype minimum and ease of usability maximum within the cost and geometric constraints.

Chapter 4

Image Processing Results

4.1 Attributes of machine vision system in surface inspection:

The chapter describes the applicability of image processing algorithms to paint surface defects of ship ballast tanks. Visual inspection along with low-voltage wet sponge pinhole detector are been widely used methods for inspection of anti-corrosion coatings [18]. So far we discussed experiments testing image understanding algorithms as an aid to visual inspection by enhancing and recognizing surface cracks and corrosion through addition of fluorescent additives in paints and observing under ultra violet light. We will discuss the performance of three image processing techniques viz. color image processing, region growing and image thresholding, and check their efficiency in detecting different surface defects. Also, a comparative study of the three techniques based on the surrounding light conditions is illustrated.

The first and most critical component of a machine vision system is illumination. Complete control of light is essential for reliable operation [20]. The type of light source and how it is applied to illuminate the scene affects all subsequent processing. Careful application of light to a scene can transform the vision task from seemingly impossible to trivial. Formation of an image of the scene on the surface of a sensing device is the next step. Image formation is performed with optical devices such as lenses, prisms and mirrors. Sensing is carried out with solid state devices that convert the light image into a proportional analog voltage image.

Because further processing will be done with digital hardware, the analog voltage must be converted into a digital image. A digital camera performs the formation, sensing and subsequent conversion of the analog voltage into a digital image [21, 22]. The result of this conversion is simply a two-dimensional array of data values (pixels) stored in the memory. Each pixel value represents the luminous intensity of a small area of the imaged scene. The size of the array determines the spatial resolution of the image and the number of gray level possible for each element determines the luminous resolution.

Enhancement of the raw acquired image is the goal of image processing. It takes an input image and produces an output image but this image is easier to process by the following stages. Enhancement is achieved by filtering noise or other unimportant data from the image. The segmentation process reduces the voluminous image data to the regions important to the vision task. Regions can be either statically or dynamically determined. In the static case, fixed windows in the image determine the areas of interest. Dynamic regions are separated from the image by either edge or connectivity relationships [26]. Measurements made on the segmented regions further reduce the data to features. Extracted features are either geometric or luminous. The interpretation process takes the extracted features and determines the systems response to the acquired image. Features can be simply compared against limits to make pass-fail decisions. Relationships between features of any regions in the image may be needed to recognize or sort objects.

4.2   Role of image segmentation in vision system:

When a human observer views a scene, the visual system processing that takes place essentially segments the scene for him [18]. This process is so efficient, that a person does not see a complex scene, but rather a collection of objects. With digital systems, holistic image analysis requires information to be extracted once the appropriate preprocessing steps of various filters are completed. In order to accomplish this, a digital image must be segmented, or partitioned into its constituent parts or objects. The segmentation process can also be viewed as separating the image into disjoint or non-overlapping regions [23]. Here a region is defined by a connected set of adjacent pixels. To be connected, a traceable path between any two pixels must be possible without ever leaving the set.

The principal objective of image segmentation process is to partition an image into meaningful regions which correspond to part of, or the whole of, objects within the scene. This is done by systematically dividing the whole image up into its constituent areas or regions. If the regions do not correspond directly to a physical object, or object surface, then they should correspond to some area of uniformity as defined by some predetermined assertion, or predicate.

(a)

(b)

(c)

(d)
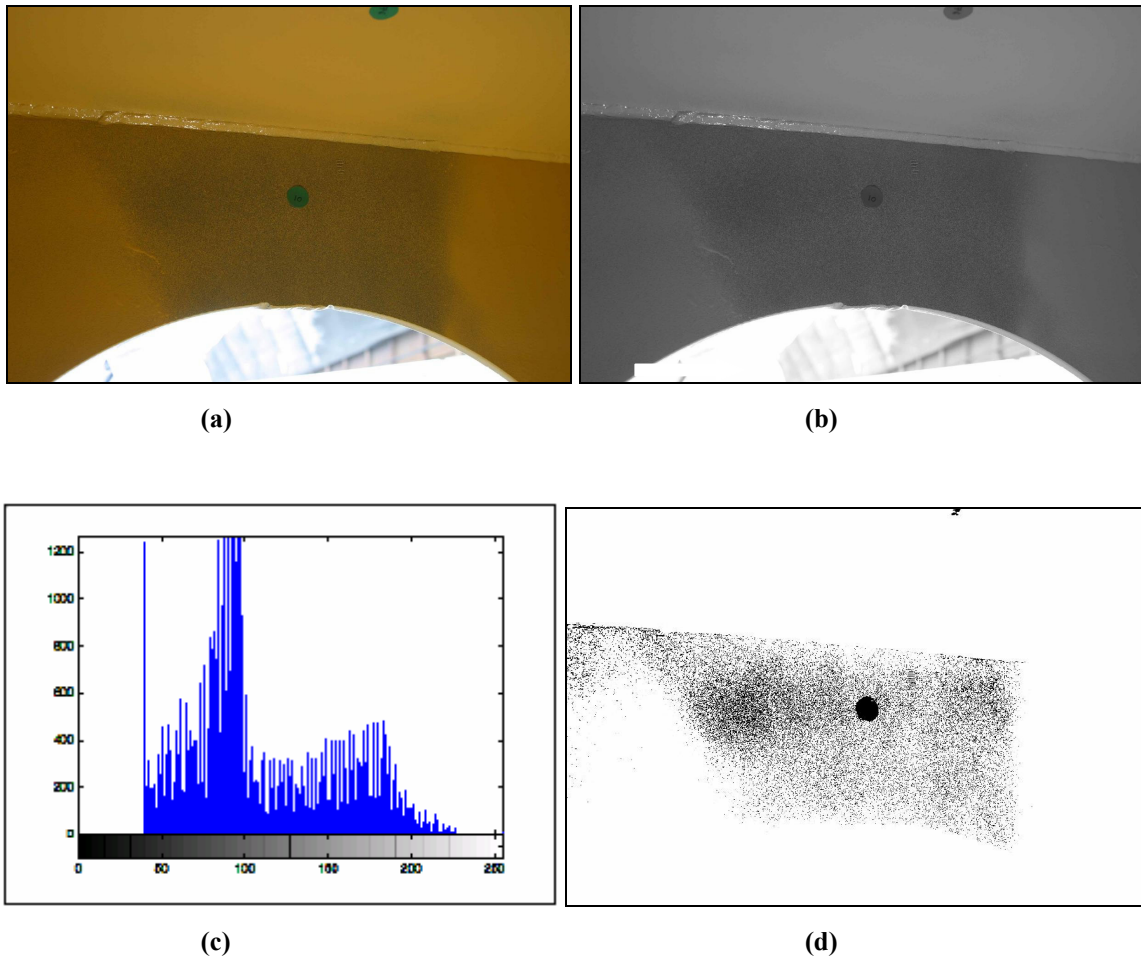
Figure 4.1 Illustration of Image Segmentation (a) Original RGB Image (b) Grey Scale Image

(c) Image Histogram (d) Segmented Image shows area of surface defects

The subdivision process should cease when all regions of interest have been identified and no further subdivision should occur. This may be easy to achieve in certain controlled applications where the outcome of segmentation is well defined (visual inspection) but it is very difficult in applications where the outcome is not known (robotic guidance). In all cases the extent to which the segmentation process is carried out will depend on the particular problem to be solved.

There is no theory of image segmentation. As a consequence, no single standard method of image segmentation has emerged. Rather, there are a collection of ad hoc methods that have received some degree of popularity. Unfortunately, no quantitative image segmentation performance metric has been developed. Segmentation has a unique position within the generic

59

model of a machine vision system as it forms the bridge between the low-level and the high-level processing operations. Low-level processing operates on image arrays of raw data and thus adopts a bottom-up, or data-driven approach to image analysis [32]. High-level processing is concerned with the manipulation of high-level, abstract data representations and thus favors a top-down, hypothesis-driven approach. Segmentation can employ either or both of these approaches.

There are two main approaches to segmentation:

a) Pixel-based or local methods;

b) Region-based or global approaches

These approaches are complimentary and should produce the same results, however in practice this is rarely the case. The pixel-based approach seeks to detect and enhance edges or edge elements within an image and then link them to create a boundary which encloses a region of uniformity. The region based approach seeks to create regions directly by grouping together pixels which share common features into areas or regions of uniformity.

4.3 Application of Image Processing Algorithms:

There are many defect detection algorithms published in the literature, and selecting an appropriate one is often a difficult task. The problem is that different algorithms typically produce different results since they make the different assumptions about the image content. For instance, the paint defects that we are going to define do not have a particular shape or size, nor do they show the same optical characteristics under different fluorescent additives. For the purpose of making the algorithms more straight forward, we have reduced the variation in the way the defects are defined and tried to categorize them under three different groups:

a) Missed areas or holidays

b) Weld defect usually found at the vertex of a welded joint

c) Under-millage defects like pinholes or areas that do not have a sufficient paint film thickness.

This chapter illustrates the application of three different image processing algorithms, depending on the type of the defect. Missed areas or holidays are detected using color image processing algorithm, the weld defects are detected using the principle of region growing, and

under-millage defects are solved using image thresholding. Each algorithm is described in detail along with illustrations.

4.3.1 Image Segmentation in RGB Vector Space:

An RGB color image is an M x N x 3 array of color pixels, where each color pixel is a triplet corresponding to the red, green and blue components of an RGB image at a specified spatial location [32, 33]. An RGB image may be viewed as a "stack" of three gray-scale images that, when fed into the red, green and blue inputs of a color monitor, produce a color image on the screen.

Color image segmentation using RGB color vectors is based on the theory of Euclidean distance between two points in color space. To objective is to segment objects of a specified color range in an RGB image. Given a set of sample points representative of a color (or range of colors) of interest, we obtain an estimate of the "average" or "mean" color that we wish to segment. Let this average color be denoted by the RGB column vector $\mathbf{m}$. The objective of segmentation is to classify each pixel in an image as having a color in the specified range or not. To perform this comparison, we need a measure of similarity. One of the simplest measures is the Euclidean distance. Let $\mathbf{z}$ denote an arbitrary point in RGB space. Then $\mathbf{z}$ is similar to $\mathbf{m}$ if the distance between them is less than a specified threshold, $\mathbf{T}$.
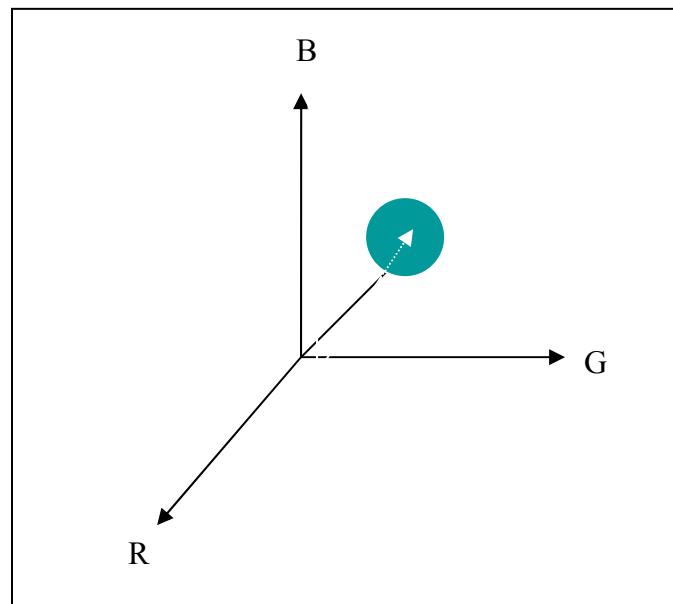

Figure 4.2 Illustration of Euclidean distance

The Euclidean distance between z and m is given by

$$D(z,m) = \|z - m\|$$

$$= \left[(z-m)^T (z-m)\right]^{1/2}$$

$$= \left[(z_R - m_R)^2 + (z_G - m_G)^2 + (z_B - m_B)^2\right]^{1/2}$$

where $\|\bullet\|$ is the norm of the argument, and the subscripts R, G, and B, denote the RGB components of vectors m and z. The locus of points, such that D (z, m) $\leq$ T, is a solid sphere of radius T. By definition, points contained within, or on the surface of, the sphere satisfy the specified color criterion; points outside the sphere do not.

The general equation of the Euclidean distance is of the form

$$D(z-m) = \left[(z-m)^T C^{-1} (z-m)\right]^{1/2}$$

where C is the covariance matrix of the samples representative of the color we wish to segment. For C = 1, the distance is referred to as Euclidean distance.

4.3.1.1 *Example 1:*

Figure 4.3 (a) shows an image of a corner defect that is observed under UV and diffused ambient light condition. The dark region in the center of the image is the area under consideration that is to be differentiated form the background region.

Step 1. In the first step, the samples representing the range of colors to be segmented are obtained. The region of interest is achieved using the MATLAB in-built function *roipoly,* which produces a binary mask of a region selected interactively.
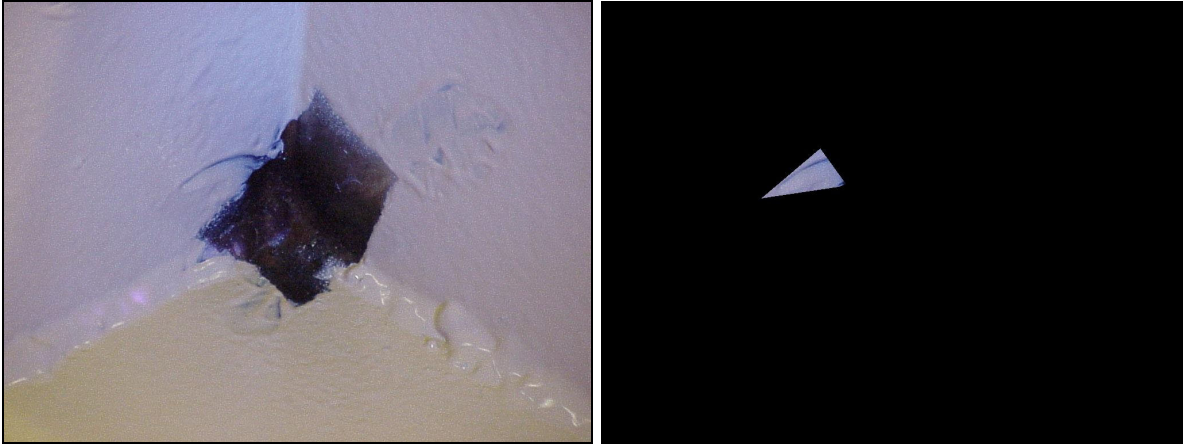
Figure 4.3 (a) RGB image of a missed corner defect (b) Region of interest

This region of interest is shown in Figure 4.3 (b) that is obtained using the following commands,

```
mask = roipoly (a);
red = immultiply (mask, a(:,:,1));
green = immultiply (mask, a(:,:,2));
blue = immultiply (mask, a(:,:,3));
g = cat (3, red, green, blue);
```

Step 2. In this step, the mean vector and the covariance matrix of the points in the ROI are computed. This can be obtained after extracting the coordinates of the points in the region of interest. This is calculated using following commands,

```
[M, N, K] = size (g);
I = reshape (g, M*N, 3);
idx = find (mask);
I = double (I (idx, 1:3));
[C, m] = covmatrix (I);
```

The final step is the determination of the threshold value T. A good starting point is to let T be a multiple of the standard deviation of one of the color components. The standard deviation is a row vector of a three components, one for each red, blue and green color respectively. The first value of T is the maximum value of the component of the std. dev. matrix. The subsequent values of T are the multiples of the first value of T.
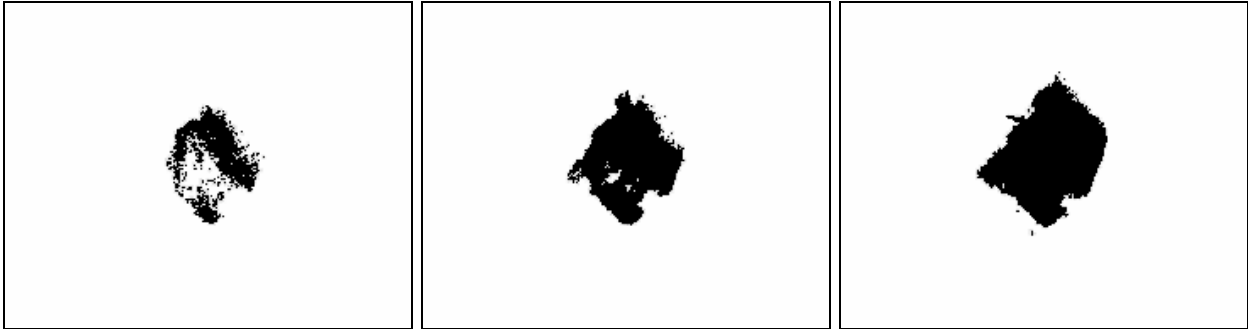
Figure 4.4 Segmented image (a) With T=Std. Dev. (b) With T= 5 (Std. Dev.) (c) With T= 15 (Std. Dev.)

Step 3.   The following commands are used and results are shown in figures. Care should be taken to decide upon when to stop iteration, to avoid oversegmentation.

d = diag (C);
sd = sqrt (d)'
a22 = colorseg ('euclidean', a, 105, m);

(a)   (b)

(c)   (d)
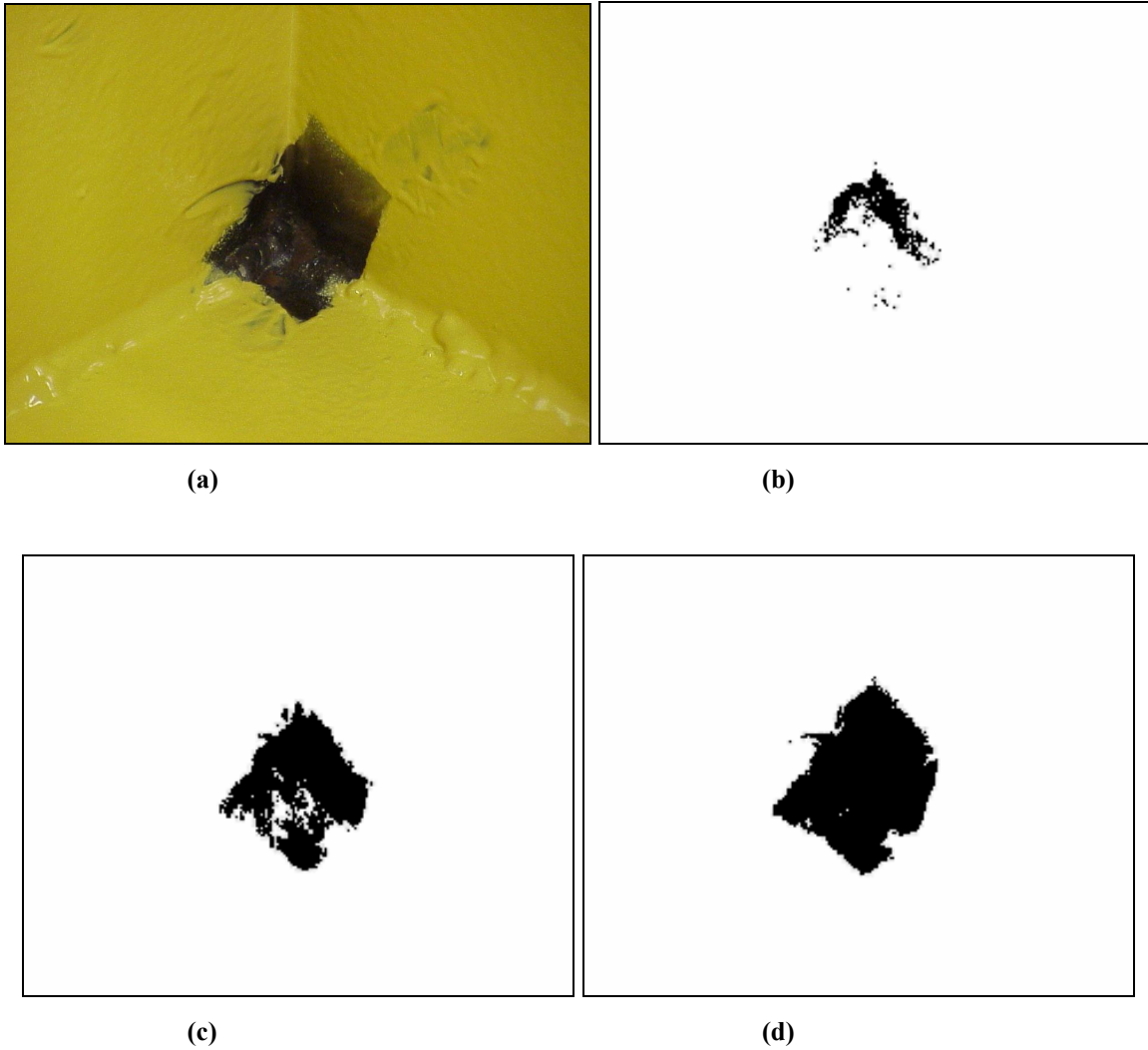
Figure 4.5 Image of a corner defect observed under ambient light only (a) RGB image
(b) Threshold = Std. Dev. (c) Threshold = 5(Std. Dev) (d) Threshold = 15(Std. Dev)

4.3.1.3 Corner Defect observed under UV and Ambient Light condition.

(a)

(b)

(c)

(d)

Figure 4.6 Image of a corner defect observed under UV and ambient light (a) RGB image (b) Threshold = Std. Dev. (c) Threshold = 5(Std. Dev) (d) Threshold = 15(Std. Dev)

4.3.1.4 Corner Defect observed under UV and Diffused Ambient Light condition.

(a)   (b)

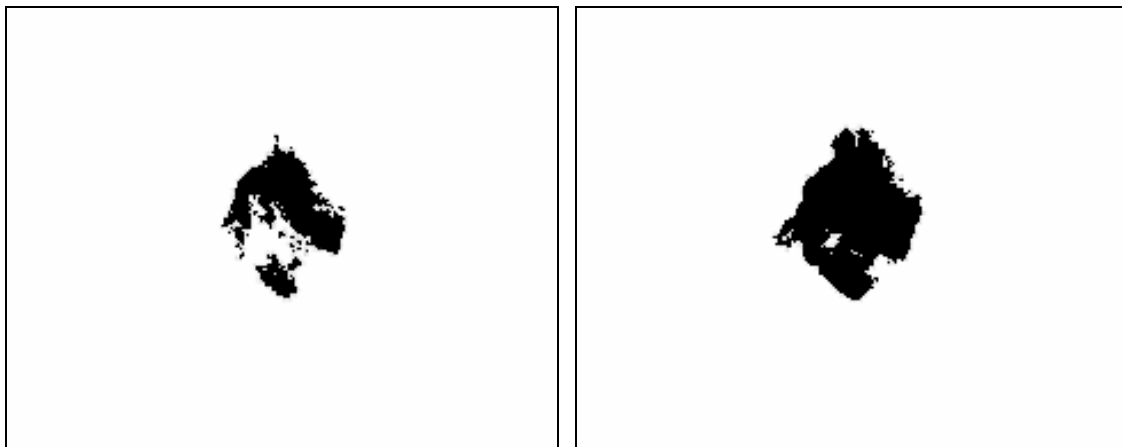(c)   (d)

Figure 4.7 Image of a corner defect observed under ambient light only (a) RGB image
(b) Threshold = Std. Dev. (c) Threshold = 5(Std. Dev) (d) Threshold = 15(Std. Dev)

(a)   (b)

(c)   (d)

Figure 4.8 Image of a missed edge observed under ambient light only (a) RGB image
(b) Threshold = Std. Dev. (c) Threshold = 5(Std. Dev) (d) Threshold = 15(Std. Dev)

4.3.1.6   Missed edge observed under UV and Ambient Light condition.

(a)   (b)

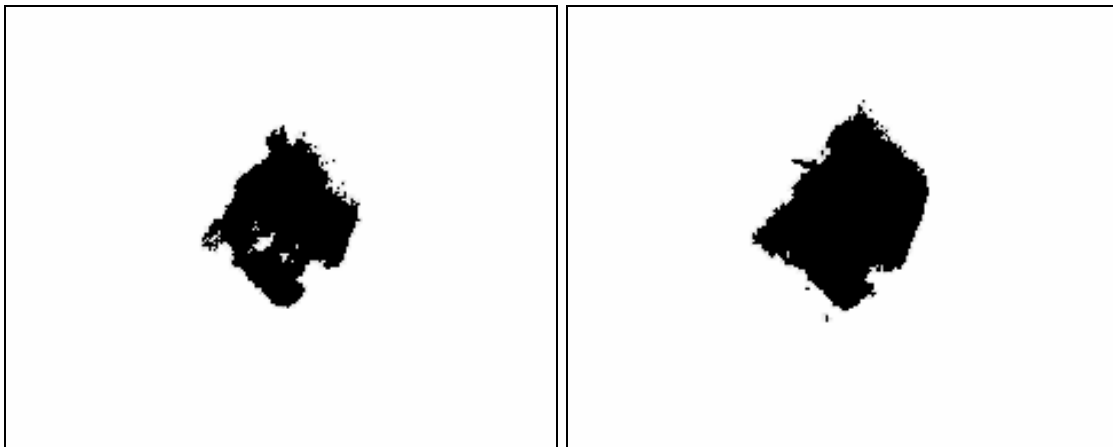(c)   (d)

**Figure 4.9 Image of missed edge observed under UV and ambient light (a) RGB image
(b) Threshold= Std. Dev. (c) Threshold = 5(Std. Dev) (d) Threshold = 15(Std. Dev)**

4.3.1.7   Missed edge observed under UV and Diffused Ambient Light condition.

(a)   (b)

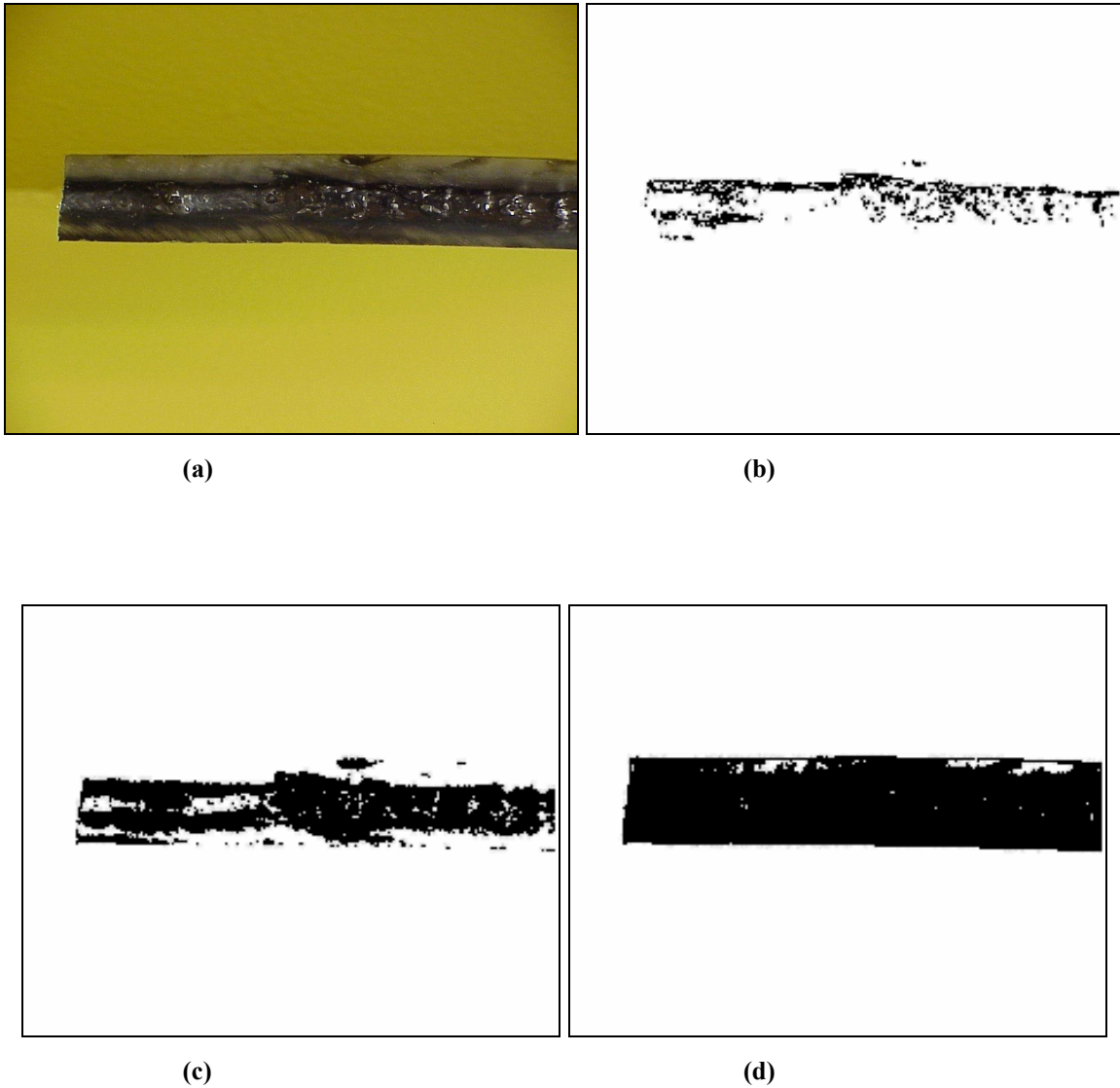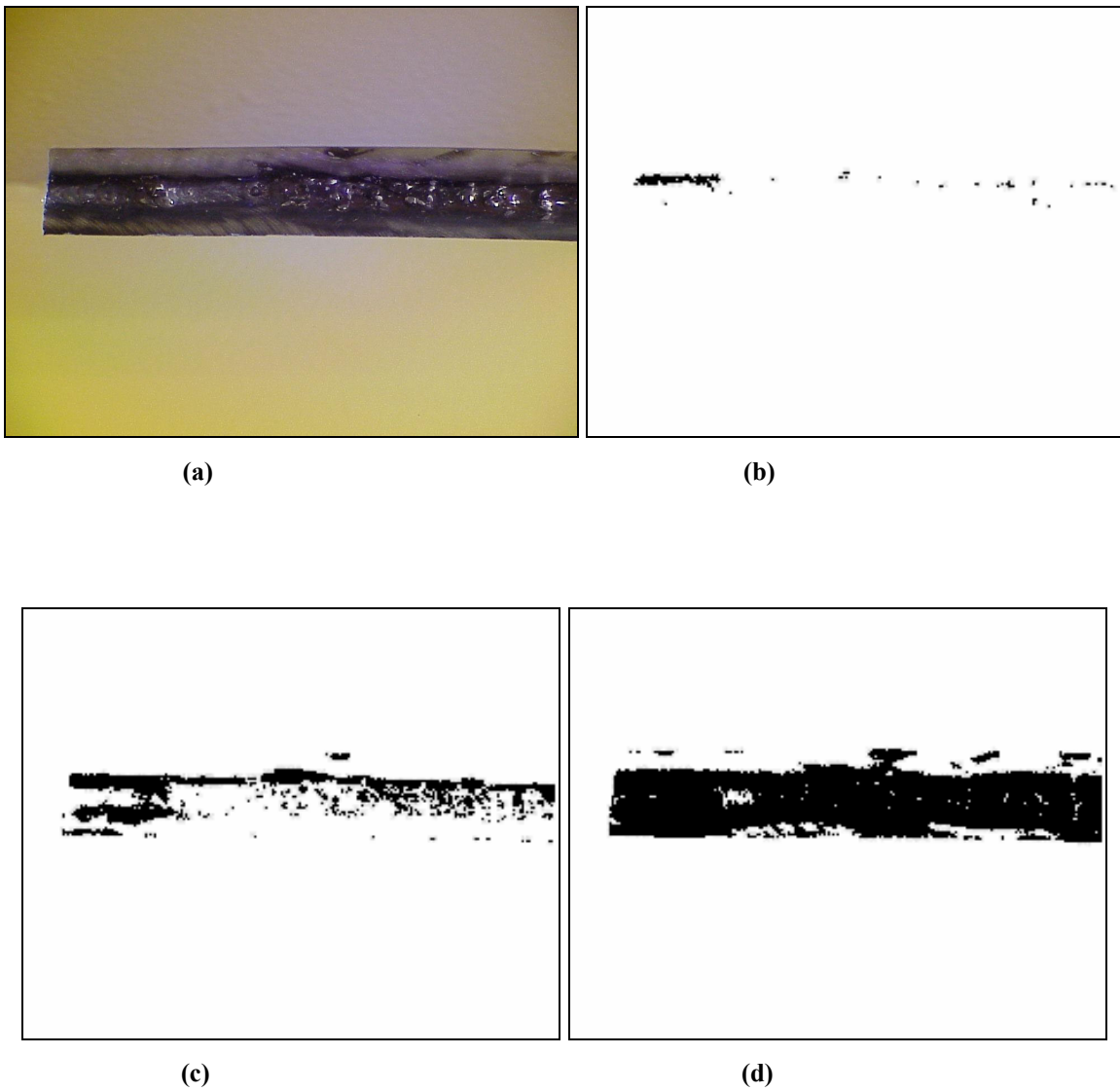(c)   (d)

Figure 4.10 Image of missed edge observed under UV and diffused ambient light (a) RGB image (b) Threshold = Std. Dev. (c) Threshold = 5(Std. Dev) (d) Threshold = 15(Std. Dev)
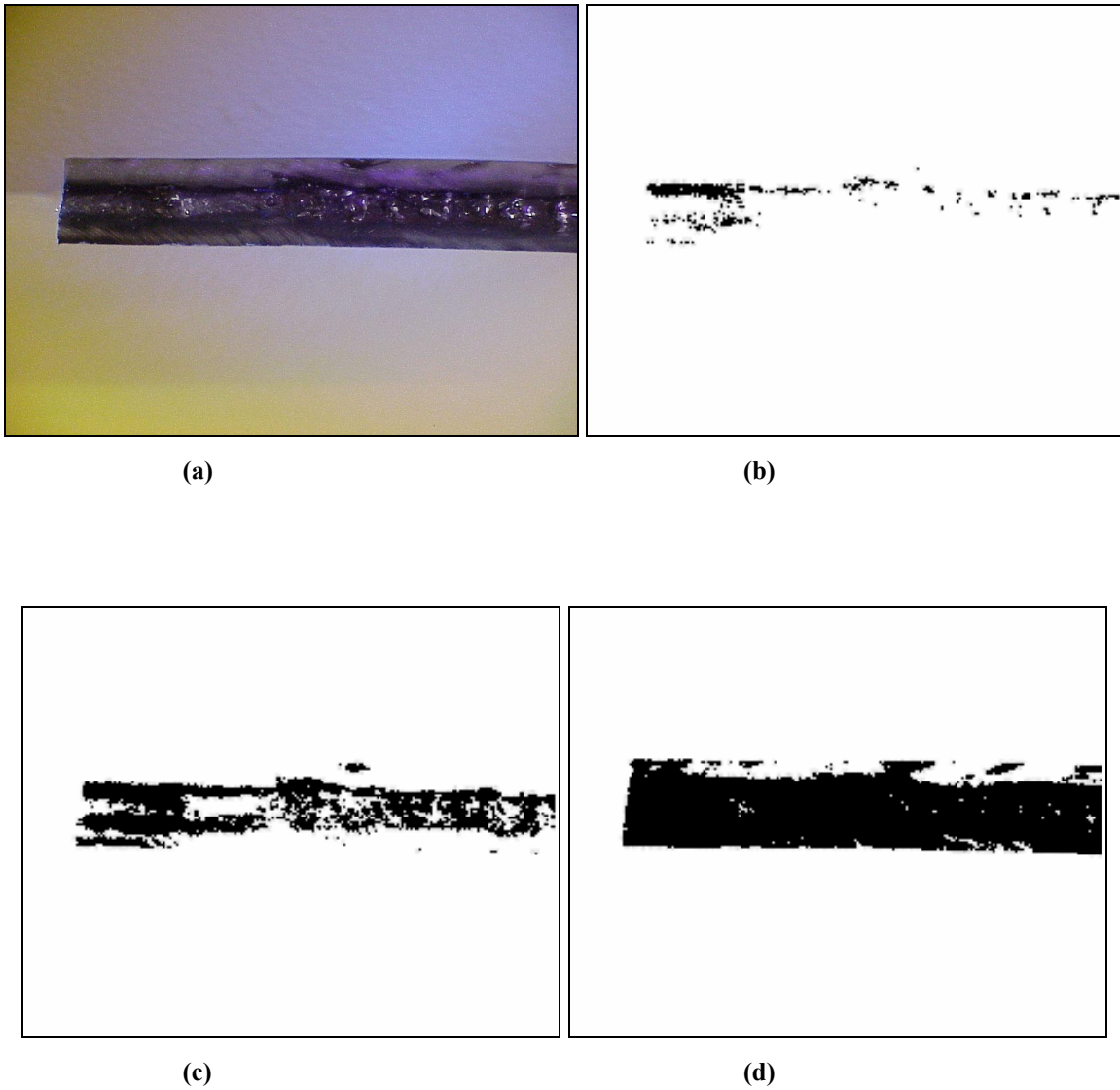
4.3.2 Region Growing:

The region based approach to segmentation seeks to create regions directly by grouping together pixels which share common features into areas, or regions of uniformity. This can be a relatively straightforward task for a high contrast image of an uncluttered scene. However, in the majority of practical cases it becomes a somewhat more complicated exercise.

Region growing is an approach to image segmentation in which neighboring pixels are examined and added to a region class of no edges are detected [32, 33]. The simplest illustration of this process is called pixel aggregation, which starts with a set of seed points and grows regions from these seeds. This process is iterated for each boundary pixel in the region. If adjacent regions are found, a region-merging algorithm is used, in which weak edges are dissolved and strong edges are left in tact.
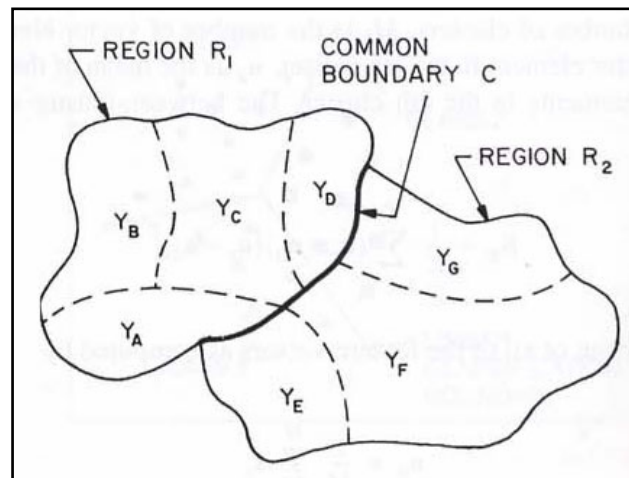
Figure 4.11 Region-growing geometry

Brice and Fenema have developed a region-growing method based on a set of simple growth rules. In the first stage of the process, pairs of quantized pixels are combined together in groups called atomic regions if they are of the same amplitude and four-connected. Two heuristic rules are next invoked to dissolve weak boundaries between atomic boundaries. As shown in the figure, let R_1 and R_2 be two adjacent regions with perimeters P_1 and P_2 respectively, which have previously been merged. After the initial stages of region growing, a region may contain previously merged sub-regions of different amplitude values. Also, let C denote the length of the common boundary and let D represent the length of that portion of C for which the amplitude

difference Y across the boundary is smaller than a significance factor ε_1. The regions R_1 and R_2 are then merged if

$$\frac{D}{MIN\{P_1, P_2\}} > \varepsilon_2$$

where ε_2 is a constant typically set at $\varepsilon_2 = \frac{1}{2}$. This heuristic prevents merger of adjacent regions of the same approximate size, but permits smaller regions to be absorbed into larger regions. The second rule merges weak common boundaries remaining after application of the first rule. Adjacent regions are merged if

$$\frac{D}{C} > \varepsilon_3$$

where ε_3 is a constant set at about $\varepsilon_3 = \frac{3}{4}$. Application of only the second rule tends to over-merge regions.

4.3.2.1 Example 1:

Figure shows a paint defect at a welded edge that is hard to detect by naked eyes. The joined edge contains several cracks and porosities (the bright, white streaks running horizontally through the middle of the image). Using the region growing segmentation, the segmented image can be included in a database of historical studies, for controlling automated welding system, and for other applications.

Step 1) The first step is to determine the initial seed points. This is achieved by first converting the image in RGB color space to HSV space. Once in the HSV space, the intensity component is extracted that will be show the region of interest. The intensity image now becomes the starting point for further evaluation of defects.

(a) (b)
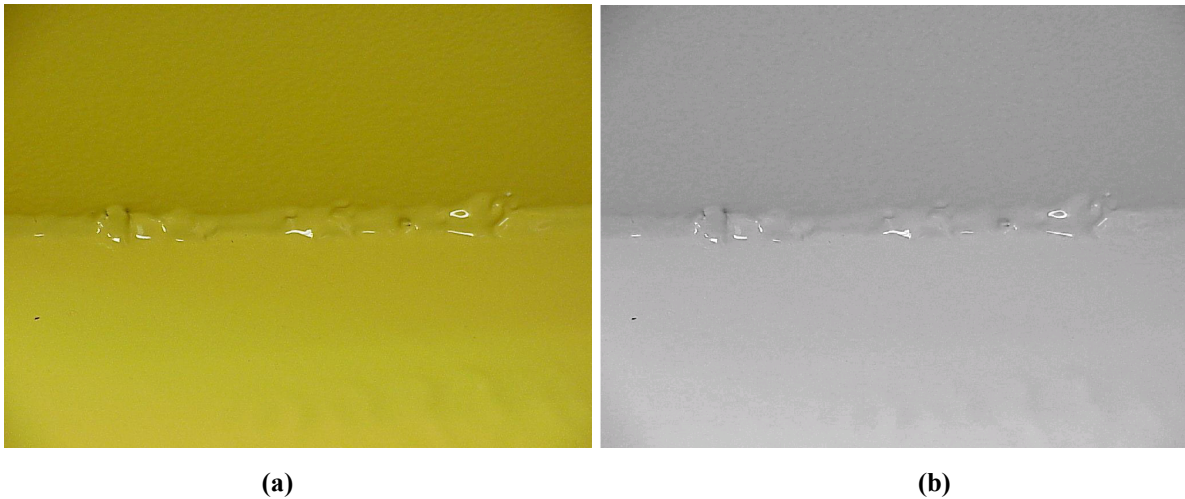
Figure 4.12 (a) RGB image of a weld defect (b) Intensity component used for further analysis

Step 2) As is seen from the intensity image, some pixels in the areas of defective welds tend to have a maximum allowable digital value (1 in this case). So, the value of S = 1.

(a) (b)
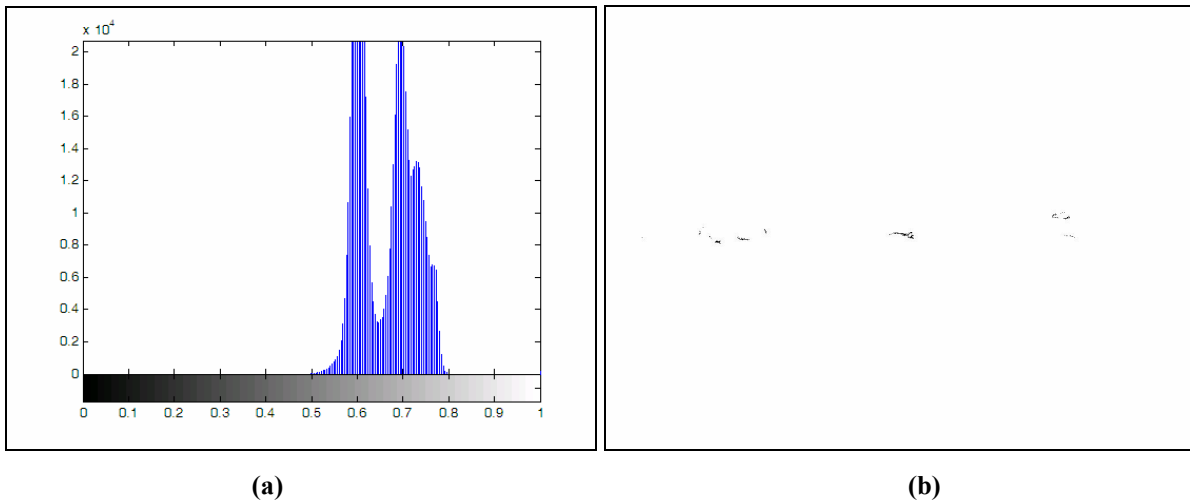
Figure 4.13 (a) Histogram of Intensity image (b) Seed points

Step 3) The next step is to choose the value of threshold T. Based on the analysis of the histogram, the value of T is decided as 0.25. This point represents the difference between 1 and the location of first major peak on the left, which is the representative of the lowest intensity value in the bright weld region. A pixel has to be 8-connected to at least one pixel in a region to be included in that region. If a pixel is found to be

connected to more than one region, the regions are automatically merged by the *regiongrow* algorithm.

(a)   (b)
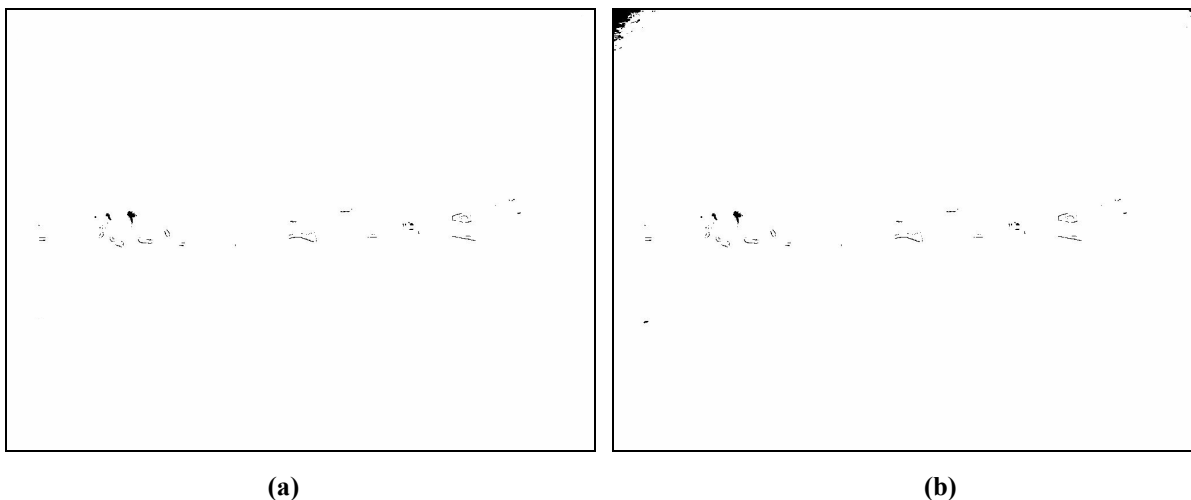
Figure 4.14 (a) Binary image showing all the pixels (in black) that passed the threshold test (b) Result after all the pixels in (c) were analyzed for 8-connectivity to the seed points.

4.3.2.2 Weld defect observed under Ambient Light condition only.

(a)

(b)

(c)

(d)
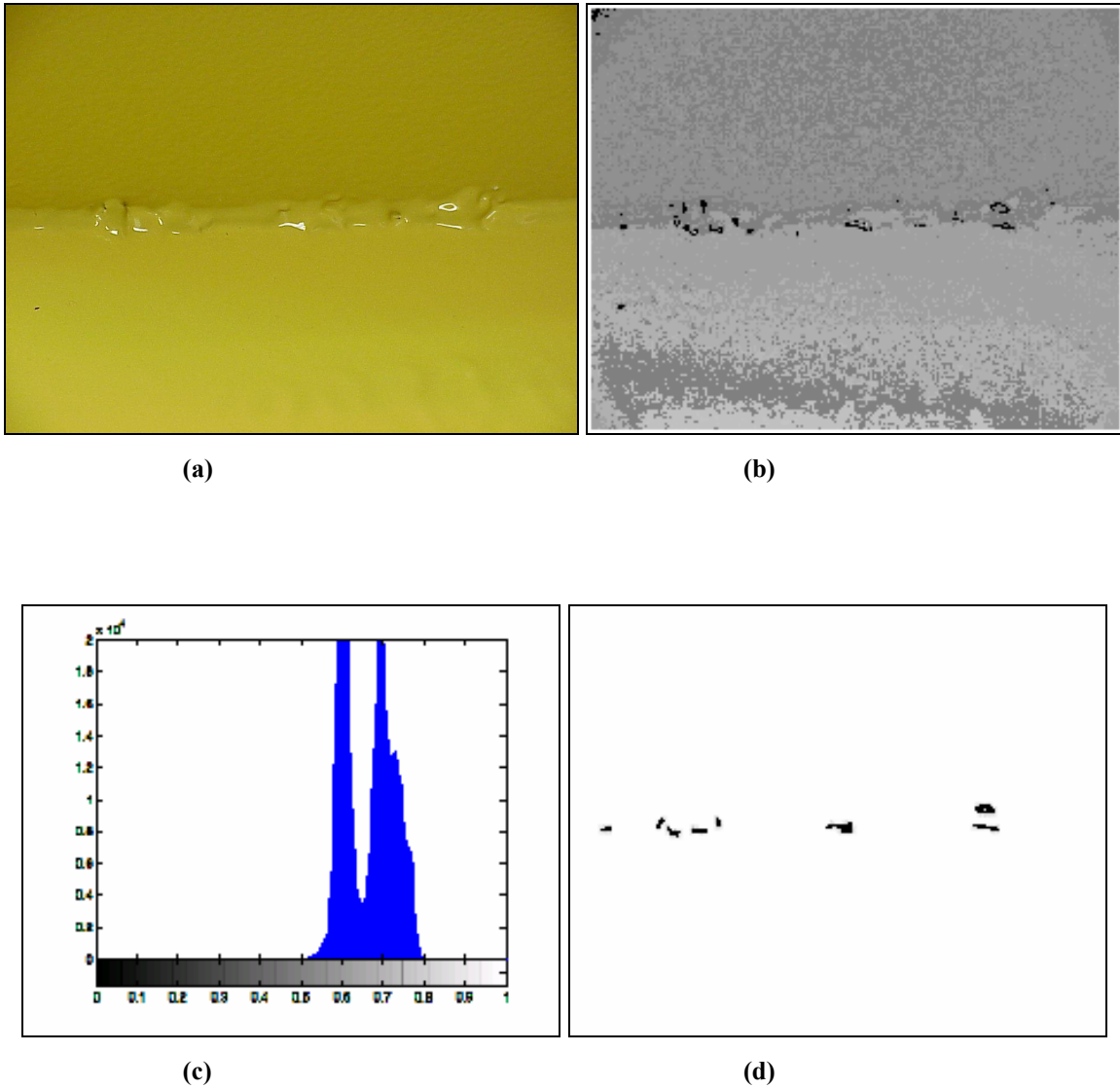
Figure 4.15 Image of weld defect observed under ambient light only (a) RGB image (b) Grey-Scale channel (c) Image Histogram (d) Segmented Image

4.3.2.3 Weld defect observed under UV and Ambient Light condition.
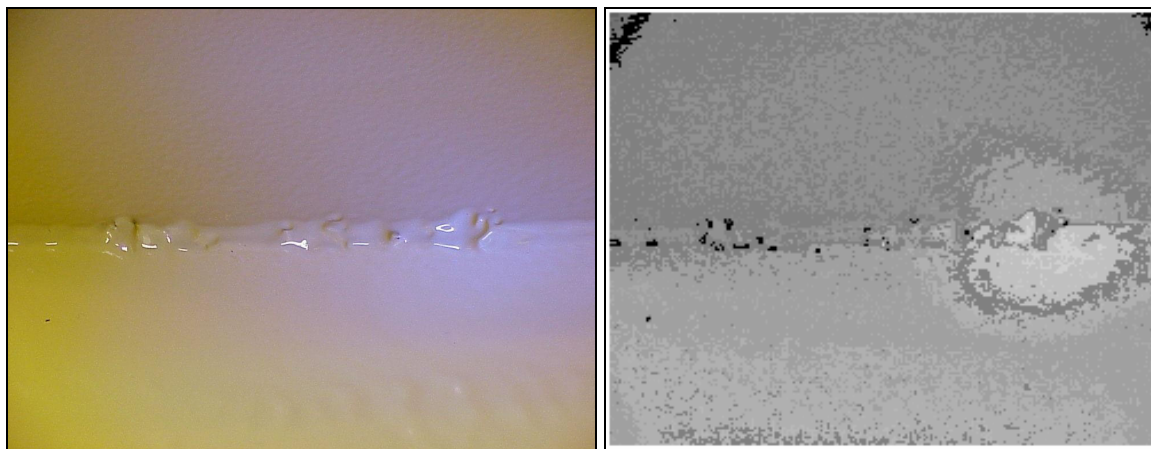
(a)

(b)

(c)

(d)

Figure 4.16 Image of weld defect observed under UV and ambient light (a) RGB image (b) Grey-Scale channel (c) Image Histogram (d) Segmented Image

(a)

(b)

(c)

(d)

Figure 4.17 Image of weld defect observed under UV and ambient light (a) RGB image

(b) Grey-Scale channel (c) Image Histogram (d) Segmented Image

4.3.2.5 Over-millage paint defect observed under Ambient Light condition only.

(a)

(b)

(c)

(d)

Figure 4.18 Image of over-millage paint defect observed under ambient light only (a) RGB image (b) Grey-Scale channel (c) Image Histogram (d) Segmented Image
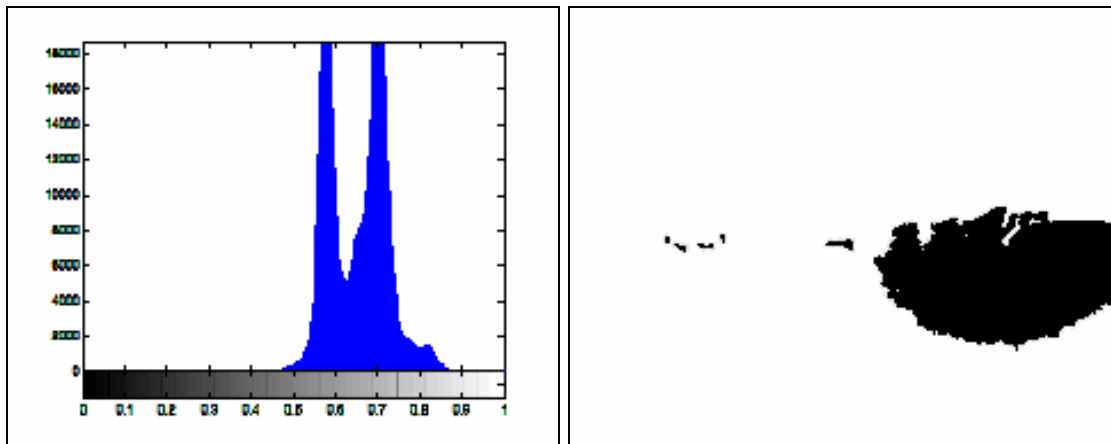
4.3.2.6 Over-millage paint defect observed under UV and Ambient Light condition.

(a)

(b)

(c)

(d)

Figure 4.19 Image of over-millage paint defect observed under UV and ambient light (a) RGB image (b) Grey-Scale channel (c) Image Histogram (d) Segmented Image

4.3.2.7 Over-millage paint defect observed under UV and Diffused Ambient Light condition.

(a)   (b)
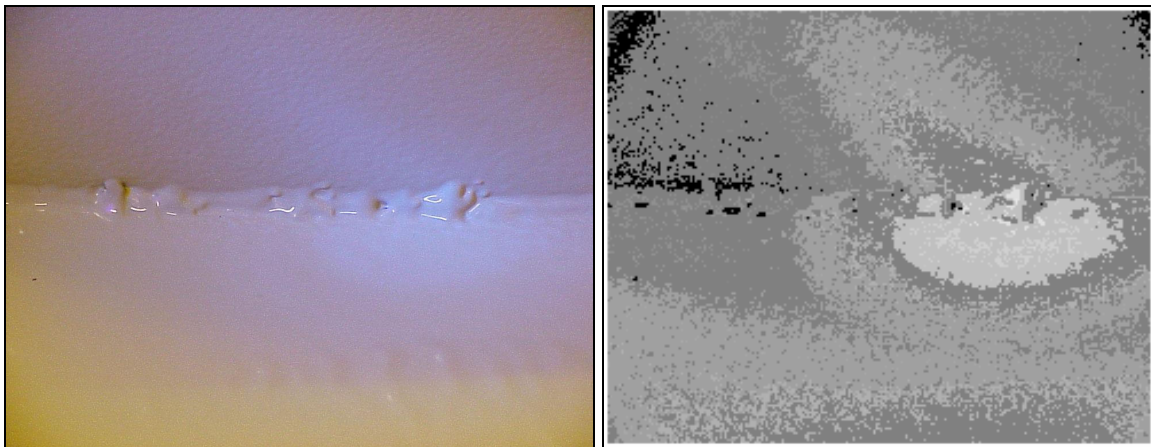

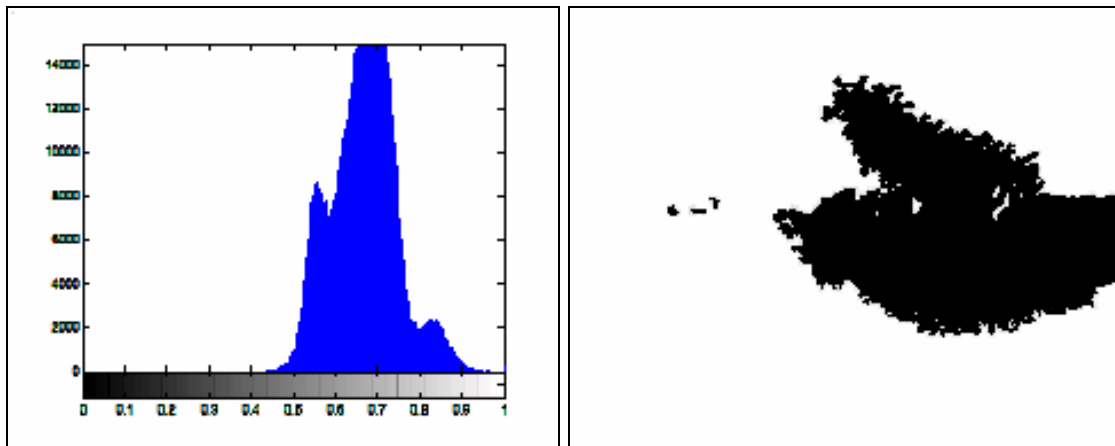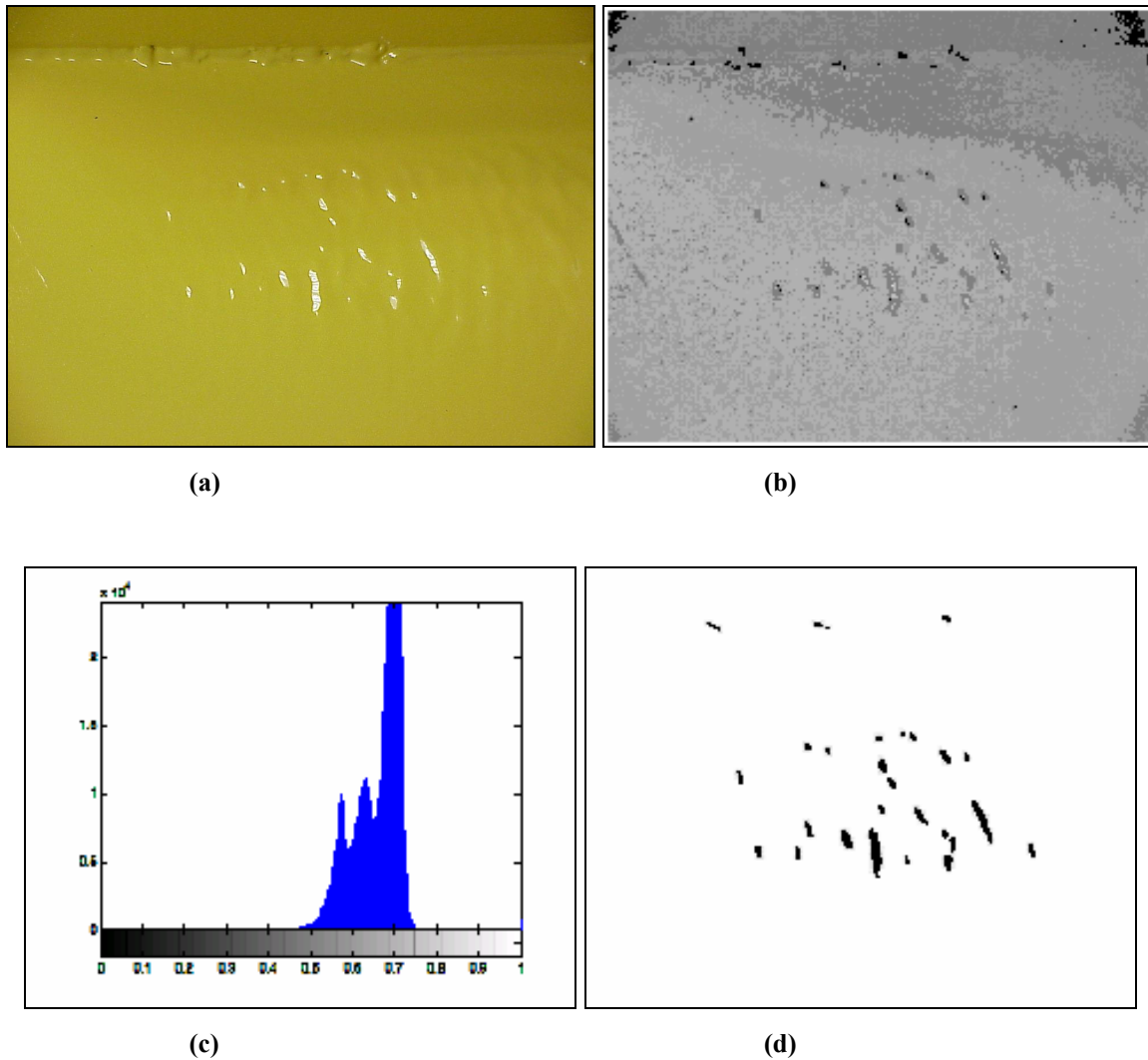(c)   (d)

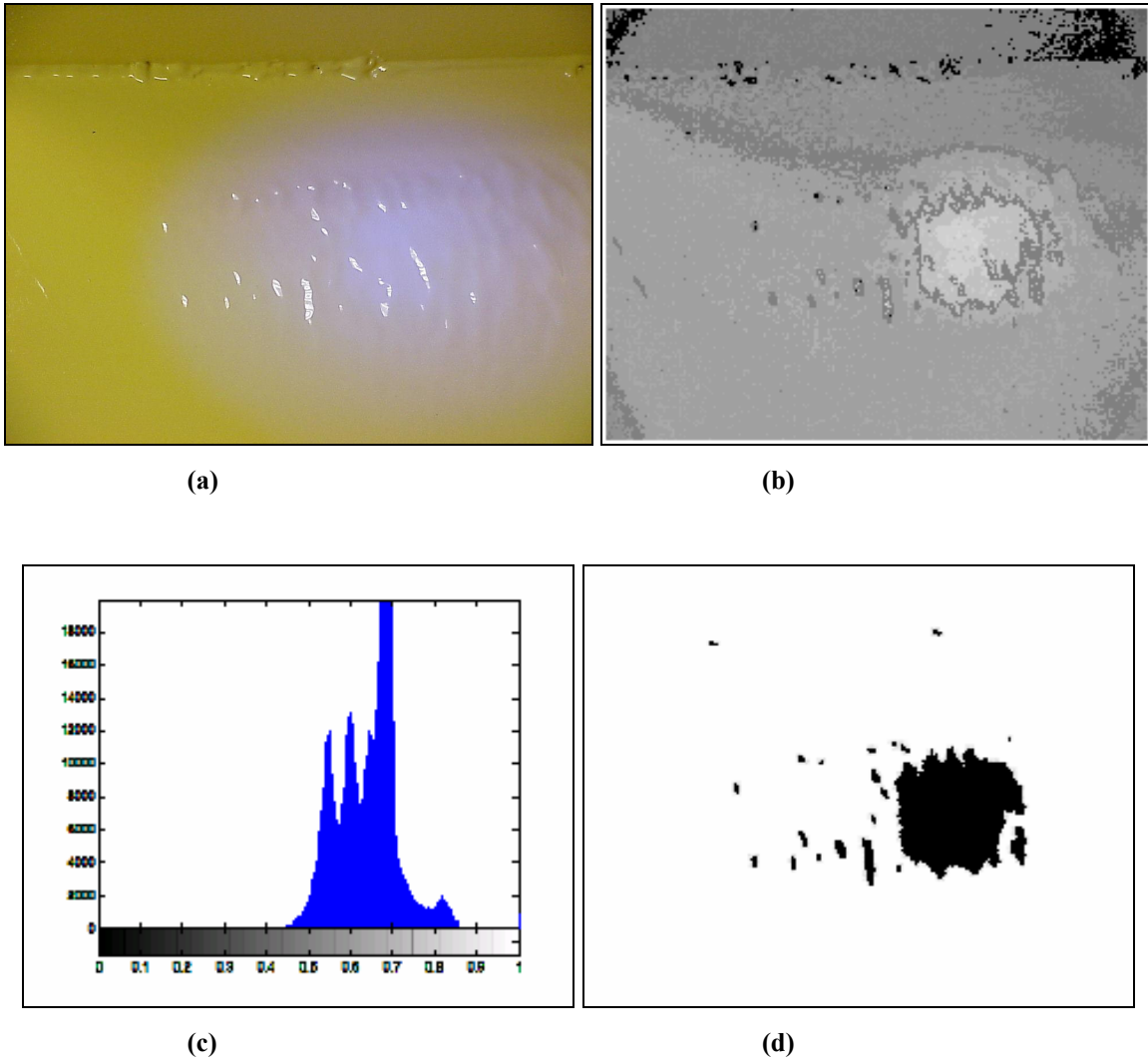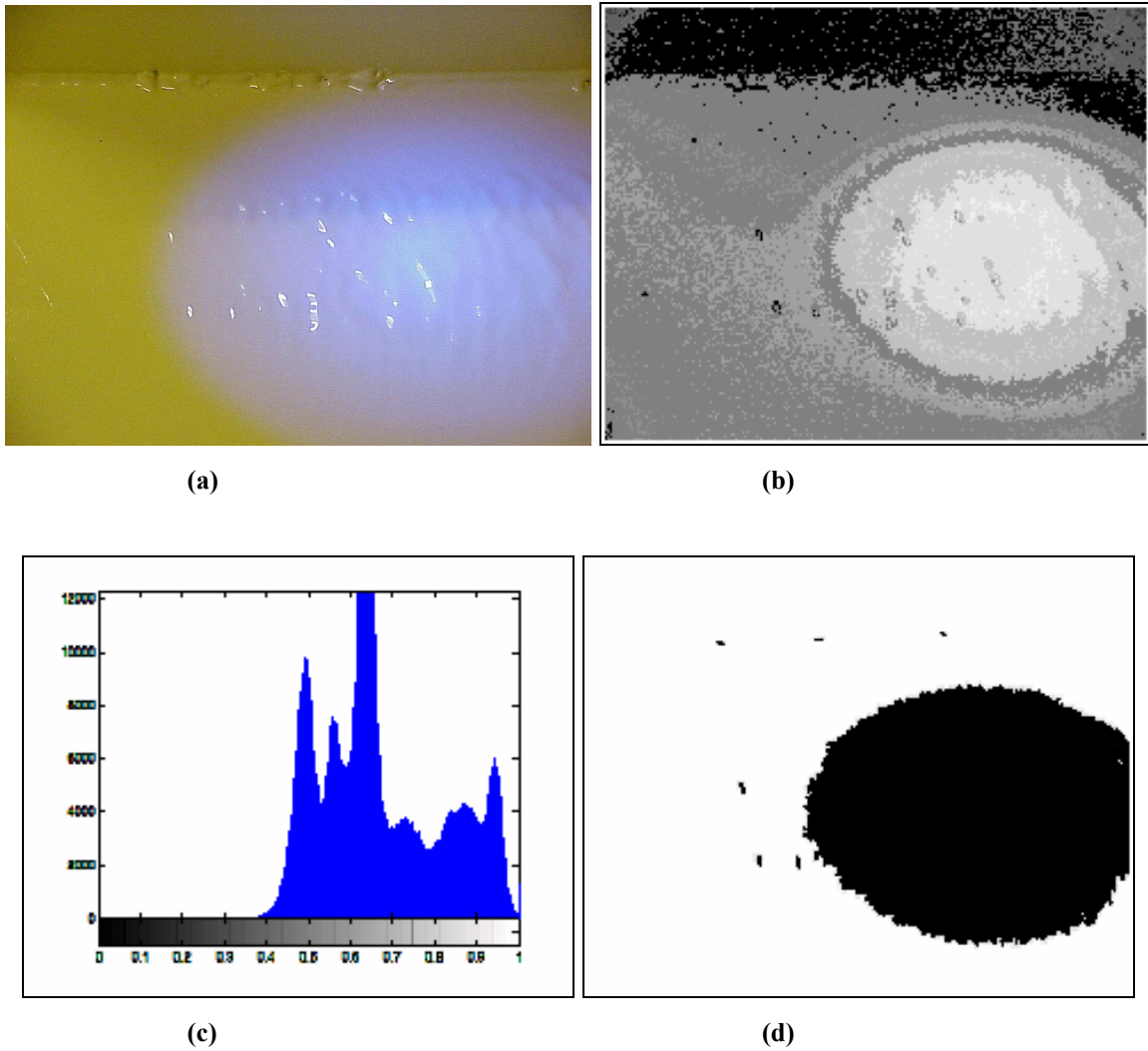**Figure 4.20 Image of over-millage paint defect observed under UV and diffused ambient light (a) RGB image (b) Grey-Scale channel (c) Image Histogram (d) Segmented Image**

4.3.3 Image Thresholding:

Thresholding is the most important technique for segmentation and is widely used for machine vision systems [32, 33]. If background lighting is arranged so as to be fairly uniform and if the objects are fairly flat, segmentation can be achieved simply by thresholding the image at a particular intensity level T.

The most common way to convert between grey-level and bi-level images is to select a single threshold value [33]. All of the grey levels below this value will be classified as black (0), and those above will be white (1). The segmentation problem becomes one of selecting a proper value for the threshold T. What is being assumed here is that the pixels in an image I belong to one of the two classes based on their grey-level. The first class is the collection of black pixels which will be given the value one, and for this class:

$$I (i, j) < T$$

The other class consists of those pixels that will become white:

$$I (I, j) \geq T$$

The threshold must be determined from the pixel values found in the image.

4.3.3.1 Under-millage defect (1) observed under Ambient Light condition.

(a)   (b)

(c)   (d)
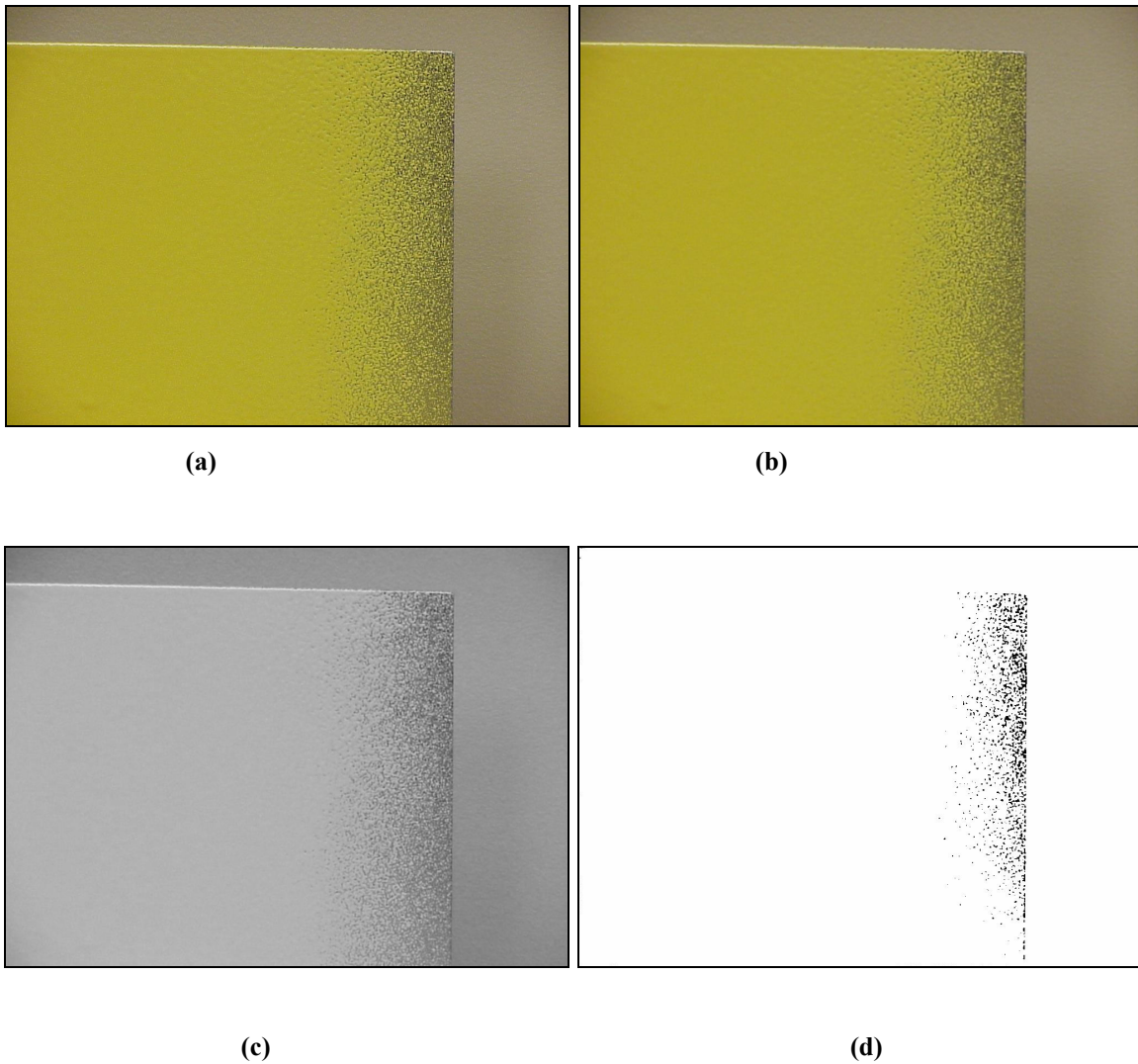
Figure 4.21 Image of under-millage (1) observed under ambient light only (a) RGB image

(b) Smoothed Image (c) Grey-Scale Image (d) Segmented Image

4.3.3.2 Under-millage defect (1) observed under UV and Ambient Light condition.

(a)

(b)

(c)

(d)
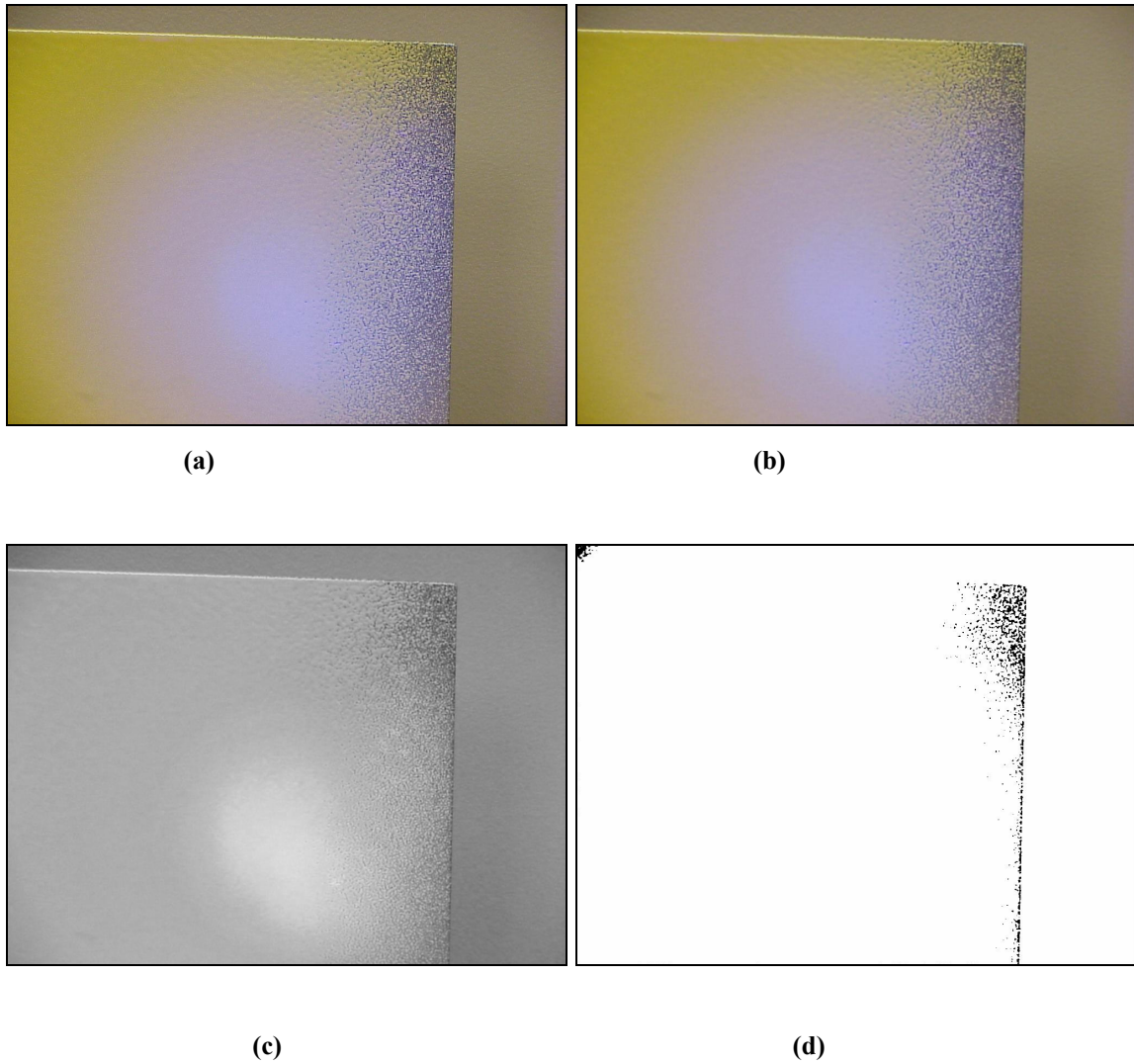
Figure 4.22 Image of under-millage (1) observed under UV and ambient light (a) RGB image (b) Smoothed Image (c) Grey-Scale Image (d) Segmented Image

4.3.3.3 Under-millage defect (1)observed under UV and Diffused Ambient Light condition.

(a) (b)

(c) (d)
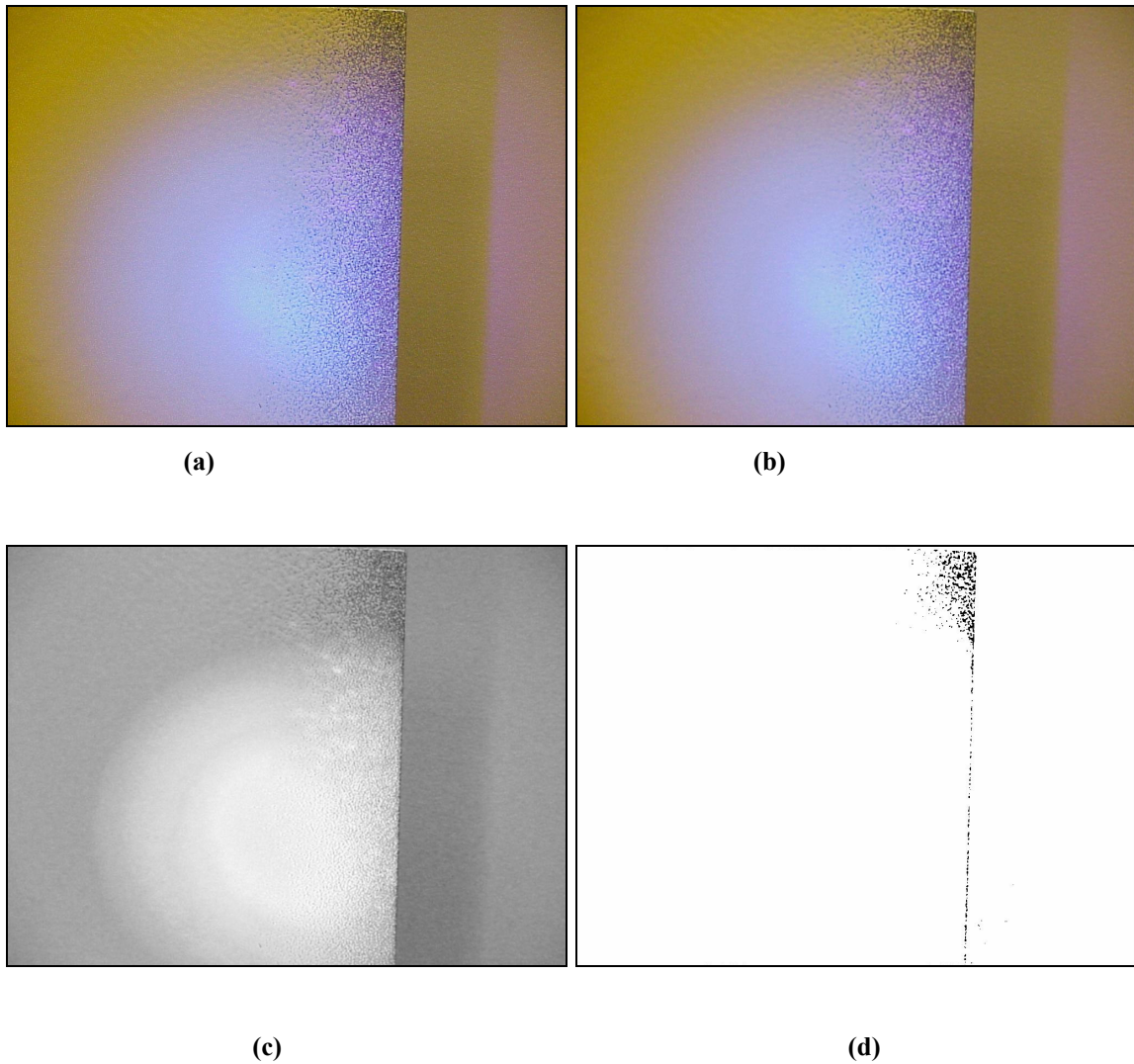
Figure 4.23 Image of under-millage (1) observed under UV and diffused ambient light (a) RGB image (b) Smoothed Image (c) Grey-Scale Image (d) Segmented Image

4.3.3.4 Under-millage defect (2) observed under Ambient Light condition.

(a)   (b)

(c)   (d)
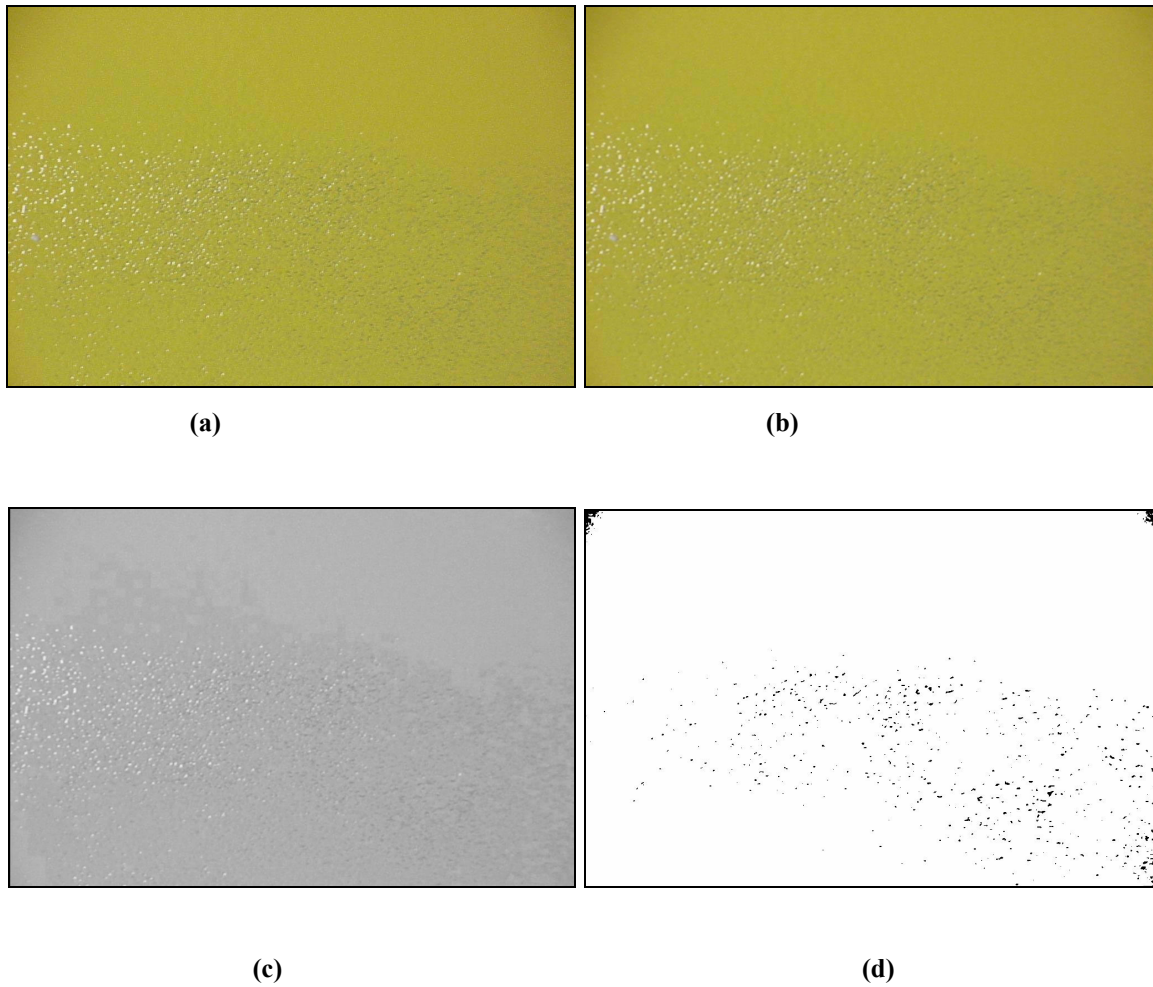
Figure 4.24 Image of under-millage (2) observed under ambient light (a) RGB image

(b) Smoothed Image (c) Grey-Scale Image (d) Segmented Image

4.3.3.5 Under-millage defect (2) observed under UV and Ambient Light condition.

(a) (b)

(c) (d)

Figure 4.25 Image of under-millage (2)observed under UV and ambient light (a) RGB image (b) Smoothed Image (c) Grey-Scale Image (d) Segmented Image

4.3.3.6 Under-millage defect (2) observed under UV and Diffused Ambient Light condition.

(a)

(b)

(c)

(d)

Figure 4.26 Image of under-millage (2) observed under UV and diffused ambient light (a) RGB image (b) Smoothed Image (c) Grey-Scale Image (d) Segmented Image
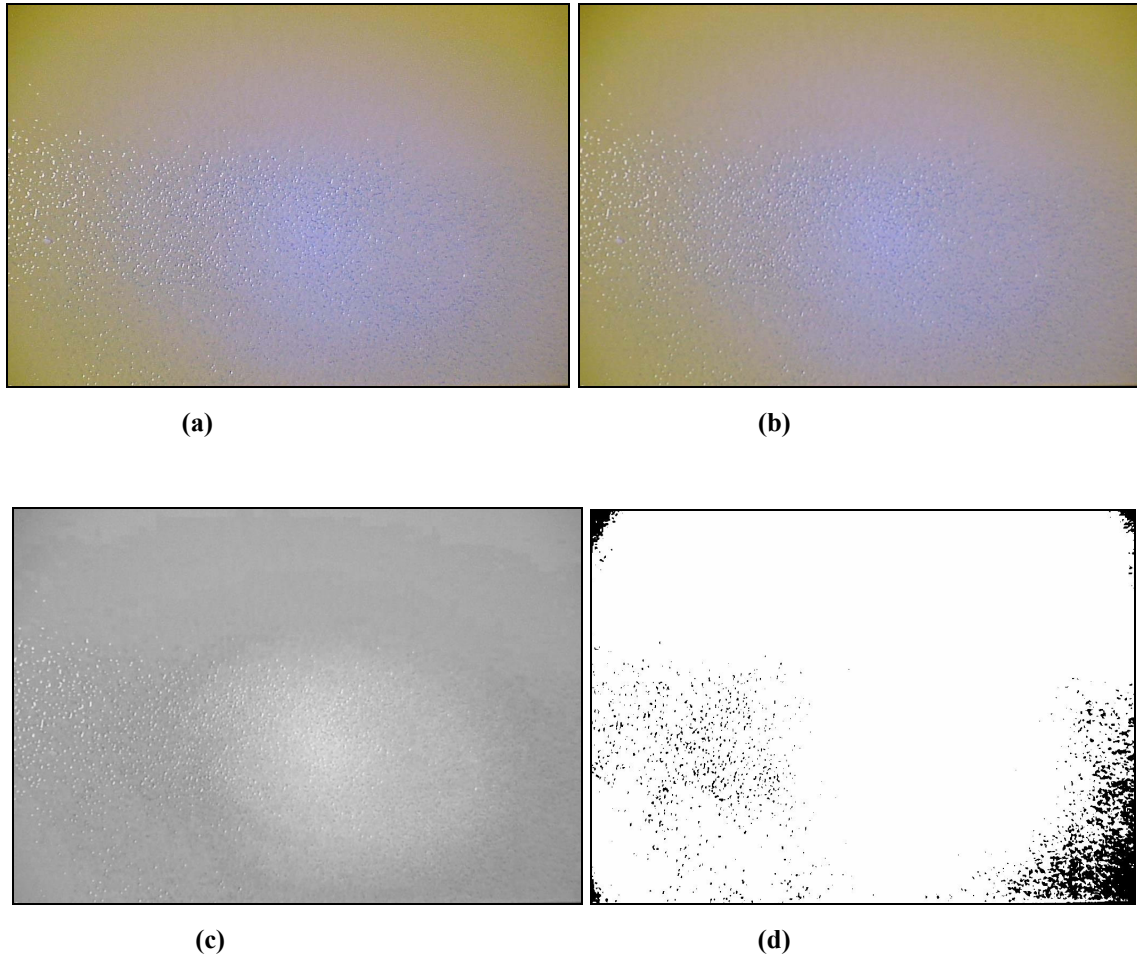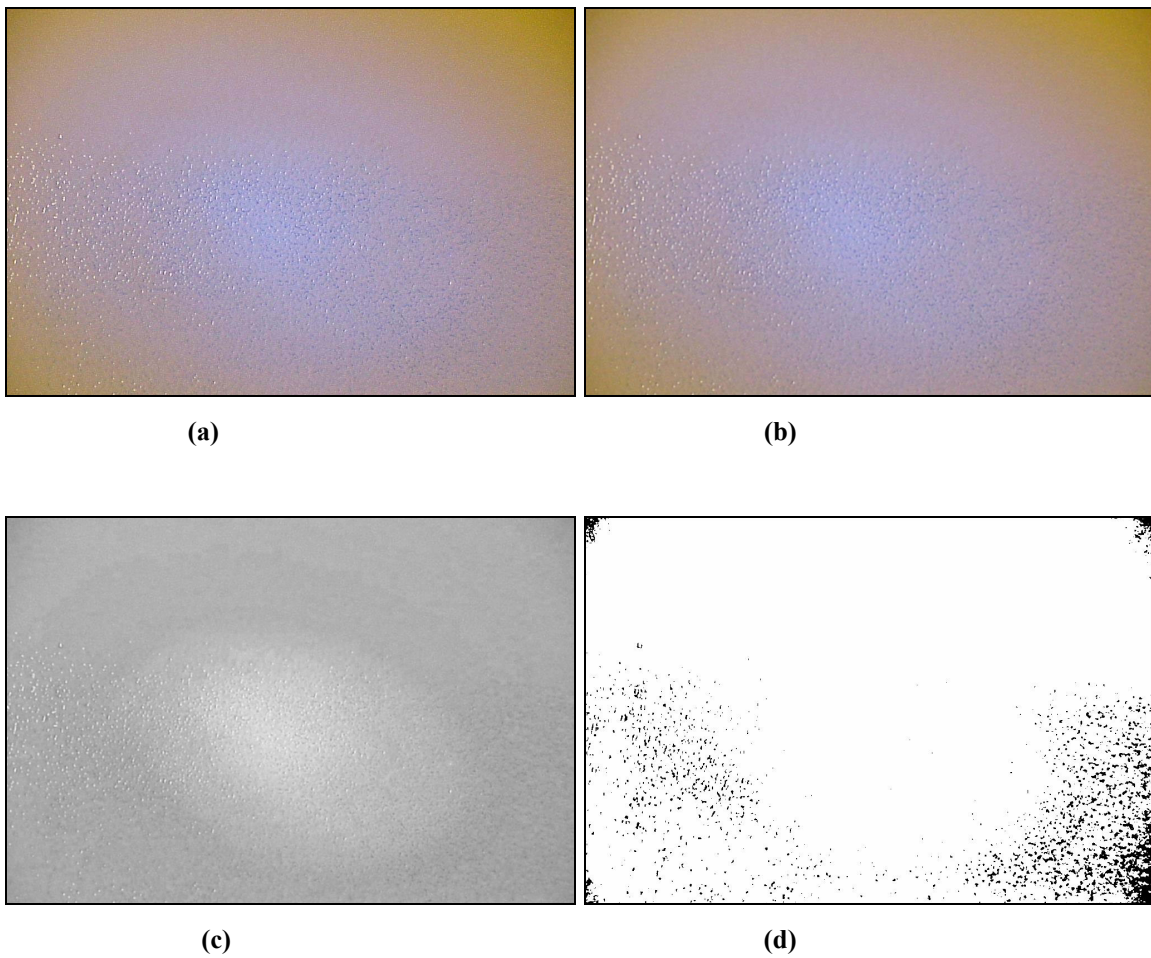
Chapter 5

Conclusion and Future Work

5.1 Summary:

The objective of the research work was to collect image data from a wide variety of samples provided from the paint vendors with a variety of ambient light and coatings conditions. Further, it was also required to develop image understanding algorithms that was make the defect identification process much simpler and less time consuming. The image data was used to fully optimize the automatic corrosion detection algorithms and an attempt was made to test its robustness with the data gathered from the field tests. Working with larger imaged areas is essential for being able to perform a tank coatings inspection in ten minutes or less. However, the use of the collimated UV light source does not allow areas more than 7" x 7" to be inspected. Other disadvantages of the light source are its circular projection of light and non-uniform intensity level over the illuminated area.

A study and analysis for three different image processing algorithms has been elaborated with examples in Chapter 5. The defects have also been categorized based on the algorithm used and the best analyzing conditions for any particular defect are discussed. The algorithms are found to produce promising results depending on the image acquisition system. A further development of these algorithms based on their adaptation to real world environments through extensive testing will significantly increase their probability of flaw detection and make them successful and productive tools for remote visual inspection.

5.2 Conclusion:

1. The technique of image acquisition and post processing of paint surface defects, using the three developed algorithms produced encouraging results. Using more controlled conditions and creating a database of possible defects can help in developing a universal and robust algorithm. This proves that the theory of using OAA incorporated with machine

vision system can be used to develop a portable gadget capable of detecting paint defects for ballast tanks of ships.

2. Three image understanding algorithms for defect detection have been described and have reported preliminary test results. These algorithms are categorized depending on the type of defects that they are capable to analyze. The image segmentation in RGB color space is used for detection of missed areas and holidays. The region growing technique works well for weld defects and over-spray problems. Under uniform illumination, simple thresholding produced excellent results for under-millage coating defects.

3. Accuracy of any image processing algorithm depends on the how uniformly the UV light and ambient light is distributed over the region of interest and is directly proportional to computational time.

4. Through field testing, we have demonstrated successfully that our remote imaging system delivers imagery of sufficient high visual quality that unskilled personnel can analyze and make decisions accordingly.

5. The experimental results show that the technique can be used to detect defects with reliable correct detection rates. Results with UV and diffused ambient light are seen to be more accurate for color image segmentation, while uniform illumination plays an important role for region-growing segmentation.

6. The results from light controlling experiments showed that a best combination of an orange filter for ambient light and a blue filter over the camera, with a 40 W bulb are the optimum parameters that can produce images suitable for processing. This data helped to decide upon the geometry and operating conditions for the prototype.

7. The experimental study also helped in deciding upon the sensor used and the helped in analyzing the prototype geometry. The study revealed the underlying drawbacks of the system such as the computation time and gave a feedback for prototype testing.

8. The repeatability of the system was tested by performing a number of experiments by changing the governing parameters. The acquired images produced good results which confirm the reliability of the system and image processing algorithms.

5.3 Recommendations for Future Work:

There is substantial scope for carrying out further research and the work presented in this thesis can be extended further. This thesis touches just one aspect of a practical vision system, with still a need to explore the other areas such as developing a user-friendly interface and real time imaging algorithms.

1. With a clear definition of the minimum size of surface defect that can be a source of corrosion, a robust algorithm can be developed that can target all the defects and can analyze the percentage defect area.

2. No single algorithm or method can be applied to different defect families. More research in the field of neural networks and creating a database of possible defects can help in developing a universal and robust algorithm.

3. Real time imaging and analysis can save a lot of money and make the inspection process more efficient and foolproof.

4. The theory of fluorescence spectroscopy can be used in conjunction with visual imaging and can help in the development of film thickness detection in addition to holiday detection.

APPENDIX

Matlab Code:

Image segmentation in RGB vector space:

```
a=imread('Edge weld A.jpg'); % Read an image in matlab
mask=roipoly(a); % Select the Region of Interest

red=immultiply(mask, a(:,:,1));
green=immultiply(mask, a(:,:,2));
blue=immultiply(mask, a(:,:,3));
g=cat(3,red,green,blue);
%figure,imshow(g)

% calculate the mean vector and covariance matrix of the points in ROI
[M, N, K]=size(g);
I=reshape(g, M*N, 3); % Rearrange the color pixels in g as rows of I
idx=find(mask); % Find row indices of color pixels that are not black
I=double(I(idx, 1:3));
[C, m]=covmatrix(I);
d=diag(C); % Compute the variances of the RGB components
sd=sqrt(d)'   % Calculate standard deviation

a22=colorseg('euclidean',a,105,m);
a22=imcomplement(a22);
figure,imshow(a22)
```

Region Growing:

```
function [g, NR, SI, TI] = regiongrow(f, S,T)


f = double(f);
% If S is a scalar, obtain the seed image.
if numel(S) == 1
   SI = f == S;
   S1 = S,
else
   SI = bwmorph(S, 'shrink', Inf);
   J = find(SI);
   S1 = f(J)
end


TI = false(size(f));
for K = 1:length(S1)
   seedvalue = S1(K)
   S = abs(f - seedvalue) <= T;
   TI = TI | S;
end


[g, NR] = bwlabel(imreconstruct(SI, TI));
```

Image thresholding :

```
I = imread('u1.jpg');
figure,imshow(I)
f_rgb = ones(3,3) / 9; % Smoothing filter for RGB image before converting to gray level image
I = imfilter(I,f_rgb); %Filter the image
hsv=rgb2hsv(I); %Convert to HSV color space
f=hsv(:,:,3);
T = graythresh(f)
g = im2bw(f, T);
figure,imshow(g)
```

References

1. Lambourne, R., Paint and surface coatings: Theory and Practice, Chichester: Ellis Horwood ; New York : Halsted Press, (1987), p. 535

2. "Engineering and Design, Painting: New Construction and Maintenance", CECW-EE Engineer Manual, Published by U.S. Army Corps of Engineers, 1995.

3. Weldon, D.G., Failure analysis of paints and coatings, (2001)

4. Stearns, S. D., Digital signal processing with examples in MATLAB, CRC Press, (2003)

5. Sharma G., Digital color imaging handbook, CRC Press, (2003)

6. Burke M.W., Handbook of machine vision engineering, (1996)

7. Zuech N., Machine vision: capabilities for Industry, (1986)

8. Jähne, B., Practical handbook on Image Processing for Scientific Applications, (1997)

9. Zuech, Nello, Applying machine vision, (1988)

10. Davies, E. R., Machine vision : Theory, Algorithms, Practicalities, (1990)

11. Awcock, G. J., Thomas R., Applied image processing, (1996)

12. Crane, Randy, Simplified approach to image processing : Classical and Modern Techniques, (1997)

13. Water Pollution Control Federation. Subcommittee on Paints and Protective Coatings. Paints and protective coatings for wastewater treatment facilities. Prepared under direction of the Technical Practice Committee by the Subcommittee on Paints and Protective Coatings. Location: Engineering Library TP935 .W395

14. Hollingum, Jack, Machine vision: The Eyes of Automation, a manager's practical guide, (1984)

15. Vision '90: conference proceedings, November 12-15, 1990, Detroit, Michigan / sponsored by Society of Manufacturing Engineers [and] Machine Vision Association of the Society of Manufacturing Engineers. Location: Engineering Library TA1632 .V553 1990

16. Vision '86: conference proceedings, June 3-5, 1986, Detroit, Michigan / sponsored by MVA/SME. Location: Engineering Library TA1632 .V550 1986

17. K.E. Lucas, E.D. Thomas, P.F. Slebodnick, "Development of a remote monitoring system for the evaluation and documentation of ballast tank coatings integrity for U.S. Navy hulls", Naval research laboratory.

18. Allgaier M.W., Ness S., McIntire P., Moore P.O., "Nondestructive testing handbook", American Society for Nondestructive testing, second edition, vol. 8, (2002).

19. B.N. Nelson, P. Slebodnick, E.J. Lemieux, "Wavelet processing for image de-noising and edge detection in automatic corrosion detection algorithms used in shipboard ballast tank video inspection systems", Proceedings of SPIE, Vol. 4391, pp 134 – 145, 2001.

20. W.Y. Wu, C.C. Hou, "Automated metal surface inspection through machine vision", Imaging Science Journal, Vol. 51, pp 79 – 88, 2003.

21. P. Gunatilake, M.W. Siegel, A.J. Jordan, G. Podnar, " Image enhancement and understanding for remote visual inspection of aircraft surface", Robotics Institute, Carnegie Mellon University.

22. P.L. Rosin, E. Ioannidis, "Evaluation of global image thresholding for change detection", Pattern Recognition Letters 24, pp 2345–2356, 2003.

23. D.W. Jacobs, P.N. Belhumeur, R. Basri, "Comparing Images Under Variable Illumination", CVPR, 1998.

24. A.S. Georghiades, D.J. Kriegman, P.N. Belhumeur, "Illumination Cones for Recognition Under Variable Lighting: Faces", CVPR, 1998.

25. O. Moselhi, T. Shehab – Eldeen, "Automated detection of surface defects in water and sewer pipes", Automation in Construction, Vol. 8, pp 581 – 588, 1999.

26. C. Hampton, T. Persons, C. Wyatt, Y. Zhang, "Survey of Image segmentation", 1998.

27. F. Lee, R.A. Ryntz, D. Britz, J. Summerville, "Analysis of coatings appearance and durability – testing – induced surface defects using image capture/processing/analysis".

28. P.L. Rosin, "Unimodal Thresholding", Brunal University.

29. Phiilippe Andrey, "Selectionist relaxation: genetic algorithms applied to image segmentation", Image and Visual Computing, Vol. 17, pp 175 – 187, 1999.

30. Y. Yang, H. Yan, "An adaptive logical method for binarization of degraded document images", Pattern Recognition Society, Vol. 33, pp 787 – 807, 2000.

31. L. Tang, L. Tian, B.L. Steward, "Color image segmentation with genetic algorithm for in-field weed sensing", American Society of Agricultural Engineers, Vol. 43(4), pp 1097 – 1027, 2000.

32. William Pratt, "Digital Image Processing", John Wiley & Sons, Inc., Third Edition, 2001.

33. R. Gonzalez, R.E. Woods, S.L. Eddins, "Digital image processing using MATLAB", Pearson Prentice Hall, 2004.

VITA

Date and place of birth

November 7, 1978 in Pune, Maharashtra, INDIA.

Education

University of Pune, Bachelor of Engineering in Mechanical Engineering (2000).

Work Experience

- Graduate Research Assistant, University of Kentucky, Lexington, KY
  (Aug. 2001 – Dec. 2003)

- Process Engineer, Atlas Copco (India) Ltd., Pune, INDIA (Jan. 2000 – Jun. 2000)

- Manufacturing Engineer, Atlas Copco (India) Ltd., Pune, INDIA (Jul. 1998 – Dec. 1998)

Technical Presentation

- "A novel approach to paint defect detection using digital image processing", Proceedings of Painting Technology Workshop, University of Kentucky, Lexington, KY, Oct 2003.